

Magdalena Traber

Synthesis and structural characterization of pseudohalide complexes with 4-hydroxymethylpyridine and 4-methoxypyridine as coligands

Master's Thesis

Graz University of Technology

Institute of Physical and Theoretical Chemistry
Head: Univ.-Prof Mag.rer.nat. Dr.phil. Georg Gescheidt-Demner

Supervisor: Ao.Univ.-Prof. Dipl.Ing. Dr.techn. Franz-Andreas Mautner

Graz, April 2017

Abstract

Fourteen pseudohalide complexes were synthesized with 4-methoxypyridine and 4-hydroxymethylpyridine as coligands. The pseudohalides were azide, cyanate, dicyanamide and rhodanide. The transition metals cadmium, cobalt, copper and zinc were used as central atoms. Among the compounds, which were prepared in aqueous solutions, nine were 4-methoxypyridine and four 4-hydroxymethylpyridine complexes. The complexes possess both monomeric and polymeric structures, except one which forms only a dimer. Compound structures were solved via single crystal structure analysis. UV-Vis and IR spectra were recorded for further characterization.

Zusammenfassung

Vierzehn Pseudohalogenid Komplexe wurden mit 4-Methoxy-pyridin und 4-Hydroxy-methyl-pyridin als Koliganden synthetisiert. Die Pseudohalogenide waren Azid, Cyanat, Dicyanamid and Rhodanid. Als Zentralatome wurden die Übergangsmetalle Cadmium, Kobalt, Kupfer und Zink verwendet. Von diesen in wässrigen Lösungen hergestellten Verbindungen waren neun 4-Methoxypyridin- und fünf 4-Hydroxymethylpyridin-Komplexe. Die Komplexe weisen polymere und monomere Strukturen auf und ein Komplex dimere Struktur. Die Struktur der Verbindungen wurde mittels Einkristallstrukturanalyse gelöst. UV-Vis- und IR-Spektren wurden zur weiteren Charakterisierung aufgenommen.

Acknowledgements

I am thankful to the head of the Physical and Theoretical Chemistry Institute Univ.-Prof. Mag.rer.nat. Dr.phil. Georg Gescheidt-Demner for the provision of the equipment and materials for synthesizing and analysing my products.

I am deeply grateful to my supervisor Ao.Univ.-Prof. Dipl.-Ing. Dr.techn. Franz A. Mautner for the intensive assistance for my master thesis.

I thank Ao. Univ.-Prof. Dr. Karl Gatterer for providing information in the spectroscopy field and help with the UV-Vis-spectrometer.

I acknowledge the generosity of Assoc.Prof. Dipl.-Ing. Dr.techn. Roland Fischer for providing the IR-spectrometer and single crystal X-ray measurements.

I am much obliged to Ing. Helmut Eisenkölbl for support in technical issues and Hilde Freißenmuth for laboratory support.

My special thanks are going out to my laboratory trainees Agnes Eck, Christine Abdelmalak, Sarah Sohar and Lea Wegger for helping out.

I appreciate the support of Manuel Strauss, BSc, for proofreading my master thesis and giving a lot of advice during the writing process.

Last but not least I want to thank my family and my friends for giving support in the years of my studies.

Contents

Abstract	ii
1. Introduction	1
I. Theory	4
2. Crystal structure analysis	5
2.1. Definitions	5
2.2. Bravais lattice	5
2.3. Diffraction	6
2.4. Bragg's Law	7
2.5. hkl indices	8
2.6. Solution of Bragg's formula	8
2.7. Reciprocal lattice	9
2.8. Intensity of diffracted X-rays	9
2.9. Atomic scattering factor and temperature factor	10
2.10. Structure factor	11
2.11. Processing data	13
2.12. Laue class	15
2.13. Direct methods	16
2.14. Patterson method	16
3. Pseudohalide complexes	18
3.1. Chemical properties	18
3.2. Azide complexes	18
3.3. Rhodanide and cyanate complexes	20
3.4. Dicyanamide complexes	21

Contents

4. Pyridines	24
4.1. 4-hydroxy-methyl-pyridine complexes	25
4.2. 4-methoxy-pyridine complexes	26
4.3. Comparison between 4-HOMepy and 4-MeOpy	28
 II. Experimental	29
5. Preparation and technical data	30
5.1. General overview	30
5.2. Used devices and programs	30
 6. 4-methoxy-pyridine complexes	32
6.1. $[\text{Co}(\text{N}_3)_2(4\text{-methoxypyridine})_4]$	32
6.1.1. Synthesis	32
6.1.2. Structural characterization	33
6.2. $[\text{Cu}(\text{N}_3)_2(4\text{-methoxypyridine})_2]_n$	37
6.2.1. Synthesis	37
6.2.2. Structural characterization	38
6.3. $[\text{Zn}(\text{N}_3)_2(4\text{-methoxypyridine})_2]$	41
6.3.1. Synthesis	41
6.3.2. Structural characterization	42
6.4. $[\text{Co}(\text{OCN})_2(4\text{-methoxypyridine})_4]$	45
6.4.1. Synthesis	45
6.4.2. Structural characterization	46
6.5. $[\text{Cd}(\text{dca})_2(4\text{-methoxypyridine})_2]_n$	50
6.5.1. Synthesis	50
6.5.2. Structural characterization	51
6.6. $[\text{Cu}(\text{dca})_2(4\text{-methoxypyridine})_2]_n$	54
6.6.1. Synthesis	54
6.6.2. Structural characterization	55
6.7. $[\text{Zn}(\text{dca})_2(4\text{-methoxypyridine})_2]_n$	58
6.7.1. Synthesis	58
6.7.2. Structural characterization	59
6.8. $[\text{Co}(\text{SCN})_2(4\text{-methoxypyridine})_4]$	62
6.8.1. Synthesis	62
6.8.2. Structural characterization	63

Contents

6.9. [Cu(SCN) ₂ (4-methoxypyridine) ₂] _n	66
6.9.1. Synthesis	66
6.9.2. Structural characterization	67
7. 4-hydroxymethylpyridine complexes	71
7.1. [Cu(N ₃) ₂ (4-hydroxymethylpyridine)] _n	71
7.1.1. Synthesis	71
7.1.2. Structural characterization	72
7.2. [Co(dca) ₂ (4-hydroxymethylpyridine) ₂] _n	77
7.2.1. Synthesis	77
7.2.2. Structural characterization	78
7.3. [Cu(dca) ₂ (4-hydroxymethylpyridine) ₂] _n	81
7.3.1. Synthesis	81
7.3.2. Structural characterization	82
7.4. [Cu(SCN) ₂ (4-hydroxymethylpyridine) ₂] ₂	85
7.4.1. Synthesis	85
7.4.2. Structural characterization	86
7.5. [Zn(SCN) ₂ (4-hydroxymethylpyridine) ₂]	90
7.5.1. Synthesis	90
7.5.2. Structural characterization	91
8. UV-VIS spectra	94
9. Discussion	97
9.1. Dicyanamide complexes	97
9.2. 4-MOP and 4-HOMP complexes	99
10. Summary	101
Appendix	103
Bibliography	112

List of Figures

1.1.	4-hydroxy-methyl-pyridine (a) and 4-methoxy-pyridine (b)	1
1.2.	Common structures of CNs	3
2.1.	Diffraction on a one dimensional lattice [4]	7
2.2.	Derivation of Bragg's Law [4]	7
2.3.	Definition of the hkl-indices through reciprocal axis intercept [4]	10
2.4.	2D- structure with two types of atoms [4]	12
3.1.	Structures of published azide complexes [17]	19
3.2.	Some thiocyanate and cyanate coordination bridging modes. Points represent metallatoms. [19]	20
3.3.	Structures of published dca complexes in the CCDC [1]	22
3.4.	Structures of possible dca complexes which are not published yet	23
4.1.	Chemical structure of pyridine	24
6.1.	IR spectrum of $[\text{Co}(\text{N}_3)_2(4\text{-MeOpy})_4]$	33
6.2.	Perspective view of $[\text{Co}(\text{N}_3)_2(4\text{-MeOpy})_4]$	35
6.3.	Packing view of $[\text{Co}(\text{N}_3)_2(4\text{-MeOpy})_4]$	35
6.4.	IR spectrum of $[\text{Cu}(\text{N}_3)_2(4\text{-MeOpy})_2]_n$	37
6.5.	Perspective view of $[\text{Cu}(\text{N}_3)_2(4\text{-MeOpy})_2]_n$	39
6.6.	Packing plot of $[\text{Cu}(\text{N}_3)_2(4\text{-MeOpy})_2]_n$	39
6.7.	IR spectrum of $[\text{Zn}(\text{N}_3)_2(4\text{-MeOpy})_2]$	41
6.8.	Perspective view of $[\text{Zn}(\text{N}_3)_2(4\text{-MeOpy})_2]$	43
6.9.	Packing view of $[\text{Zn}(\text{N}_3)_2(4\text{-MeOpy})_2]$	43
6.10.	IR spectrum of $[\text{Co}(\text{OCN})_2(4\text{-MeOpy})_4]$	45
6.11.	Perspective view of $[\text{Co}(\text{OCN})_2(4\text{-MeOpy})_4]$	48
6.12.	Packing view of $[\text{Co}(\text{OCN})_2(4\text{-MeOpy})_4]$	48

List of Figures

6.13.	IR spectrum of $[\text{Cd}(\text{dca})_2(4\text{-MeOpy})_2]_n$	50
6.14.	Perspective view of $[\text{Cd}(\text{dca})_2(4\text{-MeOpy})_2]_n$	52
6.15.	Packing plot of $[\text{Cd}(\text{dca})_2(4\text{-MeOpy})_2]_n$	52
6.16.	IR spectrum of $[\text{Cu}(\text{dca})_2(4\text{-MeOpy})_2]_n$	54
6.17.	Perspective view of $[\text{Cu}(\text{dca})_2(4\text{-MeOpy})_2]_n$	56
6.18.	Packing plot of $[\text{Cu}(\text{dca})_2(4\text{-MeOpy})_2]_n$	56
6.19.	IR-Spectrum of $[\text{Zn}(\text{dca})_2(4\text{-MeOpy})_2]_n$	58
6.20.	Perspective view of $[\text{Zn}(\text{dca})_2(4\text{-MeOpy})_2]_n$	60
6.21.	Packing plot of $[\text{Zn}(\text{dca})_2(4\text{-MeOpy})_2]_n$	60
6.22.	IR spectrum of $[\text{Co}(\text{SCN})_2(4\text{-MeOpy})_4]$	62
6.23.	Perspective view of $[\text{Co}(\text{SCN})_2(4\text{-MeOpy})_4]$	64
6.24.	Packing view of $[\text{Co}(\text{SCN})_2(4\text{-MeOpy})_4]$	64
6.25.	IR spectrum of $[\text{Cu}(\text{SCN})_2(4\text{-MeOpy})_2]_n$	66
6.26.	Perspective view of $[\text{Cu}(\text{SCN})_2(4\text{-MeOpy})_2]$	69
6.27.	View onto 2D Cu-NCS sub-lattice of $[\text{Cu}(\text{SCN})_2(4\text{-MeOpy})_2]_n$	69
7.1.	IR-Spectrum of $[\text{Cu}(\text{N}_3)_2(4\text{-HOMepy})]_n$	72
7.2.	Perspective view of $[\text{Cu}(\text{N}_3)_2(4\text{-HOMepy})]_n$	75
7.3.	Packing plot of $[\text{Cu}(\text{N}_3)_2(4\text{-HOMepy})]_n$	75
7.4.	IR spectrum of $[\text{Co}(\text{dca})_2(4\text{-HOMepy})_2]_n$	77
7.5.	Perspective view of $[\text{Co}(\text{dca})_2(4\text{-HOMepy})_2]_n$	79
7.6.	Packing plot of $[\text{Co}(\text{dca})_2(4\text{-HOMepy})_2]_n$	79
7.7.	IR spectrum of $[\text{Cu}(\text{dca})_2(4\text{-HOMepy})_2]_n$	81
7.8.	Perspective view of $[\text{Cu}(\text{dca})_2(4\text{-HOMepy})_2]_n$	83
7.9.	Packing plot of $[\text{Cu}(\text{dca})_2(4\text{-HOMepy})_2]_n$	83
7.10.	IR spectrum of $[\text{Cu}(\text{SCN})_2(4\text{-HOMepy})_2]_2$	85
7.11.	Perspective view of $[\text{Cu}(\text{SCN})_2(4\text{-HOMepy})_2]_2$	88
7.12.	Packing plot of $[\text{Cu}(\text{SCN})_2(4\text{-HOMepy})_2]_2$	88
7.13.	IR spectrum of $[\text{Zn}(\text{SCN})_2(4\text{-HOMepy})_2]$	90
7.14.	Perspective view of $[\text{Zn}(\text{SCN})_2(4\text{-HOMepy})_2]$	92
7.15.	Packing view of $[\text{Zn}(\text{SCN})_2(4\text{-HOMepy})_2]$	92
8.1.	Tanabe-Sugano-Diagramm	96

1. Introduction

4-hydroxy-methyl-pyridine and 4-methoxy-pyridine are compounds which, despite being easy to handle, see little use in synthesis of coordination compounds. This is evident in the lack of published crystal structures containing them - currently 34 contain the first and only 23 the latter one. [1] Most of these complexes employ transition metals like platinum, nickel or silver as central atom. Also only a few of them have pseudohalides as ligands.

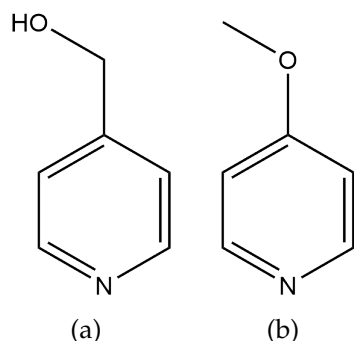


Figure 1.1.: 4-hydroxy-methyl-pyridine (a) and 4-methoxy-pyridine (b)

The aim of this master thesis was the synthesis, spectral and structural characterization of new transition metal complexes using aforementioned pyridines with pseudohalides and transition metals. Pseudohalides were chosen as anionic ligands due to their similar properties to halides. The central metal can bind to the end or middle atoms of these polyatomic ligands, making various combinations possible.

Mixing ligands and metal salts with varying ratios results in complexes with different coordination numbers (CN). Coordination numbers describe

1. Introduction

the number of donor atoms contained by ligands which are surrounding the central atom. 2, 4, 5 and 6 are common coordination numbers.

For the coordination number 2 only linear arrangements are known and these complexes are often formed with the single positively charged ions Ag^+ , Cu^+ and Au^+ . [2]

Tetrahedral and square-planar arrangements are possible for coordination number 4. Tetrahedral complexes are more common and are formed in all kinds of d-configurations whereas d^8 -configuration (or 16-electron-complexes) prefer the square planar arrangement, i.e. Pt^{2+} or Pd^{2+} . [2]

Square-pyramidal and trigonal-bipyramidal structures are forms of the seldom appearing coordination number 5. They can be transformed into each other via Berry rotation [3] and are in equilibrium at a certain temperature.

CN 6 forms are octahedron (common), trigonal antiprism or trigonal prism (rare). The metal ions Cr^{3+} , Co^{3+} and Pt^{3+} favor the octahedral arrangement.[2]

The coordination numbers with their frequent arrangements are listed in figure 1.2.

1. Introduction

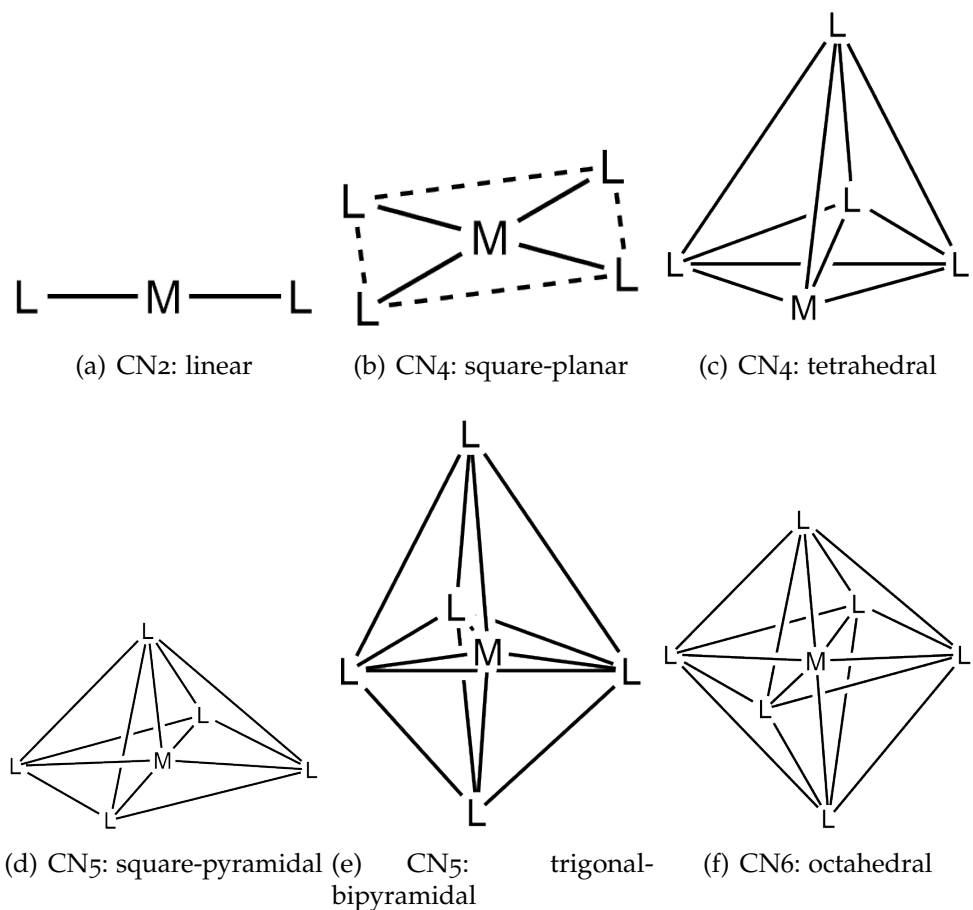


Figure 1.2.: Common structures of coordination numbers.

Part I.

Theory

2. Crystal structure analysis

Chapter 2 is adopted from the textbooks “Kristallstrukturanalyse” by W. Massa [4] and “Einführung in die Röntgenfeinstrukturanalyse” by H. Krischner [5].

2.1. Definitions

A solid that contains atoms, ions or molecules which are arranged in a periodic pattern along the three dimensions of space is described as a crystal. For an arbitrary point picked in the crystal there are infinitely many points with identical surroundings. This is called periodicity. The crystal can be considered infinitely extended in three dimensions. It can be seen as a lattice with a three dimensional array of points (lattice points). These points may not be considered as the ions or atoms in the crystal. If an atom is positioned on a lattice point, then the same atoms are at every lattice point in the crystal. [4]

2.2. Bravais lattice

7 crystal systems can be determined from a variation of the lattice parameters a , b , c and the angles α , β , γ . Together with four types of centered cells (primitive (P), body-centered (I), face-centered (F) and base-centered (B)) 14 Bravais lattice types can be defined. [6] For their determination the entire symmetry of the crystal should be contained in the smallest unit of the cell. In table 2.1 the crystal systems are listed.

2. Crystal structure analysis

Table 2.1.: Crystal systems with their types of centered cell

Crystal system	Parameter	Angles	centered cell
triclinic	$a \neq b \neq c$	$\alpha \neq \beta \neq \gamma \neq 90^\circ$	P
monoclinic	$a \neq b \neq c$	$\alpha = \gamma = 90^\circ \beta > 90^\circ$	P, B
orthorohmbic(cuboid)	$a \neq b \neq c$	$\alpha = \beta = \gamma = 90^\circ$	P, F, I, B
tetragonal	$a = b \neq c$	$\alpha = \beta = \gamma = 90^\circ$	P, I
hexagonal	$a = b \neq c$	$\alpha = \beta = 90^\circ \gamma = 120^\circ$	P
trigonal (rhomboedric)	$a = b = c$	$\alpha = \beta = \gamma \neq 90^\circ$	P
cubic	$a = b = c$	$\alpha = \beta = \gamma = 90^\circ$	P, F, I

2.3. Diffraction

Electromagnetic waves can interact with one-dimensional lattices. When monochromatic light (wavelength λ) irradiates an optical grating (period d , which is the distance between two adjacent lines) and they are in the same order of magnitude, diffraction can occur. When a point of the lattice is struck with light, becoming a spherical wave of the same wavelength, it is called elastic scattering. The waves interfere with each other depending on the angle θ of observation and the difference of the travelled path lengths by waves of the two adjacent points (optical retardation Δ). Constructive interference can occur when Δ is an integer multiple of the wavelength λ . If all scattered waves in phase reinforce one another it leads to an observable diffracted beam. Destructive interferences between scattered waves can be observed if Δ is a half integer of λ and annulles them completely. In all other cases, where the values are between constructive and destructive interference, the lattice points can be grouped in pairs and be separated by one or more lattice points. These scattered waves are out of phase and cancel each other out. The intensity of the angles which meet the requirement of constructive interference exactly will be observed, the others will not.

2. Crystal structure analysis

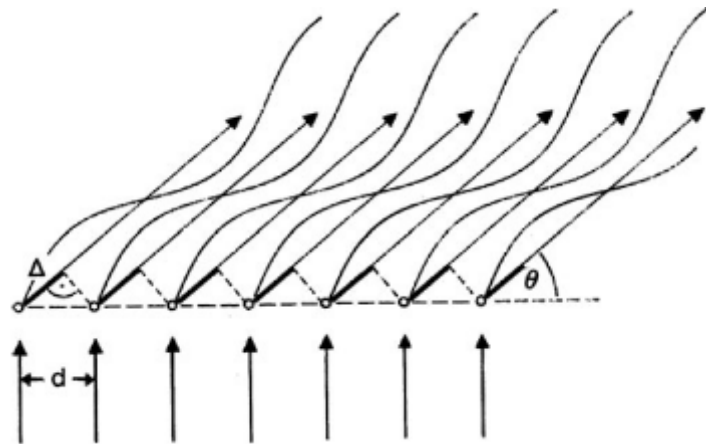


Figure 2.1.: Diffraction on a one dimensional lattice [4]

2.4. Bragg's Law

In order to obtain diffraction, X-rays are used since their wavelengths have the same order of magnitude as the inter-atomic distances in crystals, 1 \AA or 10^{-10} m . For three dimensional lattices, the one dimensional diffraction has to be adapted. The reflection of X-rays on lattice planes can be treated as diffraction. [7] Only if constructive interference occurs (retardation is whole multiple of the wavelength) the conditions are fulfilled and Bragg's Law can be derived (eq. 2.1).

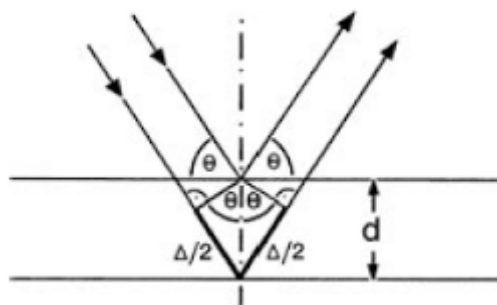


Figure 2.2.: Derivation of Bragg's Law [4]

2. Crystal structure analysis

$$2dsin(\theta) = n\lambda \quad (2.1)$$
$$n = 1, 2, 3, \dots$$

2.5. hkl indices

All of the lattice planes contain lattice points and for each lattice plane there is a set of parallel and equidistant planes. Each lattice point lies on one plane. For orientation of the planes there are the Miller Indices hkl. For the determination of the Miller indices for a set of planes, the plane nearest to the unit cell's origin (don't contain the origin) is picked. This plane intersects the a-, b- and c-axes with the distances $1/h$, $1/k$ and $1/l$ from the origin measured in the axis lengths' units. $1/h$, $1/k$ and $1/l$ can be represented as fractions, because they are rational numbers. The lattice planes can be denoted in parentheses (hkl) and hkl is used for the corresponding reflection. For parallel planes (to an axis) the intersection point lies at infinity and the Miller index is zero. For each set of lattice planes (hkl) with the characteristic distance d there is an unique angle θ for each diffraction order n at which reflection can be observed. (see Bragg's Law, eq. 2.1). Each Miller index can be multiplied by n to determine the reflection at a lattice point.

2.6. Solution of Bragg's formula

To calculate the diffraction angle θ the distance of the corresponding lattice plane must be known. The distance d depends on the Miller indices (hkl) and the geometry of the lattice. The distance can be a square number (d^2) if different crystal systems are used. If Bragg's equation 2.1 is squared and d^2 is substituted, a quadratic Braggs' law is formed. It can be used to calculate θ from the Miller indices if the unit cell is known.

2. Crystal structure analysis

2.7. Reciprocal lattice

Each reflection is equivalent to a specific set of lattice planes. These sets are described by a vector d whose direction is vertical to the planes. Its length is equal to the distance between two adjoining planes. The endpoint of the corresponding vector d represents a lattice plane. For higher diffraction angles the length of d is shorter, which can be a drawback. Also hkl cannot be used to determine the direction of d . A new coordination system can help prevent these difficulties. It is spanned by the three base vectors a^* , b^* and c^* and represents each plane (hkl) and each reflection hkl as the point $ha^* + kb^* + lc^*$. The reciprocal lattice is formed with the points of all possible coordinations of the indices, which are whole numbers. The original lattice is called the crystal lattice to distinguish the two. The reciprocal base vectors are formed from the real base vectors in eq. 2.2, where each numerator is the vector product of two real base vectors and (abc) is the triple product equal to the volume of the real unit cell.

$$\begin{aligned} a^* &= b \times c / (abc) \\ b^* &= c \times a / (abc) \\ c^* &= a \times b / (abc) \end{aligned} \tag{2.2}$$

While in orthogonal crystal systems each reciprocal base vector is parallel to its counterpart, this is not true for systems with oblique angles. Eq. 2.2 suggests that every unit vector in reciprocal space is perpendicular to a plane in real space and vice versa.

2.8. Intensity of diffracted X-rays

With the knowledge of the geometry of the crystal lattice (the metric) the angles of all possible reflections can be determined. This is used in powder and single crystal measurements. The intensities of the reflections contain information about type and location of atoms in the unit cell. They can be measured absolute or relative. Absolute values are difficult to determine but relative values can be calculated and then be scaled to absolute values. How

2. Crystal structure analysis

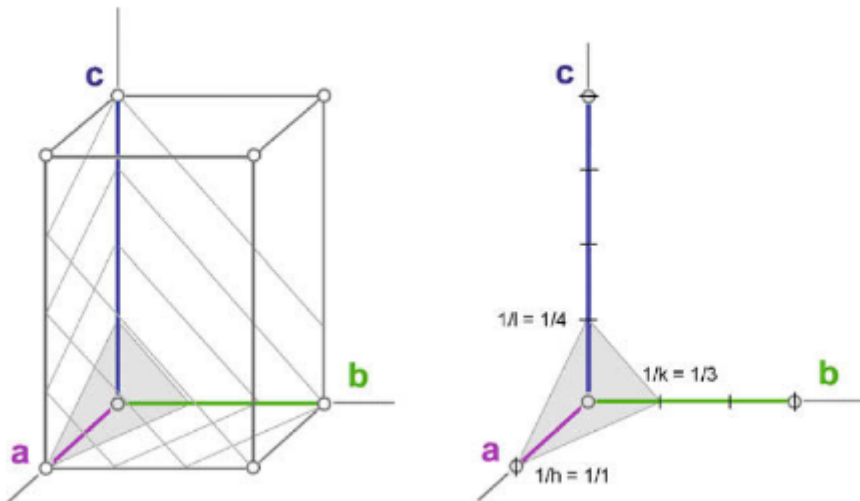


Figure 2.3.: Definition of the hkl-indices through reciprocal axis intercept [4]

the atoms are arranged in the crystal can be calculated with these values. All factors should be known because they affect the intensities.

2.9. Atomic scattering factor and temperature factor

Up to now it was considered that X-ray scattering takes place at the points of the point lattice . In reality scattering occurs at the electrons or ions of atoms and crystals. It was established that the radius of an electron shell has the same magnitude as the X-ray wavelength, but punctual scattering centers are not in the same range. Therefore rays that are scattered at different positions in the electron shell have a phase difference. This leads to a weakening of the intensities which depends on the form of the shell and on the diffraction angle. The scattering factors are scaled in a way that their values at an angle of zero are equal to the corresponding atomic number.

Atoms, depending on atom mass, chemical environment and temperature, oscillate about their equilibrium positions. X-ray beams consists of short radiation flashes that are approximately 10^{-18} s long. This is much shorter

2. Crystal structure analysis

than the period of a thermal oscillation, lasting for 10^{-14} s. Because of this a specific atom can appear at slightly different locations during measurement. The result is a phase difference which increases with larger amplitudes (u) and smaller distances of the lattice planes, i. e. larger diffraction angles. This additional weakening of the scattering factors f is taken into account by multiplying the scattering factors with an e-function. At the beginning of a calculation the oscillations are assumed to be isotropic (see equation 2.3). Substituting d in accordance with Bragg's Law eq. 2.1 and absorbing some constants in the Debye-Waller-factor B [8][9] result in eq. 2.4.

$$f' = f \cdot e^{-2\pi^2 \frac{u^2}{d^2}} \quad (2.3)$$

$$f' = f \cdot e^{-B \frac{\sin^2 \theta}{\lambda^2}} \quad (2.4)$$

This affects the determination of lighter atoms, which have both low scattering factors and high amplitudes, due to their low mass. The crystals should be cooled when they are measured because of these reasons. When refining the crystal structure, oscillations are usually considered to be anisotropic with the exception of H-atoms. The displacement is now described by a tensor, represented by a symmetric 3×3 matrix with six independent factors, U_{11} , U_{12} , U_{13} , U_{22} , U_{23} , and U_{33} . By visualizing it as a thermal ellipsoid with three axes the corresponding atom can be found within the ellipsoid with 50% probability.

$$f' = f \cdot e^{-2\pi^2 (U_{11}h^2a^{*2} + U_{22}k^2b^{*2} + U_{33}l^2c^{*2} + 2U_{23}klb^{*}c^{*} + 2U_{13}hla^{*}c^{*} + 2U_{12}hka^{*}b^{*})} \quad (2.5)$$

2.10. Structure factor

A reference point in the crystal is selected and all the other points whose surrounding are identical to that selected one are determined in order to obtain the point lattice of the crystal. If a different reference point is picked, the same lattice is given, only shifted by the translation vector. This vector

2. Crystal structure analysis

equals the difference of the spatial positioning between the first and second reference point. The same lattice applies to every atom in the unit cell, the chosen origin is the only difference. The crystal in fig. 2.4 needs to be adjusted so that the lattice plane is at an appropriate angle θ with the X-ray beam. Then the waves of all type 1 atoms are in phase with each other.

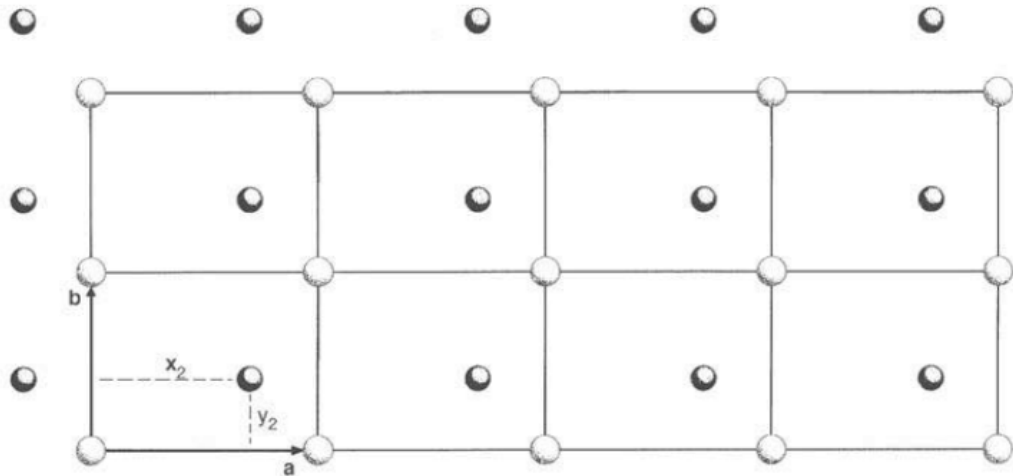


Figure 2.4.: 2D- structure with two types of atoms [4]

Waves generated by atoms of type 2 are also in phase with each other, because θ is not changed when the lattice is shifted. Since the lattice is translated a phase difference between the two diffracted rays exists. This depends on the relative position of the two atom types and on the selected lattice plane. Scattering factors are extended by a phase information, by multiplicating an exponential function with an imaginary argument:

$$F_{hkl}(n) = f_n \cdot e^{i\phi_n} \quad (2.6)$$

For each atom of type n the phase angle ϕ expresses the phase difference. Euler's formula is applied to eq. 2.6 and gives an equivalent function with the sin und cos terms:

$$F_{hkl}(n) = f_n(\cos(\phi_n) + i \cdot \sin(\phi_n)) \quad (2.7)$$

2. Crystal structure analysis

In order to calculate ϕ_n the relative coordinates x_n, y_n, z_n of atom n in the unit cell and the Miller indices of the lattice plane are taken into account:

$$\phi_n = 2\pi(hx_n + ky_n + lz_n) \quad (2.8)$$

For each reflection the diffracted waves of all atoms are added together with regard to their phase differences which leads to the final equation for the structure factor F_{hkl} for a certain reflection hkl :

$$F_{hkl} = \sum_n f_n [\cos(2\pi(hx_n + ky_n + lz_n)) + i \cdot \sin(2\pi(hx_n + ky_n + lz_n))] \quad (2.9)$$

For crystals belonging to a centro-symmetrical point group - with the origin of the crystal lattice being placed at a center of inversion - the calculation of the structure is reduced to:

$$F_{hkl} = \sum_n f_n \cos(2\pi(hx_n + ky_n + lz_n)) \quad (2.10)$$

The structure factor cannot be measured directly because it is an imaginary quantity. Its relative intensity is determined and this is proportional to the absolute value of F_{hkl}^2 . The phase angle ϕ cannot be obtained directly from the intensities, because it gets lost through the calculation - this is called the phase problem. If the crystal has an inversion center, the phase problem can be simplified to determining the sign of F_{hkl} .

2.11. Processing data

For obtaining structure factors the raw data has to be processed after measurement. First the background signal is subtracted and normalized if different periods are measured. The net intensity of each reflection is computed from the total intensity with this method. Intensities of reflections at different angles can be compared among each other when correction

2. Crystal structure analysis

factors are applied. For powder diffractometry the multiplicity factor is relevant. This factor takes in consideration that reflections of symmetry-equivalent lattice planes appear at the same angle in a powder diffractogram. The multiplicity factor normalizes the intensities since different lattice planes may have different numbers of symmetry equivalents. The value of the factor ranges from 2 to 48 (triclinic to cubic system). The diffraction of X-rays is a reflection at certain planes in the crystal. The reflection angle θ is not important for the intensity of the fraction of the reflected beam, only if the electric component lies parallel to the plane. The intensity fraction is proportional to $\cos^2(2\theta)$ for radiation whose electric vector oscillates perpendicular to the plane. The polarization factor P makes it possible. Unpolarized X-rays leave the X-ray tube as a 1:1 mixture of rays with parallel and perpendicular electric field vectors to the reflection plane. Between these two extreme cases P is simply the average of the two:

$$P = \frac{(1 + \cos^2(2\theta))}{2} \quad (2.11)$$

A reflection is a curve with a certain breadth with its peak located at θ (Bragg's angle). If a single crystal is rotated in the diffractometer the lattice planes stay in a reflection position for a period of time. It depends on the value of θ and is factored in the Lorentz factor L:

$$L = \frac{1}{\sin(2\theta)} \quad (2.12)$$

Lorentz and Polarization factor are summarized in the LP-correction:

$$LP = \frac{1 + \cos^2\theta}{2\sin 2\theta} \quad (2.13)$$

The observed structure factor F_0 may be calculated as:

$$F_0 = \sqrt{\frac{I}{LP}} \quad (2.14)$$

The absorption factor must also be taken into account. It affects the relative intensities of diffracted X-rays. While traveling through matter X-rays are

2. Crystal structure analysis

weakened by elastic scattering, inelastic scattering and ionization. These absorption effects increase approximately with the fourth potency of the atomic number of the absorbing atom and with the third potency of the wavelength of the X-rays. All effects are summarized in the linear absorption coefficient (μ) and the intensity can be calculated with eq.2.15 (s is the travelled distance of the X-ray beam):

$$I = I_0 \cdot \exp(-\mu \cdot s) \quad (2.15)$$

From tabulated values for components of the crystal, their mass fraction in the crystal and the density of the crystal μ can be obtained. Different methods for absorption corrections (for higher μ values) have been developed, e.g. numeric absorption correction, empiric absorption correction and the DIFABS method [10].

2.12. Laue class

For determination of the space group the Laue class must be derived. Each reflection is a point in the reciprocal lattice. Assigning the intensity to each reflection of its point in reciprocal space yields the intensity-weighted reciprocal lattice. Its point group is the Laue class of the crystal. The Laue class contains a center of inversion (even if the crystal has none) which is the only difference between the space group and the Laue class. The two reflections hkl and $h-k-l$ refer to the same set of lattice planes except they are only irradiated from opposing sites. All Laue groups include two or more point groups and each point group contains several space groups. For reducing the number of possible space groups systematic extinctions can be found. They are absences of reflections whose indices satisfy certain conditions. They show that glide planes, screw axes or centered unit cells can be present in the cell. For crystal systems of high symmetry the space group can be hardly determined. For these cases information about physical properties, Patterson symmetry and structure-chemical plausibility is important.

2. Crystal structure analysis

2.13. Direct methods

These methods attempt to obtain phases of the structure factors directly from measured intensities through mathematical relationships. The original works for these methods [11] found that the presence of symmetry elements gives rise to relations between structure amplitudes and certain pairs of reflection. The assumption that the electron density consists of identical and well-resolved peaks result in the equation 2.16 [12]:

$$E_{hkl} = C \sum_{h'k'l'} E_{h'k'l'} \cdot E_{h-h'k-k'l-l'} \quad (2.16)$$

To obtain the normalized structure factor E_{hkl} F_{hkl} is divided by its expectation value. This value can be calculated from the Wilson statistic. [13] Eq.2.16 applies to structures containing just one type of atom but in practice it can also be used for structures with atoms with similar atomic number; e.g. C, N, O, H. Therefore it can be applied for classes of structures that are difficult to solve via Patterson methods.

2.14. Patterson method

For crystals containing only a few heavy elements (which is the case for most metal-organic compounds) the Patterson method can be of use, as it solves the phase problem. In the Patterson function P_{uvw} , the coefficients are the directly measured F_0^2 values. To distinguish the patterson synthesis from a normal F_0 Fourier synthesis, the coordinates in Patterson space have the coordinates u, v and w. These coordinates are not directly related to atomic coordinates x, y, z, altough they refer to the same axes and unit cell. The Patterson function is defined as:

$$P_{uvw} = \frac{1}{V} \sum_{hkl} |F_{hkl}|^2 \cos(2\pi(hu + kv + lw)) \quad (2.17)$$

The Patterson function only include the information from the intensities, the interatomic vectors, because no phase information is contained in the F_0^2

2. Crystal structure analysis

values. [14]

Maxima in the function P represent distance vectors between atoms in the unit cell. P is always centrosymmetric since two distance vectors of the same length and opposite direction are associated with each pair of atoms. The intensity of a Patterson peak is simply the product of the atomic number of the two atoms involved. If a crystal contains a few heavy metal atoms, they can easily be identified by the high intensities of the corresponding peaks.

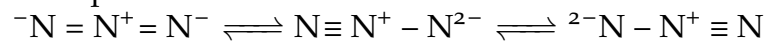
3. Pseudohalide complexes

3.1. Chemical properties

Pseudohalogens are polyatomic molecules possessing properties similar to halogenes and are therefore among the group of pseudoelements. These chemical properties are reactivity, charge and binding behavior. They can be used as substitutions for halogenes in all kinds of chemical compounds. Pseudohalides, the ionic form of pseudohalogens, are used as ligands in co-ordination complexes. Cyanide, cyanate, thiocyanate, azides and rhodanides are well known pseudohalides. The chemical properties and their behavior are identical to halide ions. The internal double or triple bonds that are often present do not affect their chemical behavior. They form strong acids (HX) and react with metals to form compounds like MX . [15]

3.2. Azide complexes

Azide (N_3^-) is the salt of hydrazoic acid. HN_3 is a weak base (pk_a of 4.75) and is highly explosive in its waterfree form. Hydrazoic acid and azides are highly toxic and should be handled with care. The linear molecule N_3^- has three possible resonance structures:



Azide can be organised in two types: inorganic (e.g. NaN_3) and organic azides (e.g. TosN_3). [15] Furthermore, azides can be subdivided in more types according to their bonding character [16]: Ionic azides, molecular azides and coordinative azides.

Azides are used for technical applications such as explosives ($\text{Pb}(\text{N}_3)_2$), airbags or pharmacy. Fig. 3.1 depicts bridging modes of azides.

3. Pseudohalide complexes

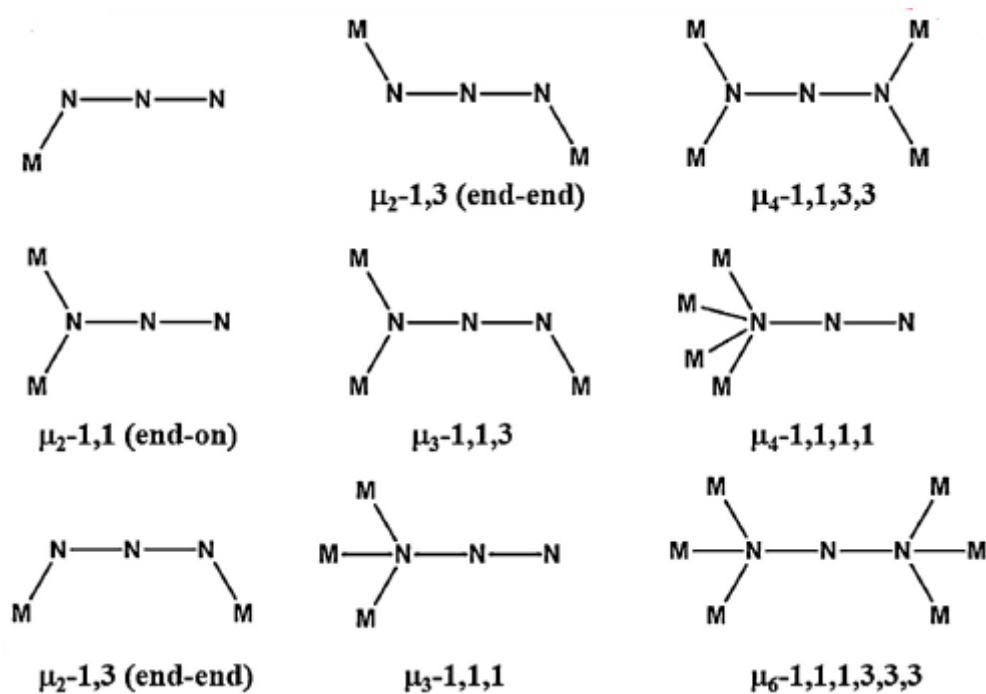
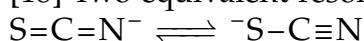


Figure 3.1.: Structures of published azide complexes [17]

3. Pseudohalide complexes

3.3. Rhodanide and cyanate complexes

Thiocyanate (alternate name rhodanide) is the conjugate base of thiocyanic acid. Common derivatives are KSCN and NaSCN. Rhodanite is an analogue of the cyanate ion (OCN^-). The name rhodanide means rose in greek and comes from the red colour of its iron complexes. If the metal or the organic group is attached to the S ($\text{R}-\text{S}-\text{C}\equiv\text{N}$) the compound is called thiocyanate and if it is bonded to the N-atom ($\text{R}-\text{N}=\text{C}=\text{S}$) its name is isothiocyanate. [18] Two equivalent resonance structures exist:



As a result thiocyanate is an ambidentate ligand, meaning that both ends (S or N) can act nucleophilic. In fig. 3.2 I-VI are listed the known bonding types. Hard acids form N-bonded isothiocyanate complexes and soft acids form S-bonded thiocyanate complexes.[15]

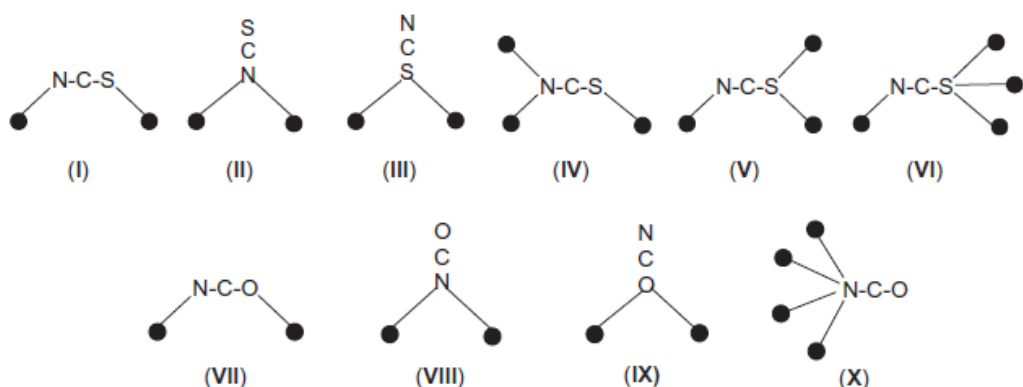


Figure 3.2.: Some thiocyanate and cyanate coordination bridging modes. Points represent metallatoms. [19]

Cyanate's chemical structure is $[\text{OCN}]^-$ or $[\text{NCO}]^-$. It has similar properties to thiocyanate. In figure 3.2 (VII) to (X) the different bonding types are shown. If the metal or the organic group is attached to the O ($\text{R}-\text{O}-\text{C}\equiv\text{N}$) the compound is called cyanate and if it is bonded to the N-atom ($\text{R}-\text{N}=\text{C}=\text{O}$) its name is isocyanate. [15]

3. Pseudohalide complexes

3.4. Dicyanamide complexes

The molecular formula for dicyanamide is $C_2N_3^-$. It is composed of two cyanide groups that are bound to a central nitrogen anion. It can be used as a counterion in organic and inorganic salts and as reactant for the synthesis of covalent organic structures. Another use would be the synthesis of pseudohalide complexes. The metal can bind on the middle and end nitrogen atoms of the dicyanamide. Therefore there are a lot of combinations how the metals can be bound to a single dicyanamide. [15] In fig. 3.3 there are examples of structures of published dca complexes. Fig. 3.4 contains structures which have not been synthesized yet but are also possible.

3. Pseudohalide complexes

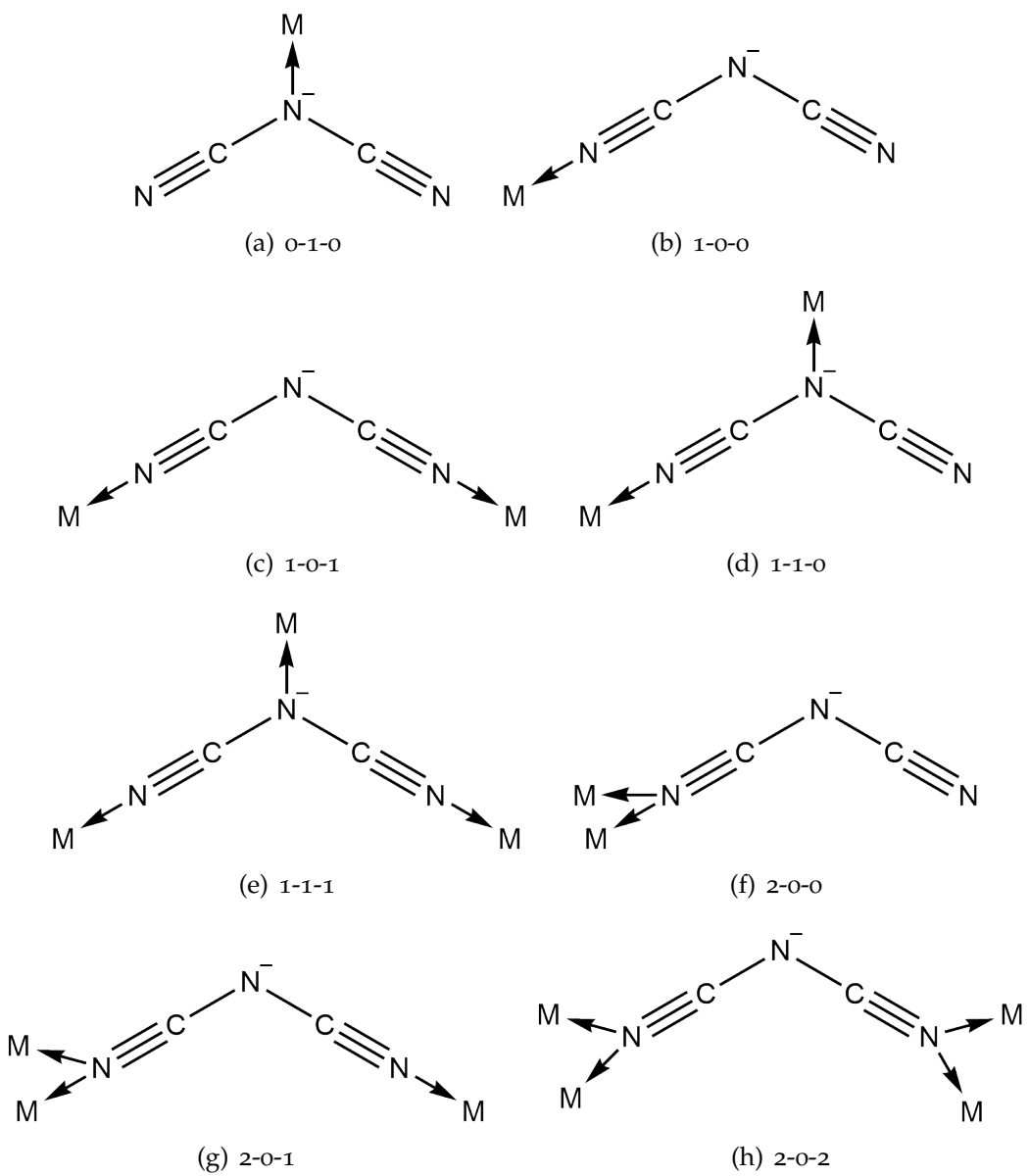


Figure 3.3.: Structures of published dca complexes in the CCDC [1]

3. Pseudohalide complexes

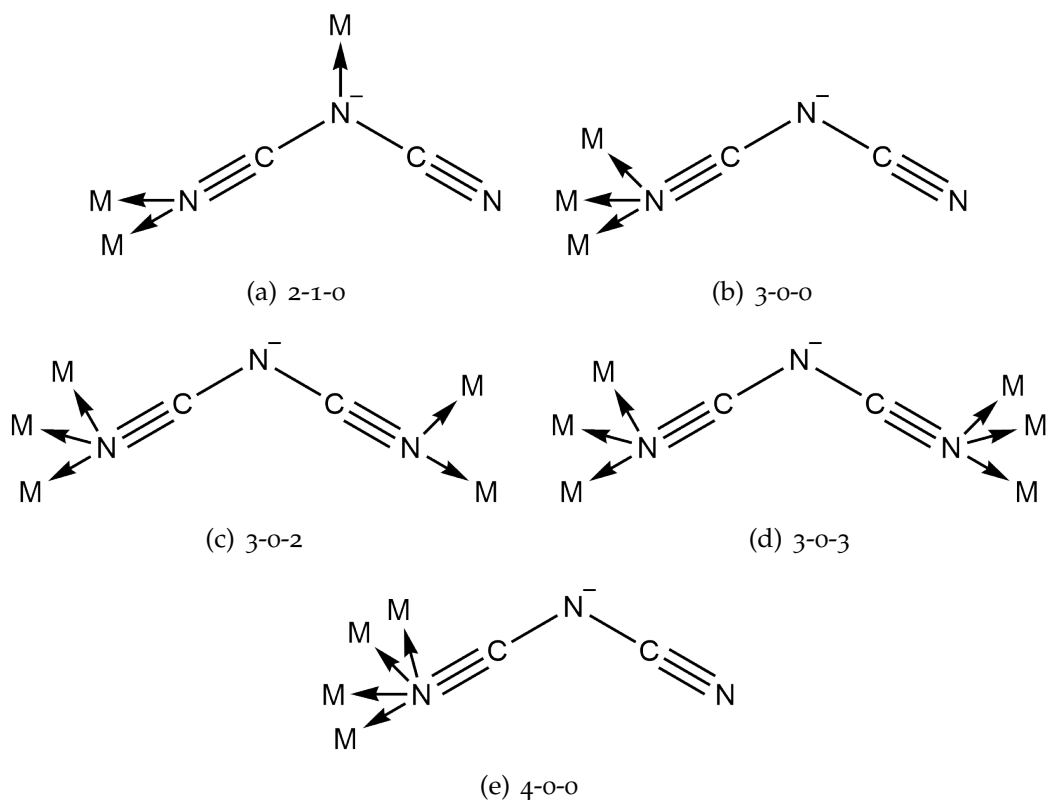


Figure 3.4.: Structures of possible dca complexes which are not published yet

4. Pyridines

Pyridines are described as six- membered heterocycles, which include a single N-atom in the ring. They are aromatic compounds and their 6π -electrons are delocalized over the entire ring. All atoms in the ring are sp^2 hybridized. The N-atom has a lone pair which does not contribute to the aromatic system and has influence on the chemical properties of the pyridine. It's hydrophilic and hydrophobic character makes it miscible with water and organic solvents. [20]

Pyridines can be involved in protonation, alkylation, acylation and N-oxidation as tertiary amines and nucleophilic substitution as aromatic compounds.

The compound itself is a weak ligand for forming complexes with transition metal ions, but its acid derivates can form strong complexes.

With a pK_a of approximately 5 pyridines are weak bases and therefore the formation of salts is favored. The electronegative nitrogen in the ring makes the pyridine an electron deficient molecule. Therefore it is more improbable for the compound to partake in electrophilic reactions unlike other benzene derivatives. Nucleophilic substitution and metalation, however, occur more often with pyridines and are conducted using strong organometallic bases. [21]

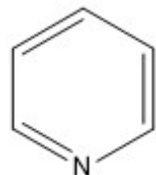


Figure 4.1.: Chemical structure of pyridine

4. Pyridines

4.1. 4-hydroxy-methyl-pyridine complexes

Table 4.1.: List of in the CCDC published 4-hydroxy-methyl-pyridine complexes [1]

trans-[PtCl ₂ NH ₃ (4-(hydroxymethyl)-pyridine)] [22]
[Mn ₆ O ₂ (O ₂ CPh) ₁₀ (4-hydroxymethylpyridine) ₃ (MeCN)] [23]
catena-((μ ₂ -pyridine-2,6-dicarboxylato)-(μ ₂ -4-(hydroxymethyl)pyridine)-copper(II)) [24]
Diaqua-(pyridine-2,6-dicarboxylato)-(4-hydroxymethyl)pyridine)-nickel(II) monohydrate [24]
[Ag(4-hydroxymethylpyridine) ₂]NO ₃ [25]
trans-[PtCl ₂ (NH ₂ CH(CH ₃) ₂ (4-py-MeOH))] [26]
trans-[PtCl ₄ (NH ₃)(4-py-MeOH)] [26]
[Cu(4-pyridylmethanol) ₄ Cl]Cl [27]
bis(Glycinato-N,O)-bis(4-hydroxymethylpyridine-N)-nickel [28]
chloro-(2-(isobutylimino)methylphenolato)-((pyridin-4-yl)(methanol))-platinum dichloromethane solvate [29]
bis(Niflumato-O)-bis(4-pyridylmethanol-N)-copper(II) methanol solvate [30]
Aqua-bis(2-chlorobenzoato-O)-bis(4-pyridylmethanol-N)-copper(II) [30]
tetrakis(μ ₂ -(2,6-Diisopropylphenyl)phosphato)-tetrakis(4-hydroxymethylpyridine)-tetra-zinc [31]
bis(μ ₄ -Oxo)-tetrakis(μ ₃ -benzoato)-hexakis(μ ₂ -benzoato)-(acetonitrile)-tris(4-hydroxymethylpyridine)-tetra-manganese(II)-di-manganese(III) acetonitrile solvate [32]
tetrakis(μ ₂ -acetato)-bis(4-pyridinemethanol)-di-rhodium) [33]
(Cyclobutane-1,1-dicarboxylato)-(bis((pyridine-4-yl)methanol)-platinum [34]
bis(μ ₂ -cyclohexane-1,2-dicarboxylic acid)-(tetrakis((pyridin-4-yl)methanol)-di-platinum dihydrate [34]
catena-[tris(μ ₂ -Azido-N ¹ ,N ¹)-(μ ₂ -Azido-N ¹ ,N ³)-tetrakis(4-hydroxymethylpyridine)-di-cadmium(II)] [35]

4. Pyridines

bis((pyridin-4-yl)methanol)-(trifluormethanesulfonato)-silver [36]
bis(pyridin-4-yl)methanol)-silver perchlorate [36]
bis((pyridin-4-yl)methanol)-silver tetrafluoroborate acetonitrile solvate [36]
tetrakis((pyridin-4-yl)methanol)-bis(thiocyanato)-nickel [37]
bis(ethanol)-bis((pyridin-4-yl)methanol)-bis(thiocyanato)-nickel [37]
diaqua-bis((pyridin-4-yl)methanol)-bis(thiocyanato)-nickel [37]
catena-[(μ -pyridin-4-ylmethanol)-(μ -thiocyanato)-(pyridin-4-ylmethanol)-(isothiocyanato-nickel] [37]
Aqua-bis(4-clofibriato-O)-bis(4-pyridylmethanol-N)-copper(II) dihydrate [38]
tris(Tetraethylammonium)-tris(μ_2 -4-pyridinemethanolato)-bis(tricarbonyl-tungsten(o)) acetonitrilo solvate [39]
chloro-tetrakis(pyrid-4-ylmethanol-N)-copper(II) chloride [38]
trans-dichloro-isopropylamine-(4-(hydroxymethyl)pyridine-N)-platinum(II) [40]
bis(pyridin-4-yl-N)methanol)-silver nitrate [36]
catena-(μ_2 -Pyridin-4-ylmethanol)-(μ_2 -thiocyanato-N,S)-isothiocyanato-(4-(hydroxymethylpyridine)-cadmium) [41]
Tetrakis(μ_2 -Acetato-O, O')-bis(4-pyridylmethanol-N)-di-copper(II) [42]
Aqua-bis(-bromobenzoato- κ O)-bis(4-pyridylmethanol- κ N)-copper(II) [43]
catena-[(μ -adipato)-bis((pyridin-4-yl)methanol)-aqua-copper] [44]

4.2. 4-methoxy-pyridine complexes

Table 4.2.: List of in the CCDC published 4-methoxy-pyridine complexes [1]

bis(acetonitrile)-tetrakis(4-methoxypyridine)-di-silver dihexafluorophosphate [45]
bis(μ_2 -iodo)-bis(4-methoxypyridine)hexamethyl-di-platinum [46]

4. Pyridines

diaqua-(chelidamato)-(4-methoxypyridine)-nickel(II) dihydrate [47]
diaqua-(chelidamato)-(4-methoxypyridine)-cobalt(II) dihydrate [47]
tetrakis(4-methoxypyridine)-dioxo-rhenium(V) hexafluorophosphate [48]
(4-Methoxypyridine)-(pyridine-2,6-dicarboxylato-N,O,O')-copper(II) [49]
bis(cyano)-(tetrakis(4-methoxypyridine))-ruthenium [50]
bis(μ_2 -cyano)-dichloro-octapyridyl-tetrakis(4-methoxypyridine)-tri-ruthenium bis(hexafluorophosphate) [50]
chloro-(p-methoxypyridine)-(2-(2-pyridyl)phenyl)-platinum(II) chloroform [51]
(benzo(h)quinolin-10-yl)-chloro-(p-methoxypyridine)-platinum(II) [51]
bis(acetato)-aqua-bis(4-methoxypyridine)-cadmium [52]
catena-(bis- μ_4 -Benzene-1,3-dicarboxylato)-bis(4-methoxypyridine)-di-zinc(II) methanol ciathrate [53]
catena-(bis μ_4 -Benzene-1,3-dicarboxylato)-bis(4-methoxypyridine)-di-zinc(II) benzene ciathrate) [53]
tricarbonyl-(4-methoxypyridine)-pyridine-2-carboxylato)-rhenium [54]
cis-1,2-Dichlorovinyl(4-methoxypyridine)-cobaloxime chloroform solvate [55]
Tetracarbonyl-(4-methoxypyridine)-(triphenylphosphine)-tungsten [56]
catena-(μ_3 -1,2-Benzoisothiazole-3-thionato-1,1-dioxide-S,S,S)-(μ_2 -1,2-benzoisothiazole-3-thionato-1,1-dioxide-S,S)-bis(4methoxypyridine)-di-silver(II) [57]
(η^2 , η^2 -Cyclo-octa-1,5-diene)-(4-methoxypyridine)-tricyclohexylphosphine-iridium hexafluorophosphate [58]
bis(4-methoxypyridine)(propane-1,3-diylbis(diphenylphosphine)-platinum bi(fluoromethanesulfonate) monohydrate [59]
bis(4-methoxypyridine)(propane-1,3-diylbis(diphenylphosphine)-palladium bis(fluoromethanesulfonate) monohydrate [59]

4. Pyridines

Chloro-(dihydrogen dimethyl glyoximato)-(4-methoxypyridine)-(dimethyl glyoximato)-cobalt diethyl ether solvate [60]

bis(4-methoxypyridine)-(2,2'.6',2''.6'',2'''-quaterpyridine)-ruthenium diperchlorate monohydrate [61]

(3,5-di-t-butylcatecholato)-(3,5-di-t-butyl-o-semiquinonanto)-bis-(4methoxypyridine)-cobalt(II) [62]

4.3. Comparison between 4-HOMepy and 4-MeOpy

4-Hydroxymethylpyridine (4-HOMP) is an alcohol. By removing the H-atom of the alcohol group, metal atoms can bind to the oxygen of the formed alkoxid group. Due to this, 4-HOMP can be used as a bridging ligand. However, this is not possible for 4-methoxypyridine (4-MOP). Hydrogen abstraction from its ether moiety is too unlikely. Thus, it can not form an additional bond, rendering 4-MOP unable to be used as a bridging ligand. With a melting point of 52-56°C and a boiling point of 107-110°C 4-HOMP is a solid at room temperature and should be stored in the fridge. 4-Methoxypyridine has the same boiling point but a melting point at 4°C and is therefore a liquid at 20°C. [63] [64]

Part II.

Experimental

5. Preparation and technical data

5.1. General overview

The chemicals used in the synthesis of the complexes were provided by Merck. No further purification was necessary. Distilled water was used as solvent for all reactions. All chemicals were handled with care and only small doses were used. For the reactions 100 mL flasks with screw caps were used. The solutions were heated in waterbaths standing on heating plates. For a slow cooling to room temperature the heating plates were shut off and the flasks were left in the waterbaths until 20°C were reached. If no crystals were obtained the screw caps were removed, so the water could slowly evaporate. The crystals were obtained using filtration under reduced pressure.

The IR spectra of the dca complexes were compared with the IR-spectrum of sodium dicyanamide in the attachment p. 104, the other complexes (azide, cyanate and rhodanide) were compared with literature. [65]

5.2. Used devices and programs

For single crystal X-ray measurement the following devices were used: A Bruker and APEX II CCD diffractometer (MoK α radiation $\lambda = 0.71073 \text{ \AA}$) with ω -scan mode and graphite-monochromator at 100K. Data was collected and processed using APEX and SAINT [66] software packages. All data was corrected, for absorption Laue symmetry requirements were applied. [67] The SHELXTL/PC program package [68] was applied for structure solution (direct methods) and structure refinement (least squares). PLATON [69] (a program for automated calculation of derived geometrical data) was used

5. Preparation and technical data

for supporting the structure solution process. Additionally a Bruker-AXS SMART APEX CCD diffractometer at 100K with Mo-radiation ($\lambda = 0.7107 \text{ \AA}$) and graphite monochromator was used. Data was collected by Assoc.Prof. Dipl.-Ing. Dr.techn. Roland Fischer and structure refinement was done by Ao. Univ.-Prof. Dr. Franz A. Mautner.

For IR-analysis an Alpha-P spectrometer by Bruker was provided. It was used to characterize specific bands from pyridines and pseudohalides. The spectra were measured in the range of 400 cm^{-1} to 4000 cm^{-1} with the program Opus. [70]

The UV-VIS-measurements were conducted using a Lambda 950 UV / VIS/ NIR spectrometer by Perkin Elmer. Measurement of the spectra ranged from 200 to 2500 nm. The program for processing and data collection was UVWINLab software. [71]

6. 4-methoxy-pyridine complexes

6.1. $[\text{Co}(\text{N}_3)_2(4\text{-methoxypyridine})_4]$

6.1.1. Synthesis

0.28 g $\text{CoSO}_4 \cdot 7\text{H}_2\text{O}$ (1 mmol), 0.13 g sodium azide (2 mmol) and 0.44 g 4-methoxy-pyridine (4 mmol) were dissolved in 20 mL distilled water. The solution was warmed up to 60°C and stirred for 2 hours and 30 minutes. The clear pink solution was stirred again after filtration for 1 hour at the same temperature and then cooled down to 20°C. Pink crystals were obtained after one day.

Anal. Calculated for $\text{C}_{24}\text{H}_{28}\text{CoN}_{10}\text{O}_4$ (579.49 g/mol) : 49.74% C; 4.87% H; 24.17% N;

Found: 49.45 % C; 4.84% H; 24.32 % N;

IR (ATR, cm^{-1}): 2037 (m), 1603 (s), 1564 (m), 1508(m), 1495 (m), 1454 (m), 1430 (m), 1291 (s), 1207 (s), 1057 (w), 1020 (s), 805 (s), 642 (w), 539 (s), 457 (w)

6. 4-methoxy-pyridine complexes

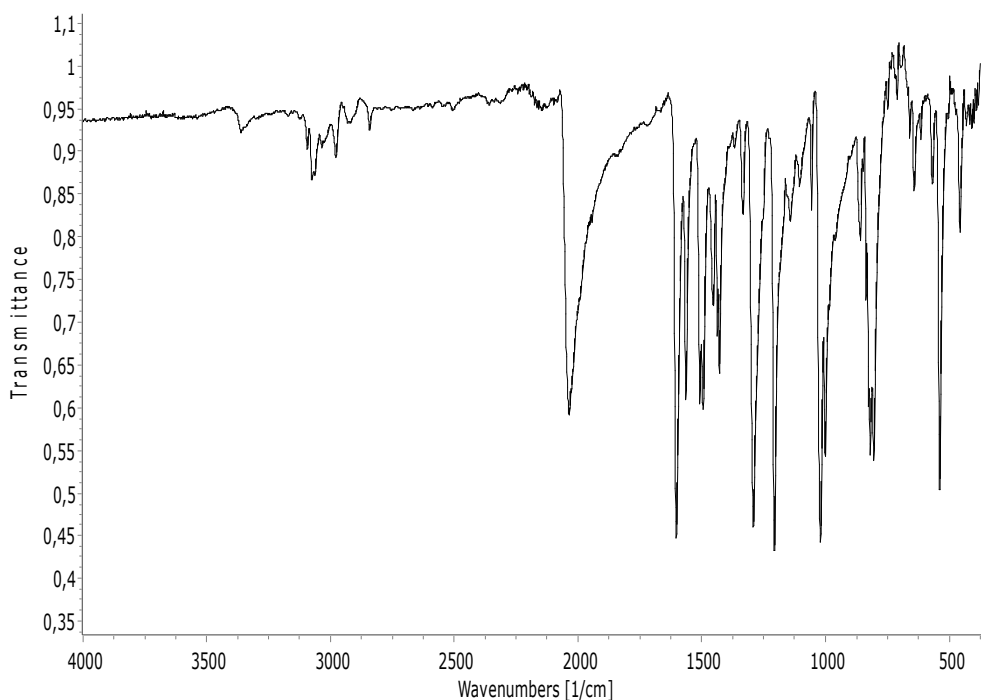


Figure 6.1.: IR spectrum of $[\text{Co}(\text{N}_3)_2(4\text{-MeOpy})_4]$

6.1.2. Structural characterization

Fig. 6.2 and fig. 6.3 show a perspective view and a packing view of $[\text{Co}(\text{N}_3)_2(4\text{-MeOpy})_4]$. Selected bond parameters are summarized in table 6.1. The complex consists of two crystallographically independent mononuclear and neutral Co(II) complexes. Each Co(II) is six-coordinated by N atoms of two terminal azido groups, as well as N-donor atoms of four neutral 4-methoxy-pyridine molecules. The CoN_6 chromophores may be described as slightly distorted octahedra with trans-arrangement of the azido ligands. The Co-N bond lengths are in the range of 2.085(3) to 2.202(3) Å, and the transoid N-Co-N bond angles within the CoN_6 octahedra vary from 171.61(11) to 177.35(12)°. The bond parameters of the terminal azido groups are: Co-N-N: from 125.6(2) to 129.1(3)°, N-N-N: from 178.3(4) to 179.3(4)°, N(x₁)-N(x₂): from 1.192(4) to 1.199(4) Å, N(x₂)-N(x₃): from 1.165(5) to 1.175(4) Å. The shortest metal-metal separation is 8.2523(8) Å.

6. 4-methoxy-pyridine complexes

Table 6.1.: Selected bond lengths (\AA) and angles ($^\circ$) for $[\text{Co}(\text{N}_3)_2(4\text{-MeOpy})_4]$

Co(1)-N(11)	$2.103(3)$	Co(2)-N(31)	$2.116(3)$
Co(1)-N(21)	$2.125(3)$	Co(2)-N(41)	$2.085(3)$
Co(1)-N(1)	$2.170(3)$	Co(2)-N(5)	$2.173(3)$
Co(1)-N(2)	$2.184(3)$	Co(2)-N(6)	$2.181(3)$
Co(1)-N(3)	$2.189(3)$	Co(2)-N(7)	$2.202(3)$
Co(1)-N(4)	$2.161(3)$	Co(2)-N(8)	$2.188(3)$
N(11)-N(12)	$1.196(4)$	N(12)-N(13)	$1.167(4)$
N(21)-N(22)	$1.194(4)$	N(22)-N(23)	$1.175(4)$
N(31)-N(32)	$1.192(4)$	N(32)-N(33)	$1.167(5)$
N(41)-N(42)	$1.199(4)$	N(42)-N(43)	$1.165(5)$
N(11)-Co(1)-N(21)	$176.97(12)$	N(31)-Co(2)-N(41)	$177.35(12)$
N(1)-Co(1)-N(3)	$175.60(11)$	N(5)-Co(2)-N(8)	$171.61(11)$
N(2)-Co(1)-N(4)	$174.15(11)$	N(6)-Co(2)-N(7)	$175.88(11)$
Co(1)-N(11)-N(12)	$125.6(2)$	N(11)-N(12)-N(13)	$178.7(4)$
Co(1)-N(21)-N(22)	$128.2(2)$	N(21)-N(22)-N(23)	$178.3(4)$
Co(2)-N(3)-N(32)	$129.1(3)$	N(31)-N(32)-N(33)	$179.3(4)$
Co(2)-N(41)-N(42)	$126.0(3)$	N(41)-N(42)-N(43)	$178.6(4)$

6. 4-methoxy-pyridine complexes

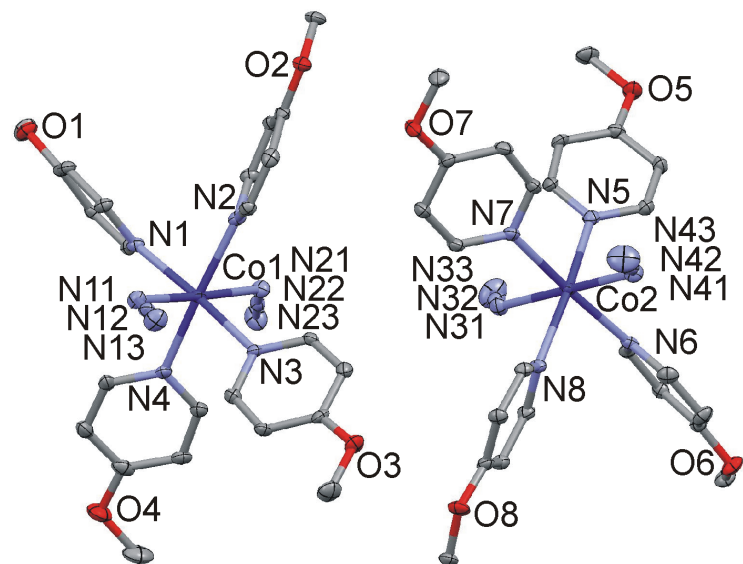


Figure 6.2.: Perspective view of $[\text{Co}(\text{N}_3)_2(4\text{-MeOpy})_4]$ with the atom numbering scheme.

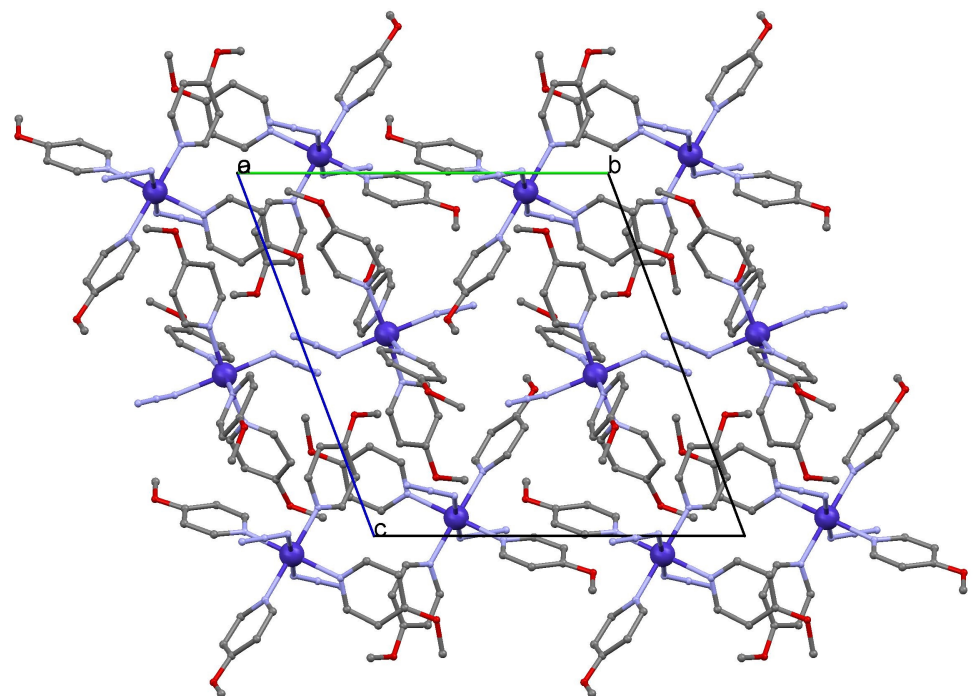


Figure 6.3.: Packing view of $[\text{Co}(\text{N}_3)_2(4\text{-MeOpy})_4]$.

6. 4-methoxy-pyridine complexes

Table 6.2.: Crystallographic data and processing parameter of $[\text{Co}(\text{N}_3)_2(4\text{-MeOpy})_4]$

Empirical formula	$\text{C}_{24}\text{H}_{28}\text{CoN}_{10}\text{O}_4$
Formula mass	579.49
System	triclinic
Space group	P-1
a (Å)	12.7449(5)
b (Å)	14.6263(6)
c (Å)	16.4750(6)
α (°)	70.309(2)
β (°)	68.118(2)
γ (°)	88.507(2)
V (Å ³)	2665.58(19)
Z	4
T (K)	100(2)
μ (mm ⁻¹)	0.695
D _{calc} (Mg/m ³)	1.444
Crystal size (mm)	0.23 x 0.17 x 0.10
θ max (°)	28.05
Data collected	12857
Unique refl. / R _{int}	12857 / —
Parameters	712
Goodness-of-Fit on F ²	1.058
R1 / wR2 (all data)	0.0608 / 0.1495
Residual extrema (e/Å ³)	0.75 / -1.27

6. 4-methoxy-pyridine complexes

6.2. $[\text{Cu}(\text{N}_3)_2(4\text{-methoxypyridine})_2]_n$

6.2.1. Synthesis

0.48 g $\text{Cu}(\text{NO}_3)_2 \cdot 3\text{H}_2\text{O}$ (2 mmol), 0.26 g Na-azide (4 mmol) and 0.44 g 4-methoxy-pyridine (4 mmol) were dissolved in 50 mL distilled H_2O . The solution was stirred for 2 hours at 50°C followed by a filtration of the resulting green solution. The mixture was stirred again for 55 minutes at the same temperature and then cooled down to room temperature. After 24 hours green needle-shaped crystals were obtained. Anal. Calculated for $\text{C}_{12}\text{H}_{14}\text{CuN}_8\text{O}_2$ (365.86 g/mol) : 39.40% C; 3.86% H; 30.63% N; Found: 39.13 % C; 3.87% H; 30.52 % N; IR (ATR, cm^{-1}): 2093 (s), 1616 (s), 1569 (m), 1512 (s), 1434 (m), 1301 (s), 1210 (s), 1062 (m), 1033 (s), 1009 (s), 822 (s), 660 (w), 602 (w), 576 (w), 533 (vs), 469 (m)

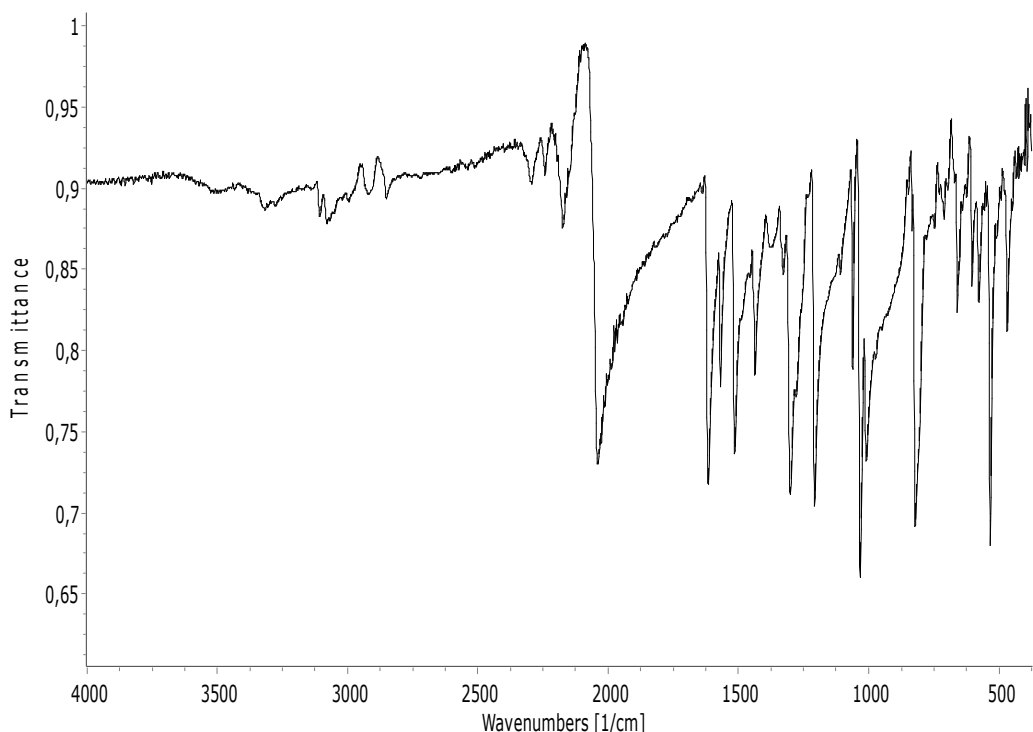


Figure 6.4.: IR spectrum of $[\text{Cu}(\text{N}_3)_2(4\text{-MeOpy})_2]_n$

6. 4-methoxy-pyridine complexes

6.2.2. Structural characterization

A perspective view of $[\text{Cu}(\text{N}_3)_2(4\text{-MeOpy})_2]_n$ is given in fig. 6.5, a packing view in fig. 6.6 and selected bond parameters are summarized in table 7.5. The Cu(1) metal center is located on an inversion center. It is coordinated via the pyridine N donor atom of two 4-MOP molecules in trans configuration and four N(11) atoms of azide groups. The latter act as bis-EO bridging ligands to generate polymeric chains of polyhedra along the a-axis of the triclinic unit cell. The CuN_6 chromophore may be described as axially elongated square bipyramid with longer Cu(1)-N(11b) bond distance of 2.736(4) Å, and shorter bond distances of 2.022(4) and 2.009(3) Å, for Cu(1)-N(11) and Cu(1)-N(1), respectively. The following bond angles are observed for the bis-EO azide bridging system: N(11)-Cu(1)-N(11c) = 79.56(14), Cu(1)-N(11)-Cu(1c) = 100.4(2), Cu(1)-N(11)-N(12) = 121.3(3) and N(11)-N(12)-N(13) = 178.0(4)°. The intra-chain Cu-Cu distance is 3.6846(14) and the shortest inter-chain metal-metal separation is 7.369(3) Å.

Table 6.3.: Selected bond lengths (Å) and angles (°) for $[\text{Cu}(\text{N}_3)_2(4\text{-MeOpy})_2]_n$

Cu(1)-N(1a)	2.009(3)	Cu(1)-N(11b)	2.736(4)
Cu(1)-N(11a)	2.022(4)	N(11)-N(12)	1.197(5)
N(12)-N(13)	1.162(5)		
N(1a)-Cu(1)-N(11a)	91.46(14)	N(11)-Cu(1)-N(11c)	79.56(4)
N(1)-Cu(1)-N(1a)	180.0	N(11)-Cu(1)-N(11a)	180.0
N(11b)-Cu(1)-N(11c)	180.0	N(11)-Cu(1)-N(11b)	100.44(14)
Cu(1)-N(11)-N(12)	121.3(3)	N(11)-N(12)-N(13)	178.0(4)

6. 4-methoxy-pyridine complexes

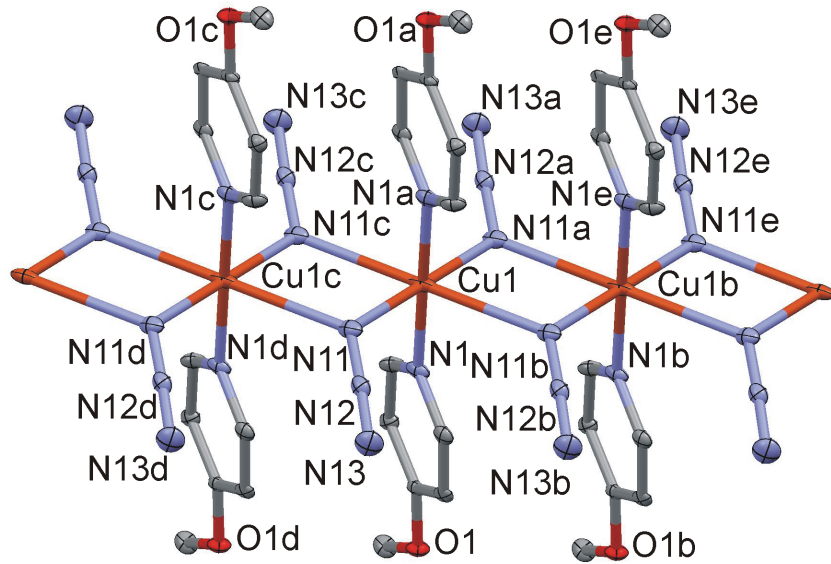


Figure 6.5.: Perspective view of a section of the polymeric chain of $[\text{Cu}(\text{N}_3)_2(4\text{-MeOpy})_2]_n$ with the atom numbering scheme. Symmetry code:(a) $1-x, 1-y, 1-z$; (b) $-1+x, y, z$; (c) $2-x, 1-y, 1-z$; (d) $1+x, y, z$; (e) $-x, 1-y, 1-z$.

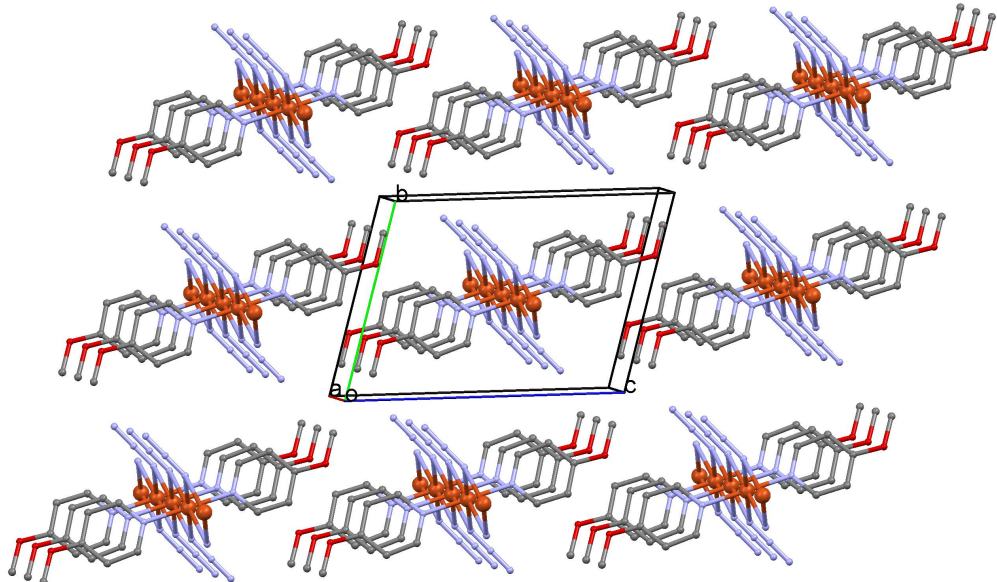


Figure 6.6.: Packing plot of $[\text{Cu}(\text{N}_3)_2(4\text{-MeOpy})_2]_n$.

6. 4-methoxy-pyridine complexes

Table 6.4.: Crystallographic data and processing parameter of $[\text{Cu}(\text{N}_3)_2(4\text{-MeOpy})_2]_n$

Empirical formula	$\text{C}_{12}\text{H}_{14}\text{CuN}_8\text{O}_2$
Formula mass	365.86
System	triclinic
Space group	P-1
a (Å)	3.6846(11)
b (Å)	8.755(3)
c (Å)	12.244(4)
α (°)	73.020(14)
β (°)	85.062(16)
γ (°)	83.034(16)
V (Å ³)	374.4(2)
Z	1
T (K)	100(2)
μ (mm ⁻¹)	1.482
D _{calc} (Mg/m ³)	1.623
Crystal size (mm)	0.32 x 0.15 x 0.09
θ max (°)	26.98
Data collected	10906
Unique refl./ R _{int}	1602 / 0.1163
Parameters	107
Goodness-of-Fit on F ²	1.149
R ₁ / wR ₂ (all data)	0.0668 / 0.1567
Residual extrema (e/Å ³)	1.39 / -1.74

6. 4-methoxy-pyridine complexes

6.3. $[\text{Zn}(\text{N}_3)_2(4\text{-methoxypyridine})_2]$

6.3.1. Synthesis

$\text{Zn}(\text{NO}_3)_2 \cdot 6\text{H}_2\text{O}$ (0.59 g, 2 mmol), NaN_3 (0.13 g, 2 mmol) and 4-methoxy-pyridine (0.22 g, 2 mmol) were added in 40 mL distilled H_2O . The solution was heated up to 80°C and stirred for 2 hours. After filtration the clear solution was stirred again for 30 minutes at the same temperature and then cooled down to RT. After 3 days needle-shaped white crystals were obtained. Anal. Calculated for $\text{C}_{12}\text{H}_{14}\text{N}_8\text{O}_2\text{Zn}$ (367.70 g/mol) : 39.20% C; 3.84% H; 30.48% N; Found: 38.96% C; 3.87% H; 30.33 % N; IR (ATR, cm^{-1}): 2094 (s), 2058 (s), 1615 (s), 1568 (s), 1513 (s), 1439 (s), 1355 (m), 1298 (s), 1210 (s), 1061 (m), 1031 (s), 819 (s), 731 (w), 659 (w), 580 (w), 535 (s), 465 (m)

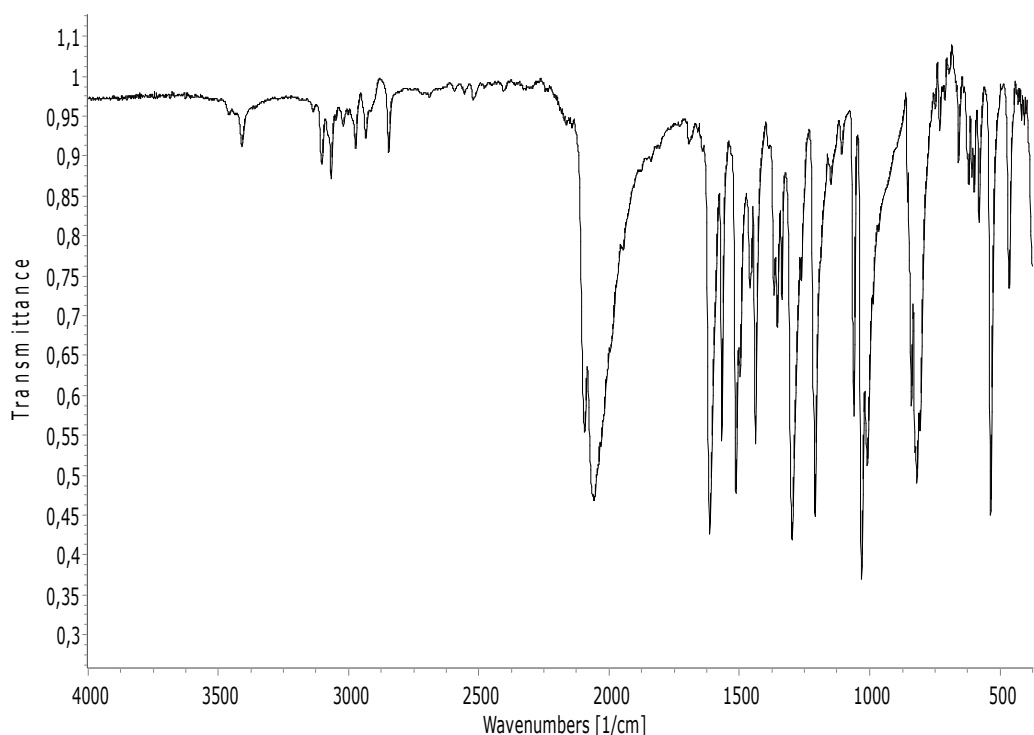


Figure 6.7.: IR spectrum of $[\text{Zn}(\text{N}_3)_2(4\text{-MeOpy})_2]$

6. 4-methoxy-pyridine complexes

6.3.2. Structural characterization

The crystal structure of $[\text{Zn}(\text{N}_3)_2(4\text{-MeOpy})_2]$ consists of mononuclear and neutral Zn(II) complexes, as depicted in figure 6.8 (perspective view) and figure 6.9 (packing view). Selected bond parameters are listed in table 6.5. Zn(1) is tetrahedrally coordinated by N(11) and N(21) of two terminal azido groups, further by N(1) and N(2) atoms of two neutral 4-methoxypyridine molecules. The Zn-N bond lengths range from 1.9330(14) to 2.0311(13) Å, and the bond angles within the ZnN_4 tetrahedron vary from 100.25(6) to 128.66(6)°. The bond parameters of the terminal azido groups are: Zn-N-N = 138.48(12) and 142.44(12)°, N-N-N = 177.17(17) and 174.52(17)°, N(x1)-N(x2) = 1.182(2) and 1.1918(19) Å, N(x2)-N(x3) = 1.156(2) and 1.148(2) Å. The shortest metal-metal separation is 5.3288(7) Å.

Table 6.5.: Selected bond lengths (Å) and angles (°) for $[\text{Zn}(\text{N}_3)_2(4\text{-MeOpy})_2]$

Zn(1)-N(11)	1.9714(14)	Zn(1)-N(1)	2.0311(13)
Zn(1)-N(21)	1.9330(14)	Zn(1)-N(2)	2.0192(13)
N(11)-N(12)	1.182(2)	N(12)-N(13)	1.156(2)
N(21)-N(22)	1.1918(19)	N(22)-N(23)	1.148(2)
N(11)-Zn(1)-N(21)	128.66(6)	N(1)-Zn(1)-N(21)	101.00(5)
N(2)-Zn(1)-N(21)	110.32(6)	N(1)-Zn(1)-N(11)	100.25(6)
N(2)-Zn(1)-N(11)	104.01(6)	N(1)-Zn(1)-N(2)	111.79(5)
Zn(1)-N(11)-N(12)	138.48(12)	N(11)-N(12)-N(13)	177.17(17)
Zn(1)-N(21)-N(22)	142.44(12)	N(21)-N(22)-N(23)	174.52(17)

6. 4-methoxy-pyridine complexes

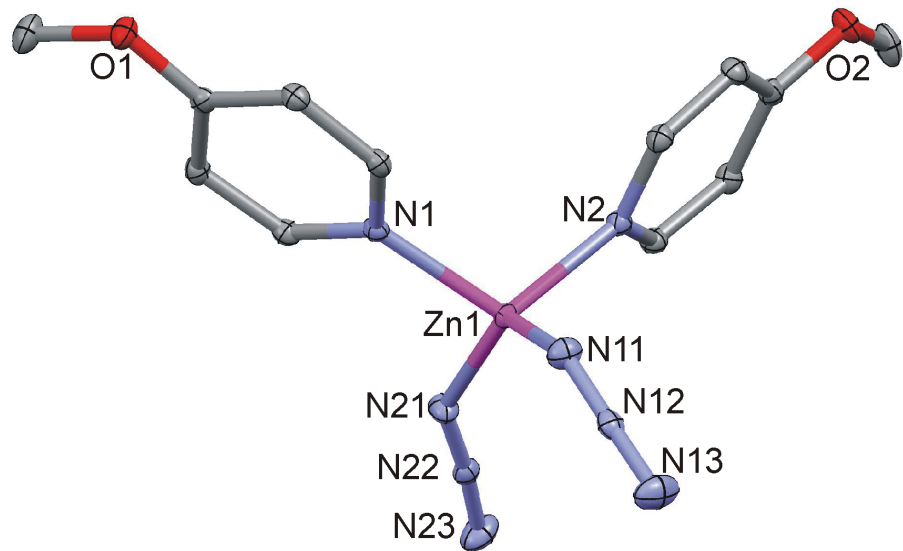


Figure 6.8.: Perspective view of $[Zn(N_3)_2(4\text{-MeOpy})_2]$ with the atom numbering scheme.
Symmetry codes: (''): $-x, y, -z+1/2$; (''): $1-x, y, -z+1/2$.

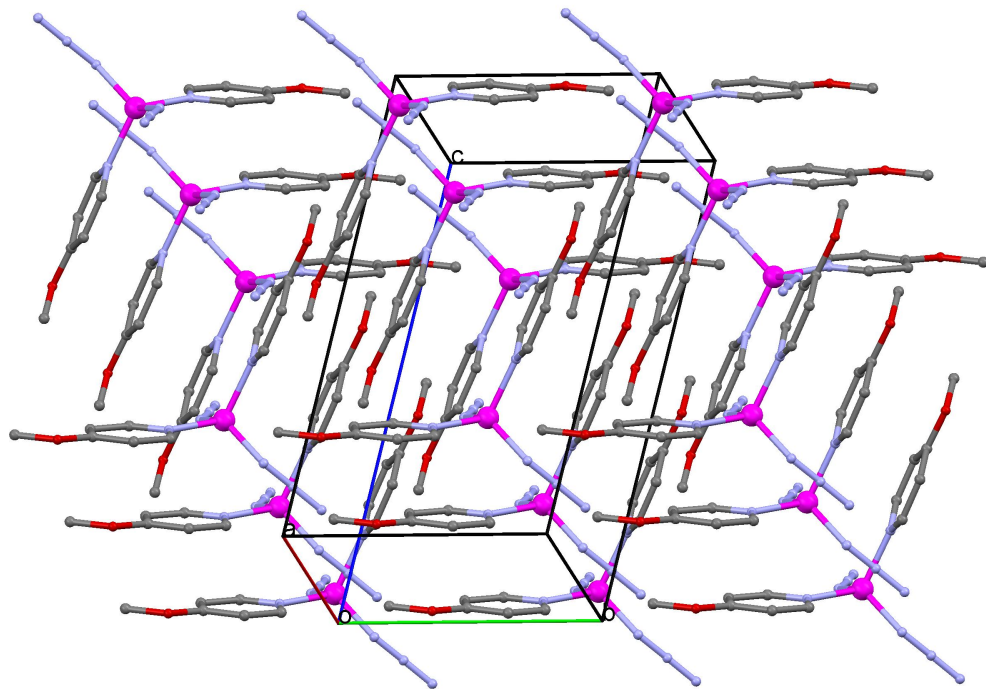


Figure 6.9.: Packing view of $[Zn(N_3)_2(4\text{-MeOpy})_2]$.

6. 4-methoxy-pyridine complexes

Table 6.6.: Crystallographic data and processing parameter of $[\text{Zn}(\text{N}_3)_2(4\text{-MeOpy})_2]$

Empirical formula	$\text{C}_{12}\text{H}_{14}\text{N}_8\text{O}_2\text{Zn}$
Formula mass	367.70
System	triclinic
Space group	P-1
a (Å)	5.3288(7)
b (Å)	9.751(1)
c (Å)	15.1580(14)
α (°)	88.877(3)
β (°)	82.068(3)
γ (°)	78.448(3)
V (Å ³)	764.26(15)
Z	2
T (K)	100(2)
μ (mm ⁻¹)	1.630
D_{calc} (Mg/m ³)	1.598
Crystal size (mm)	0.32 x 0.22 x 0.18
θ max (°)	26.35
Data collected	6131
Unique refl./ R _{int}	3069 / 0.0172
Parameters	210
Goodness-of-Fit on F ²	1.063
R1 / wR2 (all data)	0.0220 / 0.0542
Residual extrema (e/Å ³)	0.27 / -0.40

6. 4-methoxy-pyridine complexes

6.4. $[\text{Co}(\text{OCN})_2(4\text{-methoxypyridine})_4]$

6.4.1. Synthesis

0.58 g $\text{Co}(\text{NO}_3)_2 \cdot 6\text{H}_2\text{O}$ (2 mmol), 0.32 g KOCN (4 mmol) and 0.87 g 4-methoxy-pyridine (8 mmol) were dissolved in 35 mL distilled H_2O . The solution was heated up to 70°C and stirred for 1 hour and 30 minutes. After filtration the pink solution was stirred again for 45 minutes at the same temperature and then cooled to RT. After 24 hours pink needle-shaped crystals were obtained. Anal. Calculated for $\text{C}_{26}\text{H}_{28}\text{CoN}_6\text{O}_6$ (579.47 g/mol) : 53.89% C; 4.87% H; 14.50% N; Found: 53.66 % C; 4.84% H; 14.52 % N; IR (ATR, cm^{-1}): 2190 (s), 1604 (s), 1565 (m), 1497 (m), 1441 (m), 1426 (m), 1318 (w), 1288 (s), 1205 (s), 1023 (s), 1001 (m), 817 (m), 617 (s), 567 (w), 536 (s), 457 (m)

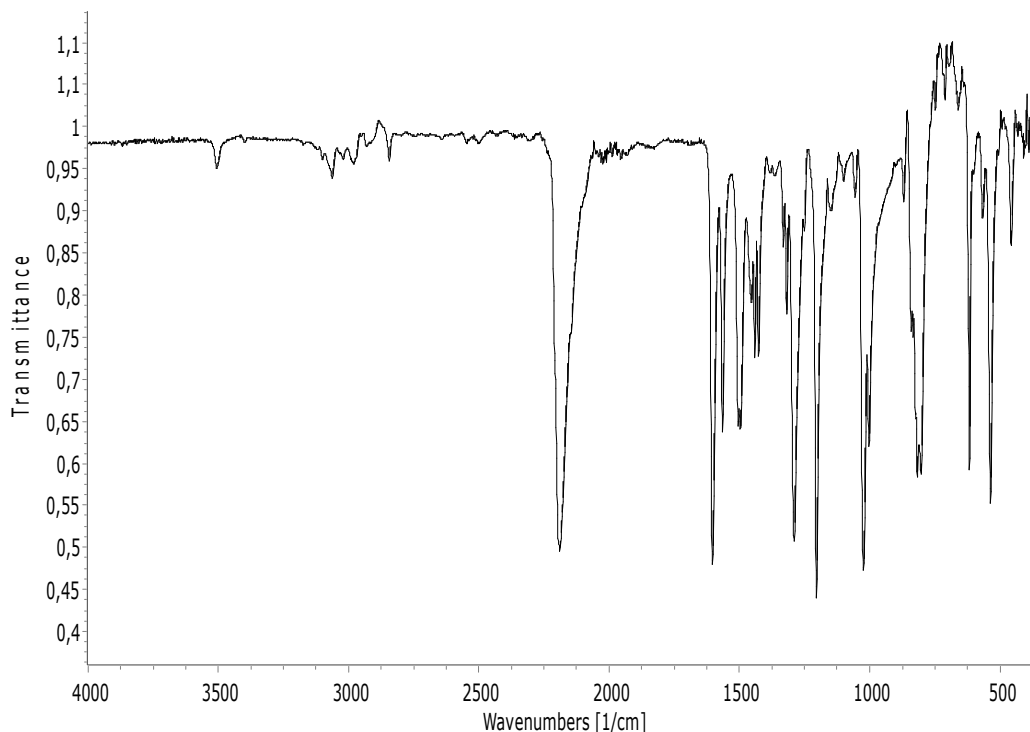


Figure 6.10.: IR spectrum of $[\text{Co}(\text{OCN})_2(4\text{-MeOpy})_4]$

6. 4-methoxy-pyridine complexes

6.4.2. Structural characterization

The crystal structure of $[\text{Co}(\text{OCN})_2(4\text{-MeOpy})_4]$ (perspective view is shown in fig. 6.11, a packing view in fig. 6.12 and selected bond parameters are summarized in table 6.7) consists of two crystallographically independent mononuclear and neutral Co(II) complexes. Each Co(II) is six-coordinated by N atoms of two terminal cyanato anions, further by N donor atoms of four neutral 4-methoxypyridine molecules. The CoN_6 chromophores may be described as slightly distorted octahedra with trans-arrangement of the cyanato ligands. The Co-N bond lengths are in the range of 2.0601(16) to 2.2185(15) Å, and the transoid N-Co-N bond angles within the CoN_6 octahedra vary from 176.19(6) to 179.04(6)°. The bond parameters of the terminal cyanato anions are: Co-N-C: from 159.34(15) to 173.73(15)°, N-C-O: from 178.5(2) to 179.5(2)°, N-C: from 1.167(2) to 1.173(2) Å, C-O: from 1.210(2) to 1.212(2) Å. The shortest metal-metal separation is 8.5608(14) Å.

6. 4-methoxy-pyridine complexes

Table 6.7.: Selected bond lengths (\AA) and angles ($^\circ$) for $[\text{Co}(\text{OCN})_2(4\text{-MeOpy})_4]$

Co(1)-N(1)	$2.0793(16)$	Co(2)-N(7)	$2.0683(16)$
Co(1)-N(2)	$2.0658(16)$	Co(2)-N(8)	$2.0601(16)$
Co(1)-N(3)	$2.1917(15)$	Co(2)-N(9)	$2.2123(15)$
Co(1)-N(4)	$2.1963(15)$	Co(2)-N(10)	$2.1829(15)$
Co(1)-N(5)	$2.2057(15)$	Co(2)-N(11)	$2.1946(16)$
Co(1)-N(6)	$2.2185(15)$	Co(2)-N(12)	$2.1748(15)$
N(1)-C(25)	$1.173(2)$	C(25)-O(1)	$1.210(2)$
N(2)-C(26)	$1.167(2)$	C(26)-O(2)	$1.210(2)$
N(7)-C(27)	$1.173(2)$	C(27)-O(7)	$1.210(2)$
N(8)-C(28)	$1.171(2)$	C(28)-O(8)	$1.212(2)$
N(1)-Co(1)-N(2)	$177.63(6)$	N(7)-Co(2)-N(8)	$179.04(6)$
N(5)-Co(1)-N(3)	$176.19(6)$	N(10)-Co(2)-N(11)	$177.55(6)$
N(6)-Co(1)-N(4)	$176.79(6)$	N(9)-Co(2)-N(12)	$176.38(6)$
Co(1)-N(1)-C(25)	$162.69(15)$	N(1)-C(25)-O(1)	$179.04(17)$
Co(1)-N(2)-C(26)	$173.73(15)$	N(2)-C(26)-O(2)	$179.5(2)$
Co(2)-N(7)-C(27)	$159.34(15)$	N(7)-C(27)-O(7)	$178.55(19)$
Co(2)-N(8)-N(28)	$161.66(15)$	N(8)-C(28)-O(8)	$178.5(2)$

6. 4-methoxy-pyridine complexes

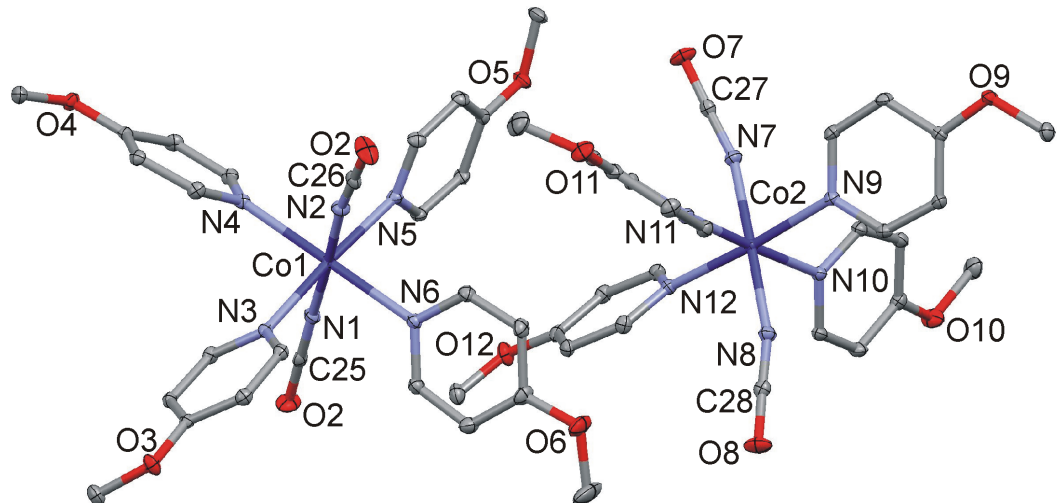


Figure 6.11.: Perspective view of $[\text{Co}(\text{OCN})_2(4\text{-MeOpy})_4]$ with the atom numbering scheme.

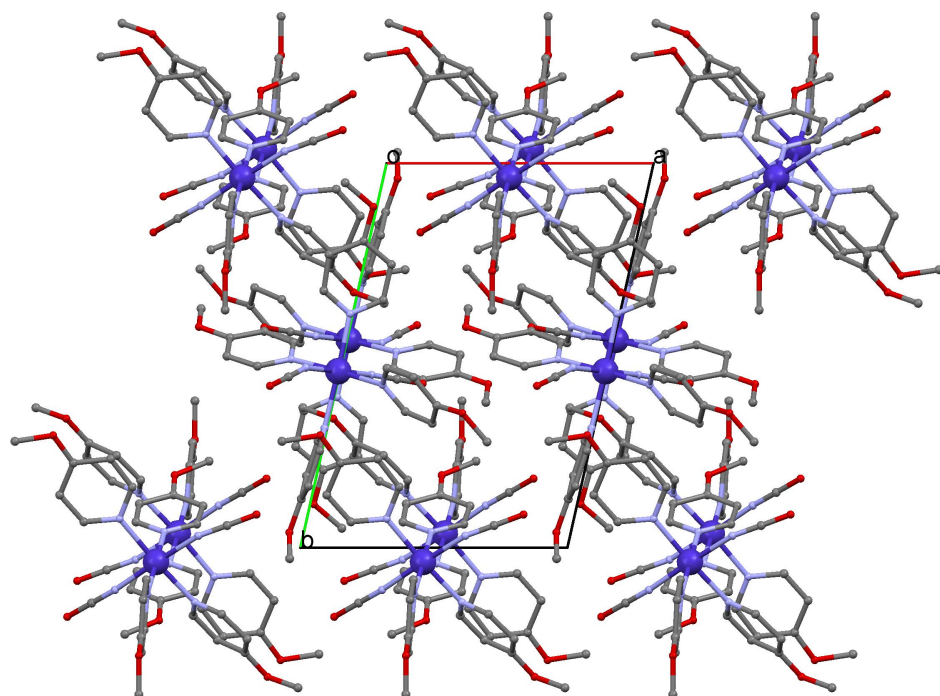


Figure 6.12.: Packing view of $[\text{Co}(\text{OCN})_2(4\text{-MeOpy})_4]$.

6. 4-methoxy-pyridine complexes

Table 6.8.: Crystallographic data and processing parameter of $[\text{Co}(\text{OCN})_2(4\text{-MeOpy})_4]$

Empirical formula	$\text{C}_{26}\text{H}_{28}\text{CoN}_6\text{O}_6$
Formula mass	579.47
System	triclinic
Space group	P-1
a (Å)	10.1989(12)
b (Å)	15.3641(18)
c (Å)	19.234(3)
α (°)	107.209(6)
β (°)	102.632(7)
γ (°)	98.012(5)
V (Å ³)	2741.1(6)
Z	4
T (K)	100(2)
μ (mm ⁻¹)	0.677
D_{calc} (Mg/m ³)	1.404
Crystal size (mm)	0.23 x 0.18 x 0.12
θ max (°)	28.00
Data collected	168102
Unique refl./ R _{int}	13238 / 0.0843
Parameters	711
Goodness-of-Fit on F ²	0.994
R1 / wR2 (all data)	0.0374 / 0.0808
Residual extrema (e/Å ³)	0.35 / -1.49

6. 4-methoxy-pyridine complexes

6.5. $[\text{Cd}(\text{dca})_2(4\text{-methoxypyridine})_2]_n$

6.5.1. Synthesis

0.52 g $\text{CdSO}_4 \cdot \frac{8}{3} \text{H}_2\text{O}$ (2 mmol), 0.36 g Na-dca (4 mmol) and 0.44 g 4-methoxypyridine (4 mmol) were dissolved in 40 mL distill. H_2O . The mixture was stirred for 140 minutes (at 70°C). After the removal of solid compounds, the colourless solution was stirred at the same temperature for 20 minutes. Thereafter the solution was allowed to cool down to RT. After one day white crystals were obtained. Anal. Calculated for $\text{C}_{16}\text{H}_{14}\text{CdN}_8\text{O}_2$ (462.76 g/mol) : 41.53% C; 3.05% H; 24.21% N; Found: 41.55 % C; 3.11% H; 24.25 % N; IR (ATR, cm^{-1}): 2295 (m), 2227 (m), 2171 (s), 1607 (s), 1566 (m), 1434 (s), 1348 (s), 1302 (s), 1206 (s), 1027 (vs), 933 (w), 813 (s), 711 (w), 675 (m), 569 (w), 521 (s), 461 (m)

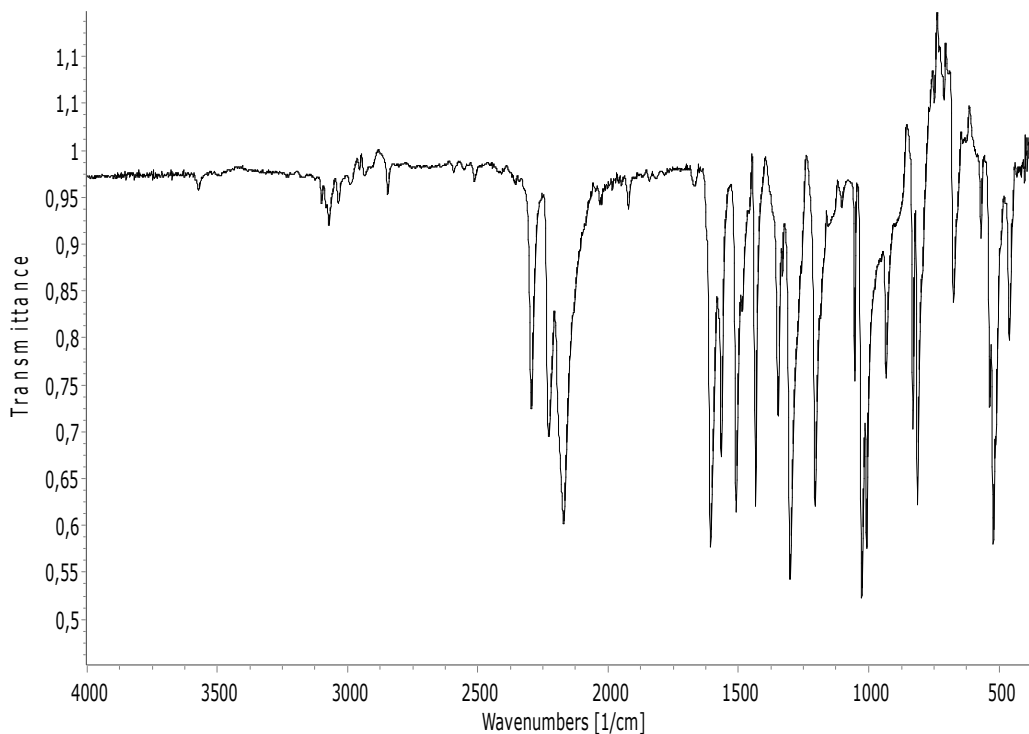


Figure 6.13.: IR spectrum of $[\text{Cd}(\text{dca})_2(4\text{-MeOpy})_2]_n$

6. 4-methoxy-pyridine complexes

6.5.2. Structural characterization

Selected bond parameters of $[Cd(dca)_2(4\text{-MeOpy})_2]_n$ are summarized in table 6.9. A perspective view of a section of the polymeric chain is given in fig. 6.14 and a packing view in fig. 6.15. The Co(1) center (located on an inversion center) is coordinated by a pyridine N donor atom for each of two 4-methoxypyridine molecules in trans configuration. Four N atoms of dicyanamide anions act in the bis- $\mu(1,5)$ -bridging mode to generate polymeric chains of polyhedra. These atoms are oriented along the b-axis of the triclinic unit cell. The CdN_6 polyhedron forms an almost regular octahedron, with Cd-N bond distances varying from 2.302(3) to 2.344(4) Å, and maximum deviation 3.34° of the N-Cd-N bond angles from 90 or 180°. The dicyanamide bridges have the following bond parameters: Cd-N-C: 161.7(4) and 155.7(4)°; N-C-N: 174.1(5) and 176.0(5)°; C-N-C: 118.9(3)°; C-N(nitril) 1.150(6) and 1.159(6) Å; C-N(amide): 1.313(6) and 1.313(6) Å. The intra-chain Cd · · · Cd distance of 7.5491(9) Å is longer than the shortest inter-chain metal · · · metal separation of 7.1028(8) Å.

Table 6.9.: Selected bond lengths (Å) and angles (°) for $[Cd(dca)_2(4\text{-MeOpy})_2]_n$; Symmetry codes: (a) 2-x, 2-y, -z; (b) 2-x, 1-y, -z; (c) x, 1+y, z; (d) x, -1+y, z; (e) 2-x, 3-y, -z; (f) 2-x, -y, -z.

$Cd(1)\text{-}N(1a)$	2.302(3)	$Cd(1)\text{-}N(4b)$	2.344(4)
$Cd(1)\text{-}N(2a)$	2.342(4)	$N(3)\text{-}C(7)$	1.313(6)
$N(2)\text{-}C(7)$	1.150(6)	$N(3)\text{-}C(8)$	1.313(6)
$N(4)\text{-}C(8)$	1.159(6)		
$N(1)\text{-}Cd(1)\text{-}N(2a)$	91.32(13)	$N(1)\text{-}Cd(1)\text{-}N(4b)$	90.58(13)
$N(4c)\text{-}Cd(1)\text{-}N(2a)$	93.34(11)	$N(2)\text{-}Cd(1)\text{-}N(2a)$	180.0
$Cd(1)\text{-}N(2)\text{-}C(7)$	161.7(4)	$N(2)\text{-}C(7)\text{-}N(3)$	174.1(5)
$Cd(1b)\text{-}N(4)\text{-}C(8)$	155.7(4)	$N(4)\text{-}C(8)\text{-}N(3)$	176.0(5)
$C(7)\text{-}N(3)\text{-}C(8)$	118.9(3)		

6. 4-methoxy-pyridine complexes

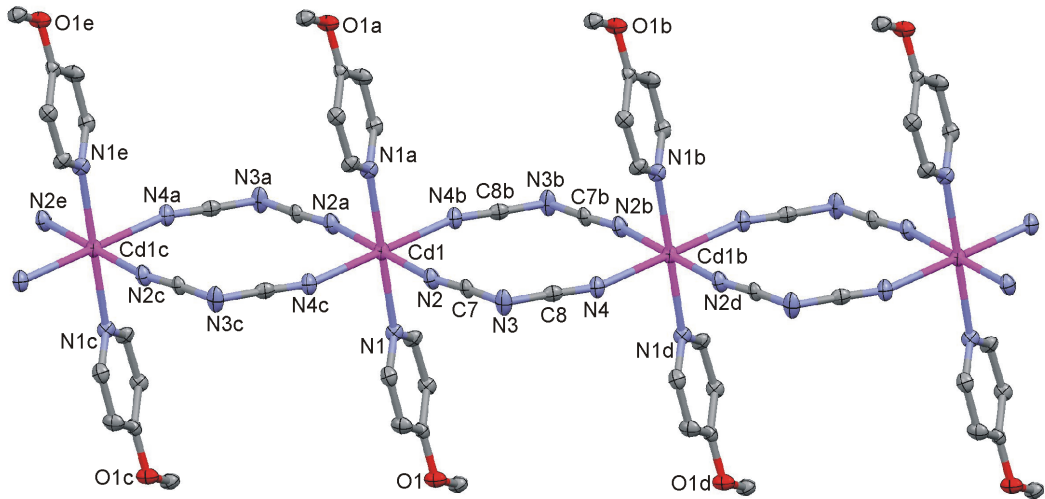


Figure 6.14.: Perspective view of a section of the polymeric chain of $[\text{Cd}(\text{dca})_2(4\text{-MeOpy})_2]_n$ together with the atom numbering scheme. Symmetry codes: (a) $2-x, 2-y, -z$; (b) $2-x, 1-y, -z$; (c) $x, 1+y, z$; (d) $x, -1+y, z$; (e) $2-x, 3-y, -z$; (f) $2-x, -y, -z$.

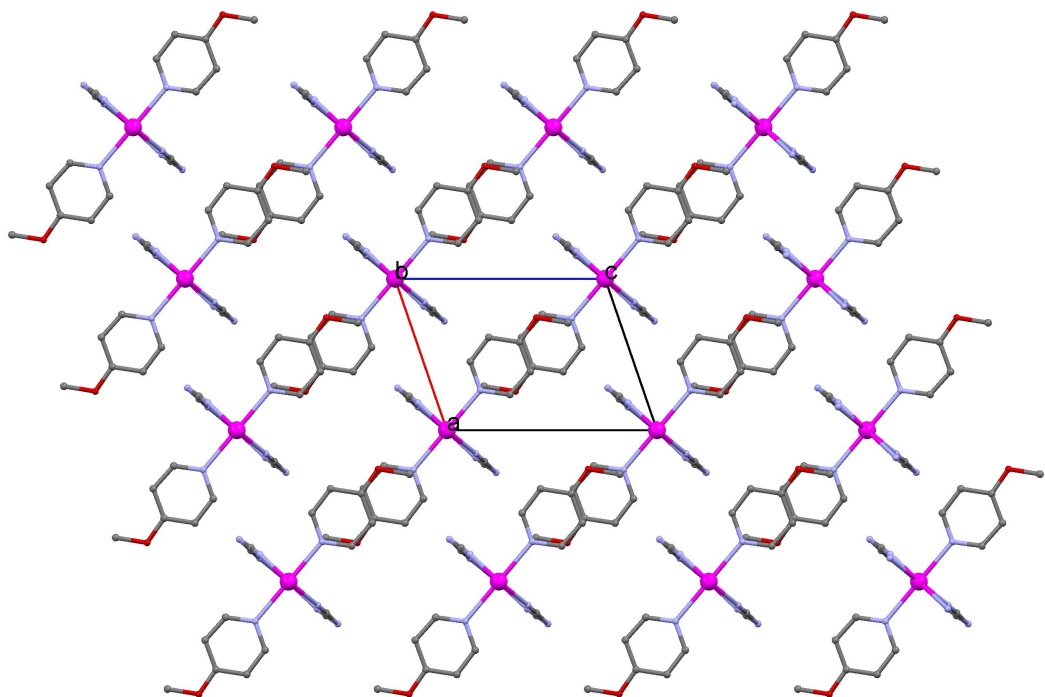


Figure 6.15.: Packing plot of $[\text{Cd}(\text{dca})_2(4\text{-MeOpy})_2]_n$.

6. 4-methoxy-pyridine complexes

Table 6.10.: Crystallographic data and processing parameter of $[Cd(dca)_2(4\text{-MeOpy})_2]_n$

Empirical formula	$C_{16}H_{14}CdN_8O_2$
Formula mass	462.76
System	triclinic
Space group	P-1
a (Å)	7.1028(8)
b (Å)	7.5491(8)
c (Å)	9.8206(11)
α (°)	71.234(5)
β (°)	70.587(5)
γ (°)	85.267(5)
V (Å ³)	470.06(9)
Z	1
T (K)	100(2)
μ (mm ⁻¹)	1.190
D _{calc} (Mg/m ³)	1.635
Crystal size (mm)	0.22 x 0.14 x 0.09
θ max (°)	27.00
Data collected	2003
Unique refl./ R _{int}	2003 / —
Parameters	126
Goodness-of-Fit on F ²	1.040
R1 / wR2 (all data)	0.0383 / 0.0836
Residual extrema (e/Å ³)	0.95 / -1.05

6. 4-methoxy-pyridine complexes

6.6. $[\text{Cu}(\text{dca})_2(4\text{-methoxypyridine})_2]_n$

6.6.1. Synthesis

2 mmol $\text{Cu}(\text{NO}_3)_2 \cdot 3 \text{H}_2\text{O}$ (0.48 g), 4 mmol Na-dicyanamide (0.36 g) and 4 mmol 4-methoxy-pyridine (0.44 g) were dissolved in 45 mL distilled H_2O . After stirring for 1 hour at 70°C , the mixture was filtered. Then the blue solution was placed in the drying oven (70°C) overnight and cooled down to RT on the next day. A few hours later plate-like blue crystals were obtained. Anal. Calculated for $\text{C}_{16}\text{H}_{14}\text{CuN}_8\text{O}_2$ (413.90 g/mol) : 46.43% C; 3.41% H; 27.07% N; Found: 46.45 % C; 3.44% H; 27.03 % N; IR (ATR, cm^{-1}): 2292 (s), 2235 (s), 2169 (s), 1614 (s), 1566 (m), 1510 (m), 1437 (m), 1348 (m), 1303 (s), 1202 (m), 1031 (s), 928 (w), 817 (s), 731 (w), 670 (m), 517 (s)

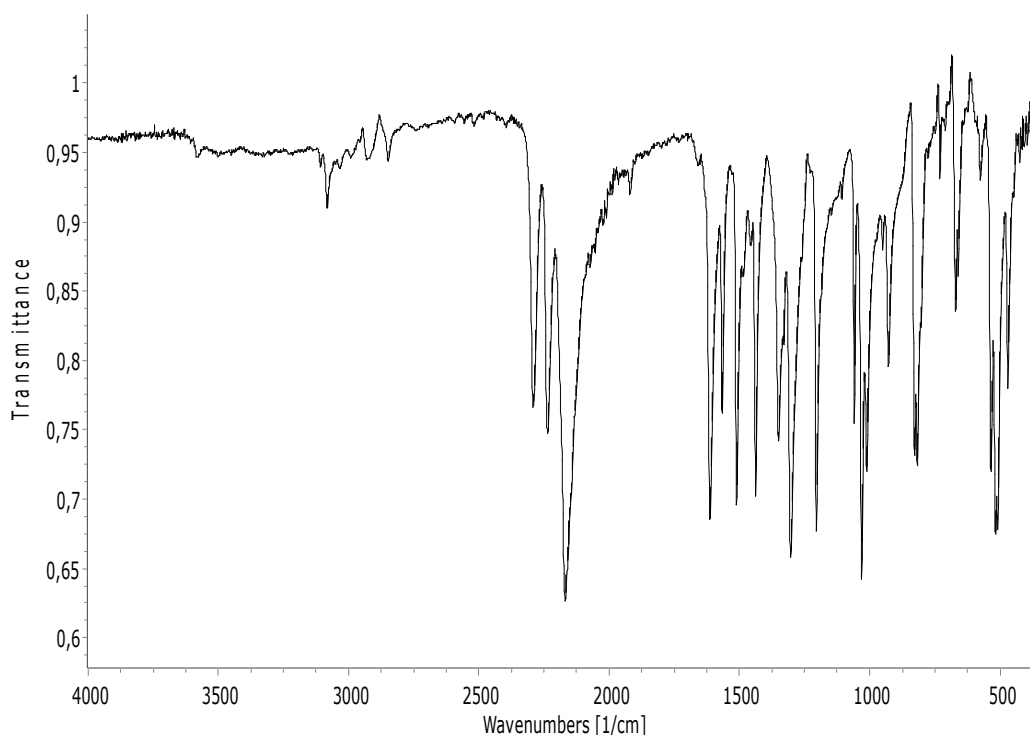


Figure 6.16.: IR spectrum of $[\text{Cu}(\text{dca})_2(4\text{-MeOpy})_2]_n$

6. 4-methoxy-pyridine complexes

6.6.2. Structural characterization

A section of the polymeric chain of $[\text{Cu}(\text{dca})_2(4\text{-MeOpy})_2]_n$ is depicted in a perspective and a packing view in fig. 6.17 and fig. 6.18. Table 6.11 shows the bond parameters which have been selected. Two 4-methoxypyridine molecules bind to Cu(1), which is placed on an inversion center. This central metal atom is also connected via the N atoms of four dicyanamide anions. The latter are acting as bis- $\mu(1,5)$ -bridging ligands, generating a chain of polyhedra along the b axis of the triclinic unit cell. The CuN_6 chromophore has an elongated square bipyramidal geometry, with short Cu(1)-N(1) and Cu(1)-N(2) bond distances of 2.0219(9) and 2.0038(10) Å, respectively, and semi-coordinative Cu(1)-N(4b,c) bond distances of 2.4556(10) Å. The asymmetric dicyanamide bridges have the following bond parameters: Cu-N-C: 169.61(9) and 148.10(9)°; N-C-N: 174.47(12) and 175.12(12)°; C-N-C: 119.26(10)°; C-N(nitril) 1.1555(15) and 1.1562(15) Å; C-N(amide): 1.3158(15) and 1.3019(15) Å. The intra-chain Cu · · · Cu distance of 7.3799(4) Å is longer than the shortest inter-chain metal · · · metal separation of 7.0318(4) Å.

Table 6.11.: Selected bond lengths (Å) and angles (°) for $[\text{Cu}(\text{dca})_2(4\text{-MeOpy})_2]_n$; Symmetry codes: (a) -x, -y, 2-z; (b) -x, 1-y, 2-z; (c) x, -1+y, z; (d) x, 1+y, z; (e) -x, -1-y, 2-z; (f) -x, 2-y, 2-z.

Cu(1)-N(1a)	2.0219(9)	Cu(1)-N(4b)	2.4556(10)
Cu(1)-N(2a)	2.0038(10)	N(3)-C(7)	1.3158(15)
N(2)-C(7)	1.1555(15)	N(3)-C(8)	1.3019(15)
N(4)-C(8)	1.1562(15)		
N(2)-Cu(1)-N(1a)	90.33(4)	N(1)-Cu(1)-N(4b)	90.31(4)
N(4c)-Cu(1)-N(2a)	92.10(4)	N(2)-Cu(1)-N(2a)	180.0
Cu(1)-N(2)-C(7)	169.61(9)	N(2)-C(7)-N(3)	174.47(12)
Cu(1b)-N(4)-C(8)	148.10(9)	N(4)-C(8)-N(3)	175.12(12)
C(7)-N(3)-C(8)	119.26(10)		

6. 4-methoxy-pyridine complexes

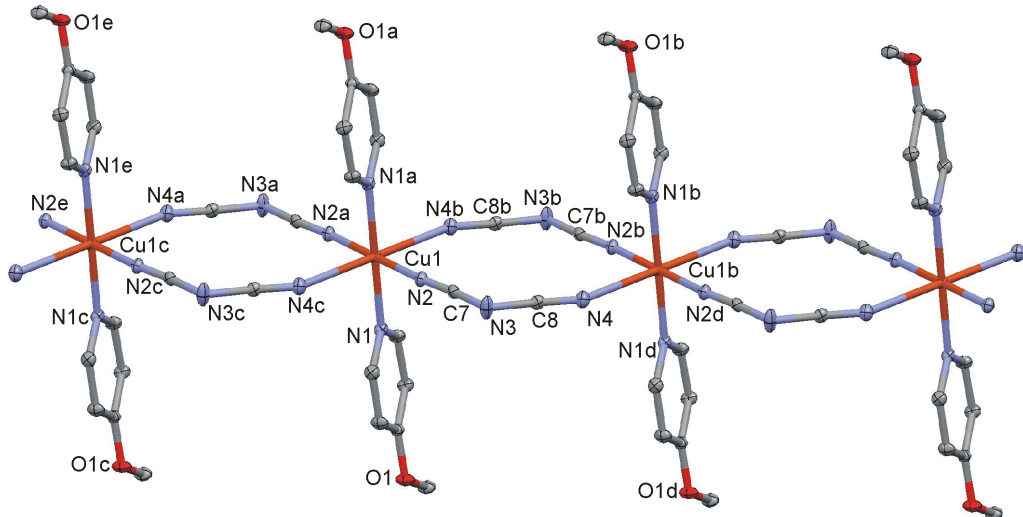


Figure 6.17.: Perspective view of a section of the polymeric chain of $[\text{Cu}(\text{dca})_2(4\text{-MeOpy})_2]_n$ together with the atom numbering scheme. Symmetry codes: (a) $-x, -y, 2-z$; (b) $-x, 1-y, 2-z$; (c) $x, -1+y, z$; (d) $x, 1+y, z$; (e) $-x, -1-y, 2-z$; (f) $-x, 2-y, 2-z$.

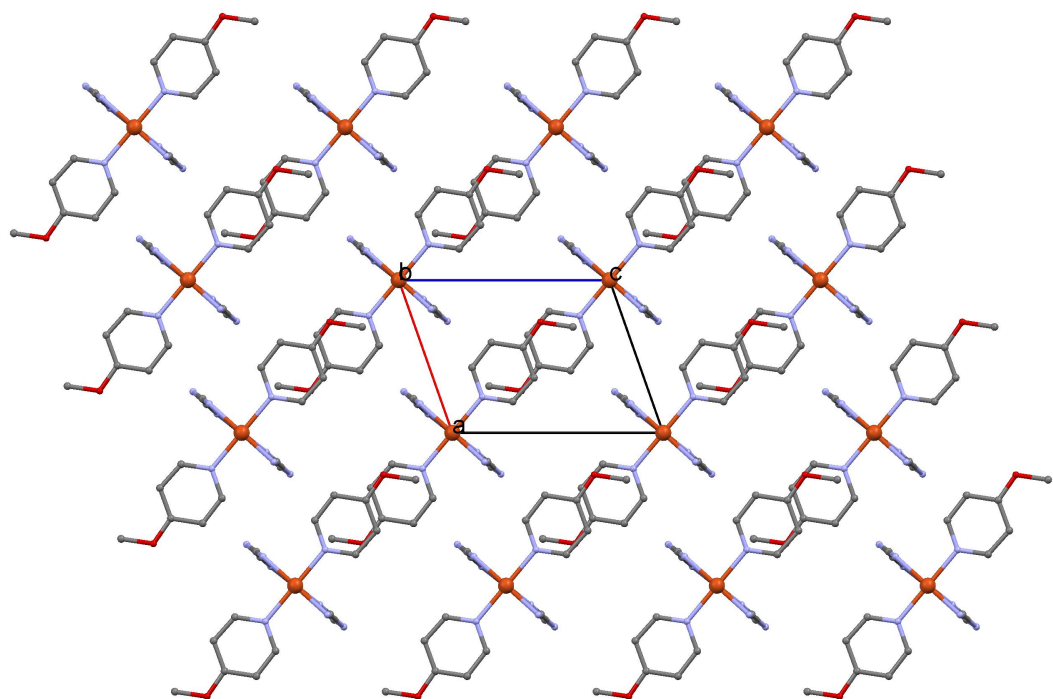


Figure 6.18.: Packing plot of $[\text{Cu}(\text{dca})_2(4\text{-MeOpy})_2]_n$.

6. 4-methoxy-pyridine complexes

Table 6.12.: Crystallographic data and processing parameter of $[\text{Cu}(\text{dca})_2(4\text{-MeOpy})_2]\text{n}$

Empirical formula	$\text{C}_{16}\text{H}_{14}\text{CuN}_8\text{O}_2$
Formula mass	413.90
System	triclinic
Space group	P-1
a (Å)	7.0318(3)
b (Å)	7.3799(3)
c (Å)	9.7467(5)
α (°)	69.519(2)
β (°)	70.257(2)
γ (°)	85.367(2)
V (Å ³)	445.57(4)
Z	1
T (K)	100(2)
μ (mm ⁻¹)	1.256
D_{calc} (Mg/m ³)	1.543
Crystal size (mm)	0.25 x 0.15 x 0.10
θ max (°)	29.63
Data collected	24435
Unique refl./ R _{int}	2514 / 0.0361
Parameters	125
Goodness-of-Fit on F ²	1.121
R1 / wR2 (all data)	0.0203 / 0.0578
Residual extrema (e/Å ³)	0.42 / -0.43

6. 4-methoxy-pyridine complexes

6.7. $[\text{Zn}(\text{dca})_2(4\text{-methoxypyridine})_2]_n$

6.7.1. Synthesis

20 mL distilled H₂O were used as a solvent for 0.30 g Zn(NO₃)₂ · 6 H₂O (1 mmol), 0.18 g Na-dicyanamide (2 mmol) and 0.22 g 4-methoxypyridine (2 mmol). The solution was heated up to 80°C and stirred for 1 hour. After filtration, the clear solution was put in the drying oven at 80°C overnight and then slowly cooled down to 20° in a waterbath. A few hours later white crystals were obtained. Anal. Calculated for C₁₆H₁₄N₈O₂Zn (415.74 g/mol) : 46.28% C; 3.40% H; 26.98% N; Found: 46.23 % C; 3.43% H; 26.98 % N; IR (ATR, cm⁻¹): 2294 (m), 2233 (m), 2170 (s), 1922 (w), 1667 (w), 1611 (s), 1566 (s), 1512 (s), 1433 (s), 1345 (s), 1304 (vs), 1206 (s), 1056 (m), 1008 (s), 936 (m), 830 (s), 814 (s), 673 (m), 571 (w), 526 (s), 463 (m)

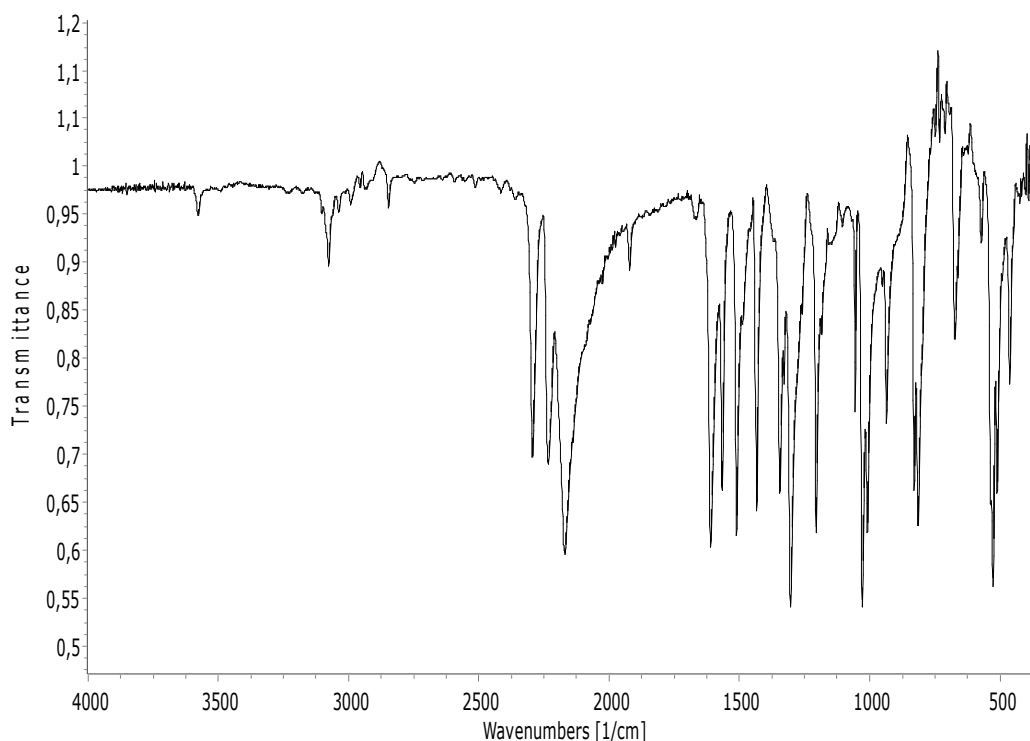


Figure 6.19.: IR-Spectrum of $[\text{Zn}(\text{dca})_2(4\text{-MeOpy})_2]_n$

6. 4-methoxy-pyridine complexes

6.7.2. Structural characterization

The selected bond parameters of $[Zn(dca)_2(4\text{-MeOpy})_2]_n$ are summarized in table 6.13. Its crystal structure is displayed in fig. 6.20 (perspective view) and fig. 6.21 (packing view). Zn(1) is situated on an inversion center and connected to six ligands: four of them are dicyanamide anions which act in bis- $\mu(1,5)$ -bridging mode, forming a polymeric chain along the axis of the triclinic cell. The others are 4-MOP molecules in trans configuration. The ZnN_6 polyhedron forms an almost regular octahedron, with Zn-N bond distances varying from $2.1288(15)$ to $2.1733(19)$ Å, and a maximum deviation of 0.89° of the N-Zn-N bond angles from 90 or 180° . The dicyanamide bridges have the following bond parameters: Zn-N-C: $162.01(18)$ and $159.00(19)^\circ$; N-C-N: $174.9(2)$ and $175.6(2)^\circ$; C-N-C: $118.38(17)^\circ$; C-N(nitril) $1.154(3)$ and $1.158(3)$ Å; C-N(amide): $1.310(3)$ and $1.309(3)$ Å. The intra-chain Zn · · · Zn distance of $7.3706(4)$ Å is longer than the shortest inter-chain metal · · · metal separation of $7.0620(4)$ Å.

Table 6.13.: Selected bond lengths (Å) and angles (°) for $[Zn(dca)_2(4\text{-MeOpy})_2]_n$; Symmetry codes: (a) $2-x, 2-y, -z$; (b) $2-x, 1-y, -z$; (c) $x, 1+y, z$; (d) $x, -1+y, z$; (e) $2-x, 3-y, -z$; (f) $2-x, -y, -z$.

Zn(1)-N(1a)	2.1288(15)	Zn(1)-N(4b)	2.1733(19)
Zn(1)-N(2a)	2.1710(19)	N(3)-C(7)	1.310(3)
N(2)-C(7)	1.154(3)	N(3)-C(8)	1.309(3)
N(4)-C(8)	1.158(3)		
N(1)-Zn(1)-N(2a)	90.59(7)	N(1a)-Zn(1)-N(4b)	90.28(7)
N(4c)-Zn(1)-N(2a)	90.89(6)	N(2)-Zn(1)-N(2a)	180.0
Zn(1)-N(2)-C(7)	162.01(18)	N(2)-C(7)-N(3)	174.9(2)
Zn(1b)-N(4)-C(8)	159.00(19)	N(4)-C(8)-N(3)	175.6(2)
C(7)-N(3)-C(8)	118.38(17)		

6. 4-methoxy-pyridine complexes

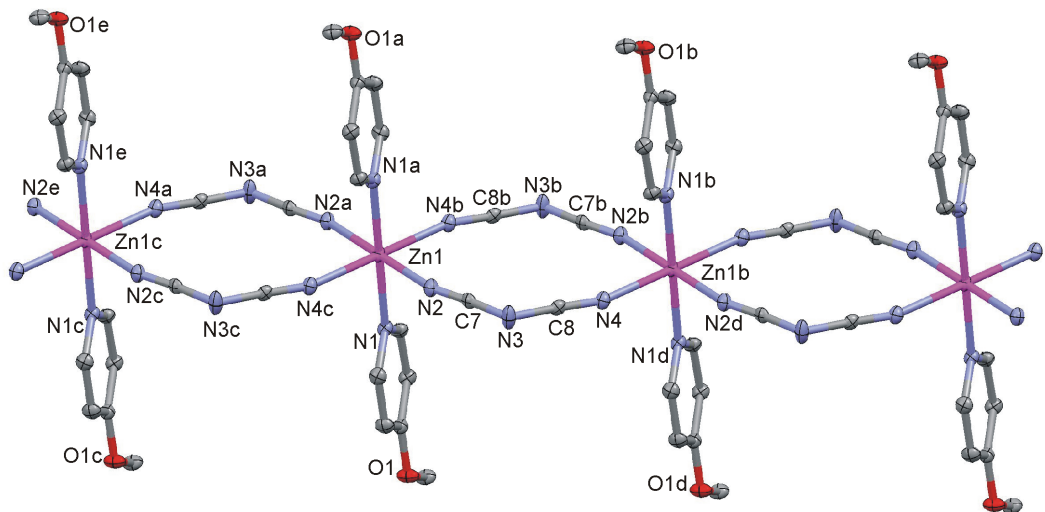


Figure 6.20.: Perspective view of a section of the polymeric chain of $[\text{Zn}(\text{dca})_2(4\text{-MeOpy})_2]_n$ together with the atom numbering scheme. Symmetry codes: (a) $2-x, 2-y, -z$; (b) $2-x, 1-y, -z$; (c) $x, 1+y, z$; (d) $x, -1+y, z$; (e) $2-x, 3-y, -z$; (f) $2-x, -y, -z$.

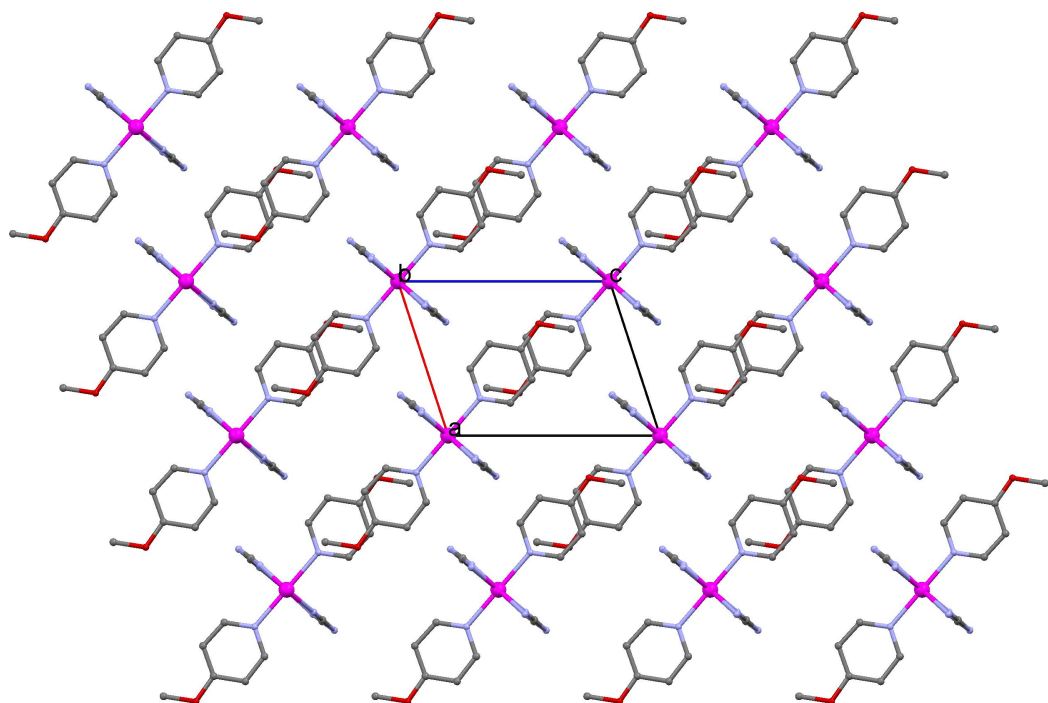


Figure 6.21.: Packing plot of $[\text{Zn}(\text{dca})_2(4\text{-MeOpy})_2]_n$.

6. 4-methoxy-pyridine complexes

Table 6.14.: Crystallographic data and processing parameter of $[Zn(dca)_2(4\text{-MeOpy})_2]_n$.

Empirical formula	$C_{16}H_{14}N_8O_2Zn$
Formula mass	415.74
System	triclinic
Space group	P-1
a (Å)	7.0620(4)
b (Å)	7.3706(4)
c (Å)	9.8134(5)
α (°)	69.847(2)
β (°)	71.759(3)
γ (°)	86.183(3)
V (Å ³)	454.94(4)
Z	1
T (K)	100(2)
μ (mm ⁻¹)	1.379
D _{calc} (Mg/m ³)	1.518
Crystal size (mm)	0.26 x 0.21 x 0.12
θ max (°)	28.00
Data collected	2188
Unique refl./ R _{int}	2188 / —
Parameters	126
Goodness-of-Fit on F ²	1.148
R1 / wR2 (all data)	0.0282 / 0.0798
Residual extrema (e/Å ³)	0.40 / -0.40

6. 4-methoxy-pyridine complexes

6.8. $[\text{Co}(\text{SCN})_2(4\text{-methoxypyridine})_4]$

6.8.1. Synthesis

0.58 g $\text{Co}(\text{NO}_3)_2 \cdot 6\text{H}_2\text{O}$ (2 mmol), 0.38 g KSCN (4 mmol) and 0.87 g 4-methoxy-pyridine (8 mmol) were dissolved in 40 mL distilled H_2O . The solution was heated up to 70°C and stirred for 1 hour. After filtration the clear pink solution was placed in the drying oven (70°C) overnight and then cooled down to RT. After a few hours pink crystals were obtained. Anal. Calculated for $\text{C}_{26}\text{H}_{28}\text{CoN}_6\text{O}_4\text{S}_2$ (611,59 g/mol): 51.06% C; 4.61% H; 13.74% N; 10.49 % S; Found: 50.94 % C; 4.65% H; 13.80 % N; 10.30% S; IR (ATR, cm^{-1}): 2061 (s), 1608 (s), 1567 (s), 1508 (s), 1493 (s), 1460 (w), 1426 (m), 1293 (s), 1205 (s), 1024 (vs), 822 (s), 659 (w), 540 (s), 458 (m)

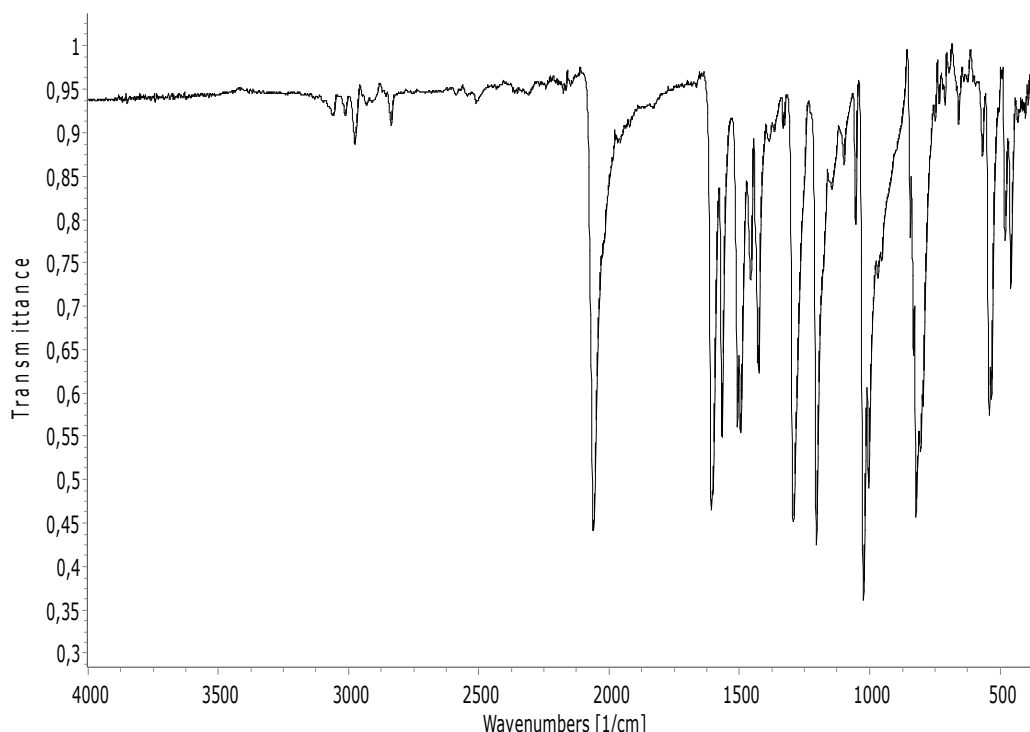


Figure 6.22.: IR spectrum of $[\text{Co}(\text{SCN})_2(4\text{-MeOpy})_4]$

6. 4-methoxy-pyridine complexes

6.8.2. Structural characterization

The crystal structure of $[\text{Co}(\text{SCN})_2(4\text{-MeOpy})_4]$ consists of mononuclear and neutral Co(II) complexes. A perspective view is shown in fig. 6.23, a packing view in fig 6.24 and selected bond parameters are summarized in table 6.17. Co(1) is six-coordinated by N atoms of two terminal isothiocyanato anions, further by N donor atoms of four neutral 4-methoxypyridine molecules. The CoN_6 chromophore may be described as a slightly distorted octahedron with trans-arrangement of the isothiocyanato ligands. The Co-N bond lengths range from 2.089(5) to 2.195(5) Å, and the transoid N-Co-N bond angles within the CoN_6 octahedra vary from 175.08(17) to 178.96(18)°. The bond parameters of the terminal isothiocyanato anions are: Co-N-C: 153.9(4) and 163.4(5)°, N-C-S: 178.0(5) and 179.4(6)°, N-C: 1.160(7) and 1.167(7) Å, C-S: 1.637(5) and 1.628(6) Å. The shortest metal-metal separation is 9.1969(19) Å.

Table 6.15.: Selected bond lengths (Å) and angles (°) for $[\text{Co}(\text{SCN})_2(4\text{-MeOpy})_4]$

Co(1)-N(1)	2.096(5)	Co(1)-N(4)	2.195(5)
Co(1)-N(2)	2.089(5)	Co(1)-N(5)	2.136(5)
Co(1)-N(3)	2.174(5)	Co(1)-N(6)	2.155(5)
N(1)-C(1)	1.160(7)	C(1)-S(1)	1.637(5)
N(2)-C(2)	1.167(7)	C(2)-S(2)	1.628(6)
N(1)-Co(1)-N(2)	178.96(18)	N(3)-Co(1)-N(5)	175.08(17)
N(4)-Co(1)-N(6)	1.178.44(17)	Co(1)-N(2)-C(2)	153.9(4)
Co(1)-N(1)-C(1)	163.4(5)	N(2)-C(2)-S(2)	178.0(5)
N(1)-C(1)-S(1)	179.4(6)		

6. 4-methoxy-pyridine complexes

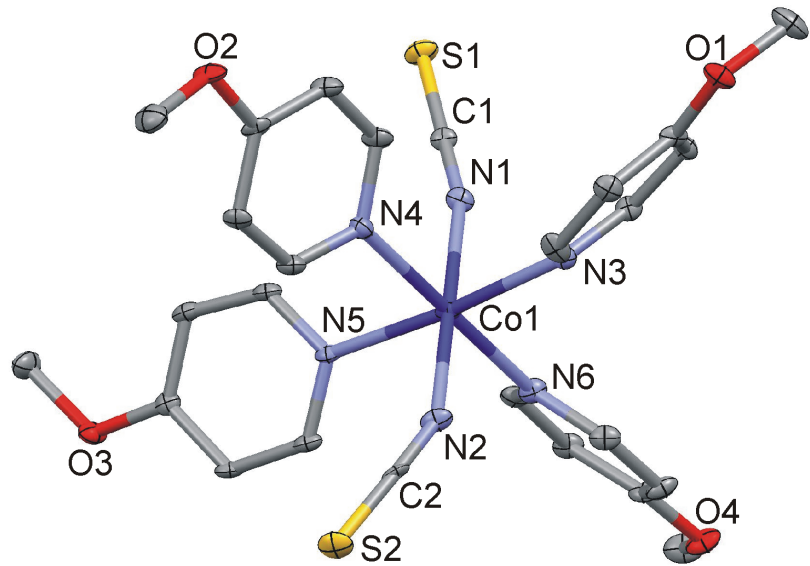


Figure 6.23.: Perspective view of $[\text{Co}(\text{SCN})_2(4\text{-MeOpy})_4]$ with the atom numbering scheme.

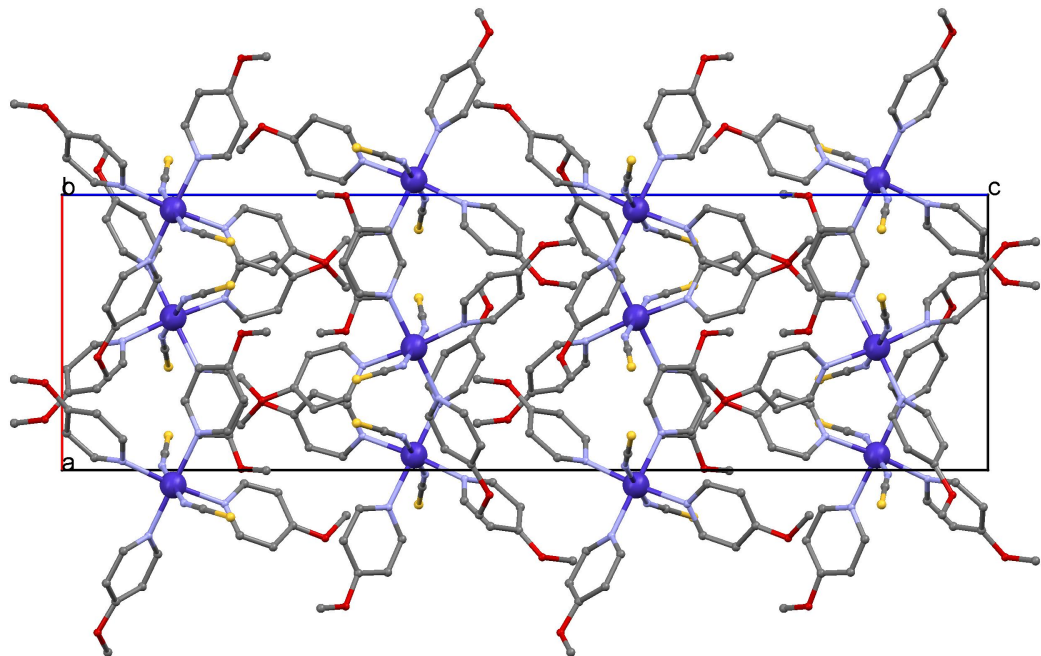


Figure 6.24.: Packing view of $[\text{Co}(\text{SCN})_2(4\text{-MeOpy})_4]$.

6. 4-methoxy-pyridine complexes

Table 6.16.: Crystallographic data and processing parameter of $[\text{Co}(\text{SCN})_2(4\text{-MeOpy})_4]$

Empirical formula	$\text{C}_{26}\text{H}_{28}\text{CoN}_6\text{O}_4\text{S}_2$
Formula mass	611.59
System	orthorhombic
Space group	Pbca
a (Å)	10.1815(17)
b (Å)	16.574(3)
c (Å)	34.268(6)
α (°)	90
β (°)	90
γ (°)	90
V (Å ³)	5782.6(17)
Z	8
T (K)	100(2)
μ (mm ⁻¹)	0.780
D _{calc} (Mg/m ³)	1.405
Crystal size (mm)	0.19 x 0.16 x 0.09
θ max (°)	25.50
Data collected	33321
Unique refl. / R _{int}	5372 / 0.1050
Parameters	356
Goodness-of-Fit on F ²	1.154
R1 / wR2 (all data)	0.0763 / 0.1570
Residual extrema (e/Å ³)	0.64 / -0.85

6. 4-methoxy-pyridine complexes

6.9. $[\text{Cu}(\text{SCN})_2(4\text{-methoxypyridine})_2]_n$

6.9.1. Synthesis

0.48 g $\text{Cu}(\text{NO}_3)_2 \cdot 3 \text{H}_2\text{O}$ (2 mmol), 0.39 g KSCN (4 mmol) and 0.44 g 4-methoxy-pyridine (4 mmol) were mixed with 40 mL distilled H_2O . Stirring was conducted for 2 hours and 30 minutes at 60°C . After filtration the green solution was stirred again for 50 minutes at the same temperature and then cooled down to RT. Over the course of 24 hours green crystals precipitated. Anal. Calculated for $\text{C}_{14}\text{H}_{14}\text{CuN}_4\text{O}_2\text{S}_2$ (397.96 g/mol) : 42.25% C; 3.55% H; 14.08% N; 16.11% S; Found: 41.84 % C; 3.51% H; 14.14 % N; 15.69% S; IR (ATR, cm^{-1}): 2086 (s), 2072 (s), 1614 (s), 1566 (s), 1512 (s), 1434 (s), 1299 (s), 1205 (s), 1059 (m), 1030 (s), 1012 (m), 844 (m), 817 (s), 732 (w), 659 (w), 573 (w), 535 (s), 464 (s)

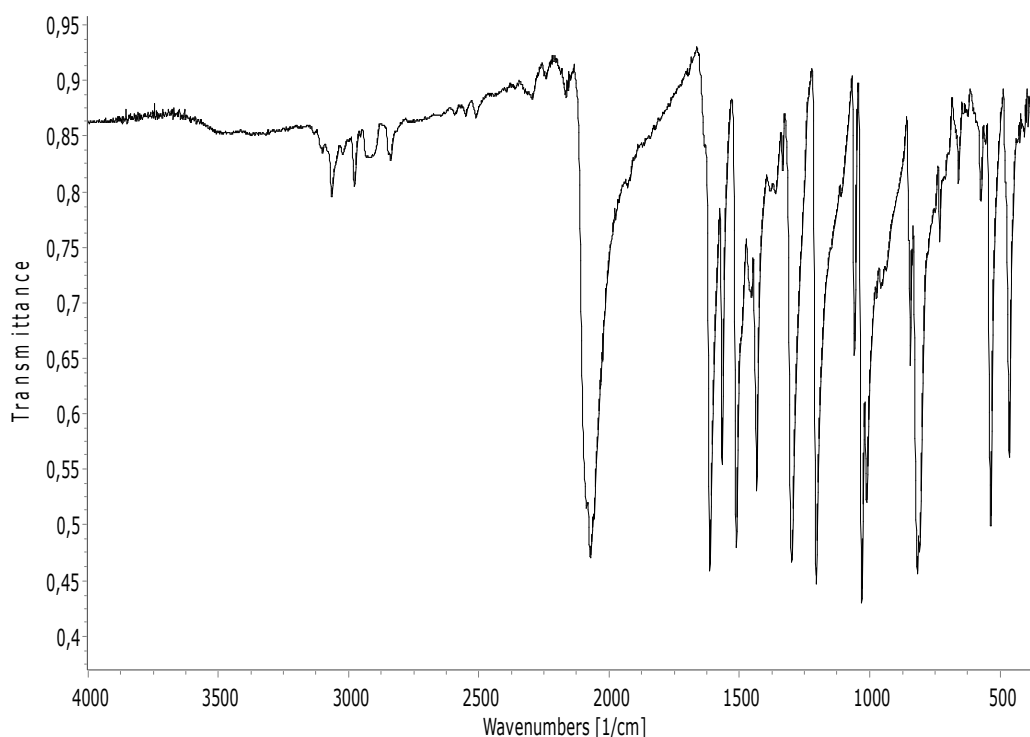


Figure 6.25.: IR spectrum of $[\text{Cu}(\text{SCN})_2(4\text{-MeOpy})_2]_n$

6. 4-methoxy-pyridine complexes

6.9.2. Structural characterization

A perspective view of $[\text{Cu}(\text{SCN})_2(4\text{-MeOpy})_2]_n$ is given in fig. 6.26. The 2D layer system of the Cu-NCS sublattice is displayed in fig. 6.27. Table 6.17 lists the chosen bond parameters. The three crystallographically independent Cu(II) metal centers in the structure of $\text{Cu}(\text{SCN})_2(4\text{-MeOpy})_2$ are located on inversion centers. Taking into account the semi-coordinative Cu-S bond distances, each Cu(II) is bound to four N and two S atoms, whereas two N belong to two 4-MOPs in trans configuration. The remaining 4 atoms each belong to a isothiocyanate anion. The Cu-N(py) bond distances vary from 2.010(3) to 2.037(2) Å, the Cu-N(NCS) bond distances vary from 1.953(2) to 1.970(3) Å, whereas the semi-coordinative Cu-S bond lengths are in the range of 2.930(2) to 3.112(2) Å. The three NCS-groups behave in a different manner. N(2)-C(2)-S(2) acts as N-terminal ligand only, N(1)-C(1)-S(1) acts as $\mu(\text{N},\text{S})$ ligand, to bridge Cu(1) and Cu(3) centers, N(3)-C(3)-S(3) acts as $\mu(\text{N},\text{S},\text{S}')$ -bridging ligand to connect all three different metal centers. The 2D system of $\text{Cu}(\text{SCN})_2(4\text{-MeOpy})_2$ may be described as polymeric chains of alternating Cu(1) and Cu(3) polyhedra oriented along the c-axis. These chains are formed via di- μ -(N,S) bridging NCS-anions. This is where the Cu(1) polyhedra are further connected by Cu(2) polyhedra along the b-axis of the triclinic unit cell (Fig. 6.27). The N(1)-C(1)-S(1) $\mu(\text{N},\text{S})$ bridge has a Cu-N \cdots S-Cu torsion angle of +64.1°, and the N(3)-C(3)-S(3) $\mu(\text{N},\text{S},\text{S}')$ -bridge forms Cu-N \cdots S-Cu torsion angles of -27.1 and -165.7°.

6. 4-methoxy-pyridine complexes

Table 6.17.: Selected bond lengths (\AA) and angles ($^\circ$) for $[\text{Cu}(\text{SCN})_2(4\text{-MeOpy})_2]_n$. Symmetry codes: (') $1-x, -y, 2-z$; (*) $1-x, 1-y, -z$; (") $1-x, 2-y, 1-z$.

$\text{Cu}(1)\text{-N}(1')$	1.953(2)	$\text{Cu}(1)\text{-N}(5')$	2.037(2)
$\text{Cu}(2)\text{-N}(2^*)$	1.958(3)	$\text{Cu}(2)\text{-N}(6^*)$	2.027(2)
$\text{Cu}(3)\text{-N}(3'')$	1.970(3)	$\text{Cu}(3)\text{-N}(7'')$	2.010(3)
$\text{N}(1)\text{-C}(1)$	1.159(4)	$\text{C}(1)\text{-S}(1)$	1.635(3)
$\text{N}(2)\text{-C}(2)$	1.145(4)	$\text{C}(2)\text{-S}(2)$	1.622(4)
$\text{N}(3)\text{-C}(3)$	1.157(4)	$\text{C}(3)\text{-S}(3)$	1.641(3)
$\text{N}(1')\text{-Cu}(1)\text{-N}(5')$	90.87(10)	$\text{N}(2^*)\text{-Cu}(2)\text{-N}(6^*)$	90.16(10)
$\text{N}(3)\text{-Cu}(3)\text{-N}(7'')$	90.02(11)	$\text{N}(21)\text{-Cu}(1)\text{-N}(11a)$	91.04(9)
$\text{Cu}(1)\text{-N}(1)\text{-C}(1)$	162.3(2)	$\text{N}(1)\text{-C}(1)\text{-S}(1)$	179.6(3)
$\text{Cu}(2)\text{-N}(2)\text{-C}(2)$	155.0(3)	$\text{N}(2)\text{-C}(2)\text{-S}(2)$	179.4(3)
$\text{Cu}(3)\text{-N}(3)\text{-C}(3)$	168.3(2)	$\text{N}(3)\text{-C}(3)\text{-S}(3)$	178.8(3)

6. 4-methoxy-pyridine complexes

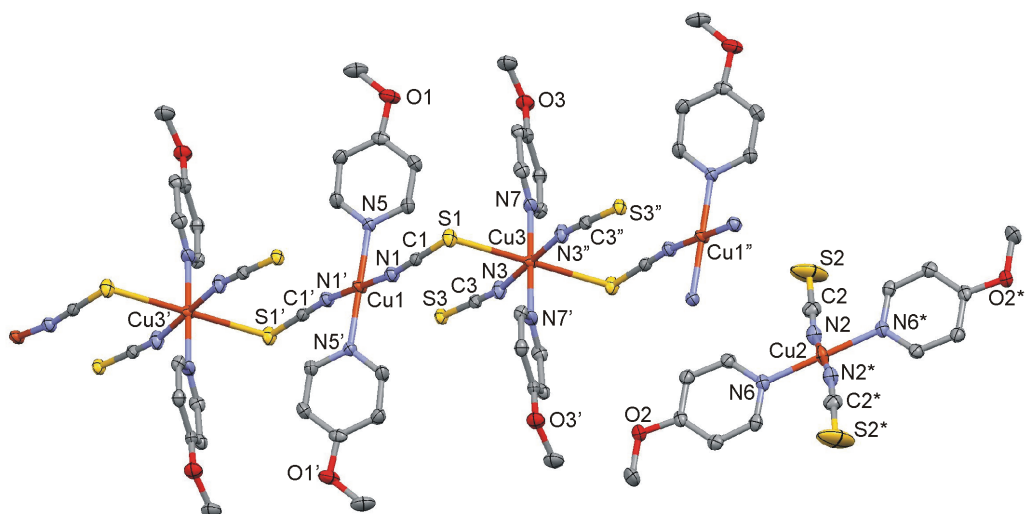


Figure 6.26.: Perspective view of $[\text{Cu}(\text{SCN})_2(4\text{-MeOpy})_2]_n$ with the atom numbering scheme. Symmetry codes: ('') 1-x, -y, 2-z; (*) 1-x, 1-y, -z; ('') 1-x, 2-y, 1-z.

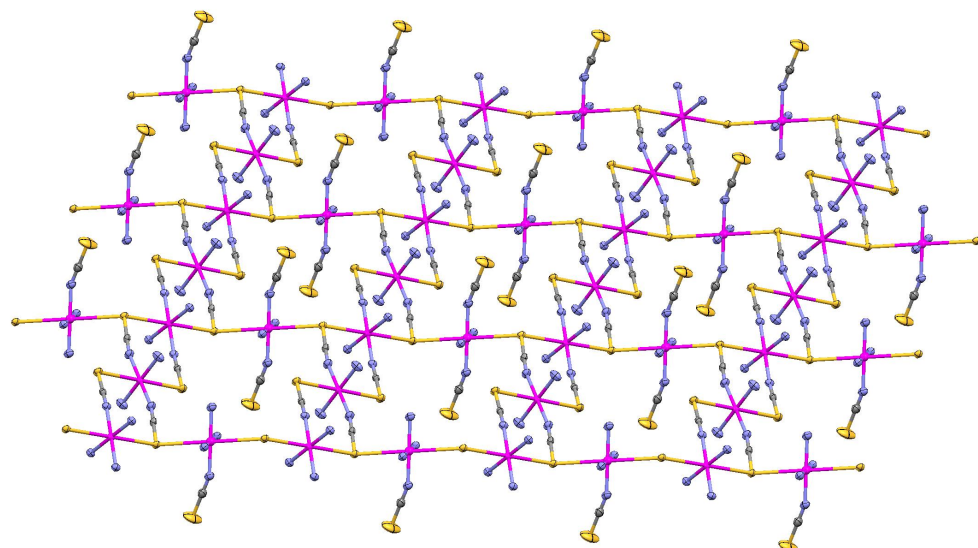


Figure 6.27.: View onto 2D Cu-NCS sub-lattice of $[\text{Cu}(\text{SCN})_2(4\text{-MeOpy})_2]_n$.

6. 4-methoxy-pyridine complexes

Table 6.18.: Crystallographic data and processing parameter of $[\text{Cu}(\text{SCN})_2(4\text{-MeOpy})_2]_n$

Empirical formula	$\text{C}_{14}\text{H}_{14}\text{CuN}_4\text{O}_2\text{S}_2$
Formula mass	397.96
System	triclinic
Space group	P-1
a (Å)	10.981(2)
b (Å)	11.296(2)
c (Å)	11.531(2)
α (°)	112.524(3)
β (°)	99.366(3)
γ (°)	98.311(2)
V (Å ³)	1269.6(4)
Z	3
T (K)	100(2)
μ (mm ⁻¹)	1.549
D _{calc} (Mg/m ³)	1.561
Crystal size (mm)	0.34 x 0.18 x 0.04
θ max (°)	26.37
Data collected	10186
Unique refl. / R _{int}	5122 / 0.0266
Parameters	384
Goodness-of-Fit on F ²	1.047
R1 / wR2 (all data)	0.0410 / 0.0998
Residual extrema (e/Å ³)	1.23 / -1.29

7. 4-hydroxymethylpyridine complexes

7.1. $[\text{Cu}(\text{N}_3)_2(4\text{-hydroxymethylpyridine})]_n$

7.1.1. Synthesis

0.48 g $\text{Cu}(\text{NO}_3)_2 \cdot 3 \text{H}_2\text{O}$ (2 mmol), 0.26 g sodium azide (4 mmol) and 0.22 g 4-(hydroxymethyl)pyridine (2 mmol) were added to 40 mL distilled water. The solution was heated up for 120 minutes at 70°C. After filtration the solution was heated up 50 minutes at 70°C and then cooled down to RT. Green needles were obtained after one day.

Anal. Calculated for $\text{C}_6\text{H}_7\text{CuN}_7\text{O}$ (256.74 g/mol): 28.07% C; 2.75% H; 38.19% N;

Found: 28.09 % C; 2.78% H; 38.09 % N;

IR (ATR, cm^{-1}): 3355 (w), 2025 (vs), 1616 (m), 1562 (w), 1505 (w), 1432 (m), 1289 (m), 1221 (m), 1034 (s), 960 (w), 806 (m), 618 (m), 587 (m), 483 (m)

7. 4-hydroxymethylpyridine complexes

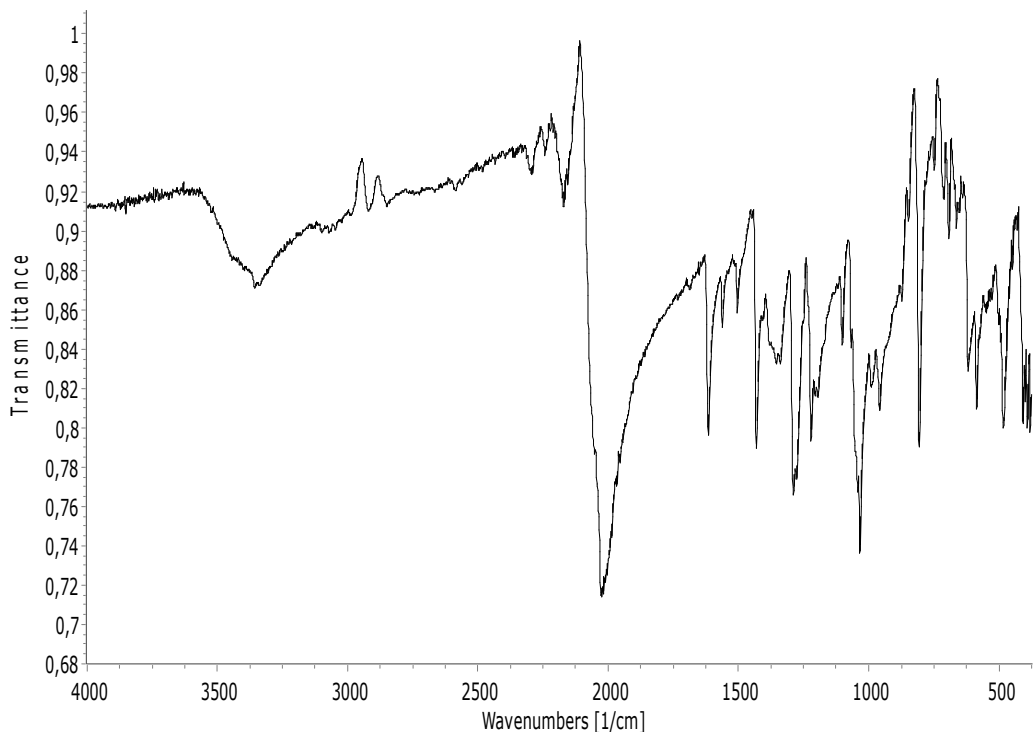


Figure 7.1.: IR-Spectrum of $[\text{Cu}(\text{N}_3)_2(4\text{-HOMepy})]_n$

7.1.2. Structural characterization

Selected bond parameters of $[\text{Cu}(\text{N}_3)_2(4\text{-HOMepy})]_n$ are summarized in table 7.1, a perspective view of a section of the polymeric chain is given in fig. 7.2 and a packing view in fig. 7.3. The Cu(1) metal center is penta-coordinated by pyridine N donor atom of a 4-hydroxymethylpyridine molecule and four N atoms of azide groups. The CuN_5 chromophore forms a distorted square pyramid (SP) with a τ -value of 0.24 (τ -values of 1 and 0 refer to ideal geometries of trigonal bipyramidal (TBP) and square pyramid (SP), respectively) [72]. The apical site is occupied by N(23b) [$\text{Cu}(1)\text{-N}(23b) = 2.462(2)$ Å]. The basal Cu-N bond distances range from 1.972(2) to 2.005(2) Å. The azide groups behave differently. Azide groups N(11)-N(12)-N(13) and N(11a)-N(12a)-N(13a) act as di-EO bridges to connect the polyhedra of

7. 4-hydroxymethylpyridine complexes

Cu(1) and Cu(1a) to centrosymmetric dimeric subunits. The bond parameters within their four-membered Cu₂N₂ rings are: Cu(1)-N(11)-Cu(1a) = 101.82(10), N(11)-Cu(1)-N(11a) = 78.18(10), Cu(1)-N(11)-N(12) = 128.59(18) and Cu(1a)-N(11)-N(12) = 125.00(18)^o. The azide group N(21)-N(22)-N(23) act as asymmetrical single EE azido bridge, with N(21) ligated in basal position and N(23) ligated in axial position. Four such single EE azide bridges connect the centrosymmetric dimeric Cu(1)..Cu(1a) subunits to generate double chains of polyhedra oriented along the a-axis of the unit cell. The Cu(1)-N(21)-Cu(1c)-N(23)-N(22) bond angles are 123.98(19) and 110.51(18)^o, respectively, and the Cu(1)-N(21)..N(23)-Cu(1c) torsion angle is -92.3^o. The intra-chain Cu(1)..Cu(1a) and Cu(1)..Cu(1c) distances are 3.1042(6) and 5.2153(9) Å, and the shortest inter-chain metal-metal separation is 7.5484(12) Å. The bond distances and bond angle of the EO azide bridge are 1.220(3) Å, 1.139(4) Å, and 177.8(3)^o, whereas the corresponding bond parameters for the EE azide bridge are 1.199(3) Å, 1.161(3) Å, and 176.9(3)^o. The 4-hydroxypyridine molecule forms hydrogen bond of the type O-H · · · N(O(17)-H(91) · · · N(13') = 144(6)^o, O(17) · · · N(13') = 2.990(6) Å; symmetry code (''): 1-x,2-y,1-z).

7. 4-hydroxymethylpyridine complexes

Table 7.1.: Selected bond lengths (\AA) and angles ($^\circ$) for $[\text{Cu}(\text{N}_3)_2(4\text{-HOMepy})]_n$. Symmetry codes: (a) $2-x, 1-y, 1-z$; (b) $-1+x, y, z$; (c) $2-x, 1-y, 1-z$; (d) $1+x, y, z$; (e) $-x, 1-y, 1-z$; (g) $-2x, y, z$.

$\text{Cu}(1)\text{-N}(11\text{a})$	2.005(2)	$\text{Cu}(1)\text{-N}(23\text{b})$	2.462(2)
$\text{Cu}(1)\text{-N}(1)$	1.981(2)	$\text{Cu}(1)\text{-N}(11)$	1.995(2)
$\text{Cu}(1)\text{-N}(21)$	1.972(2)	$\text{N}(11)\text{-N}(12)$	1.220(3)
$\text{N}(12)\text{-N}(13)$	1.139(4)	$\text{N}(21)\text{-N}(22)$	1.199(3)
$\text{N}(22)\text{-N}(23)$	1.161(3)		
$\text{N}(21)\text{-Cu}(1)\text{-N}(1)$	94.55(9)	$\text{N}(21)\text{-Cu}(1)\text{-N}(11)$	159.74(10)
$\text{N}(11)\text{-Cu}(1)\text{-N}(1)$	96.01(9)	$\text{N}(21)\text{-Cu}(1)\text{-N}(11\text{a})$	91.04(9)
$\text{N}(11)\text{-Cu}(1)\text{-N}(11\text{a})$	78.18(10)	$\text{N}(21)\text{-Cu}(1)\text{-N}(23\text{b})$	103.39(9)
$\text{N}(1)\text{-Cu}(1)\text{-N}(23\text{b})$	93.42(9)	$\text{N}(11)\text{-Cu}(1)\text{-N}(23\text{b})$	93.19(9)
$\text{N}(11\text{a})\text{Cu}(1)\text{-N}(23\text{b})$	86.84(9)	$\text{N}(1)\text{-Cu}(1)\text{-N}(11\text{a})$	174.18(9)
$\text{Cu}(1)\text{-N}(11)\text{-N}(12)$	128.5(18)	$\text{N}(11)\text{-N}(12)\text{-N}(13)$	177.8(3)
$\text{Cu}(1)\text{-N}(21)\text{-C}(22)$	123.98(19)	$\text{N}(21)\text{-N}(22)\text{-N}(23)$	176.9(3)
$\text{Cu}(1\text{a})\text{-N}(11)\text{-N}(12)$	125.00(18)	$\text{Cu}(1)\text{-N}(11)\text{-Cu}(1\text{a})$	101.82(10)
$\text{Cu}(1\text{c})\text{-N}(23)\text{-N}(22)$	110.51(18)		

7. 4-hydroxymethylpyridine complexes

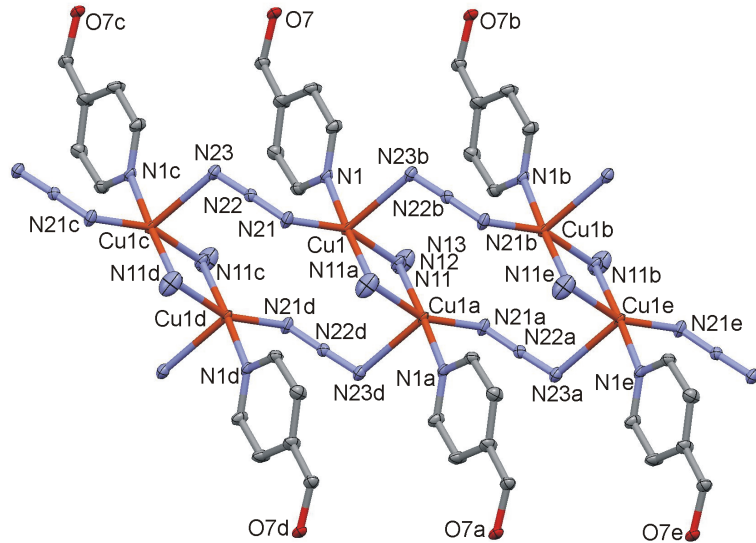


Figure 7.2.: Perspective view of a section of the polymeric chain of $[\text{Cu}(\text{N}_3)_2(4\text{-HOMepy})]_n$ with the atom numbering scheme. Symmetry codes:(a) $2-x, 1-y, 1-z$; (b) $1+x, y, z$; (c) $-1+x, y, z$; (d) $1-x, 1-y, 1-z$; (e) $3-x, 1-y, 1-z$.

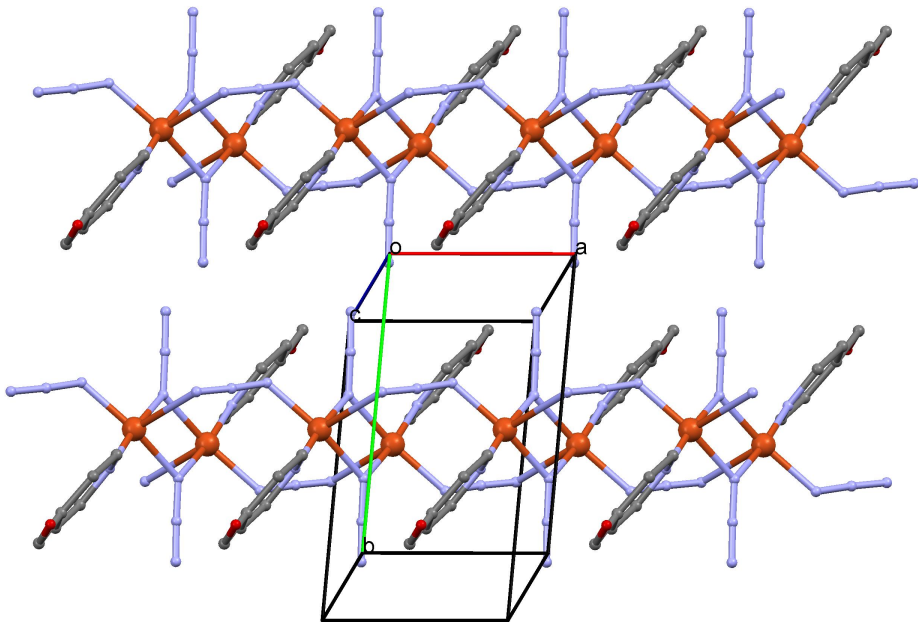


Figure 7.3.: Packing plot of $[\text{Cu}(\text{N}_3)_2(4\text{-HOMepy})]_n$.

7. 4-hydroxymethylpyridine complexes

Table 7.2.: Crystallographic data and processing parameter of $[\text{Cu}(\text{N}_3)_2(4\text{-HOMepy})]_n$

Empirical formula	$\text{C}_6\text{H}_7\text{CuN}_7\text{O}$
Formula mass	256.74
System	triclinic
Space group	P-1
a (Å)	5.2153(8)
b (Å)	9.6409(15)
c (Å)	9.7206(15)
α (°)	106.898(3)
β (°)	97.332(3)
γ (°)	94.151(3)
V (Å ³)	460.73(12)
Z	2
T (K)	100(2)
μ (mm ⁻¹)	2.354
D_{calc} (Mg/m ³)	1.851
Crystal size (mm)	0.10 x 0.15 x 0.02
θ max (°)	29.99
Data collected	12368
Unique refl./ R _{int}	2692 / 0.0207
Parameters	160
Goodness-of-Fit on F ²	1.369
R1 / wR2 (all data)	0.0313 / 0.0878
Residual extrema (e/Å ³)	0.59 / -0.68

7. 4-hydroxymethylpyridine complexes

7.2. $[\text{Co}(\text{dca})_2(4\text{-hydroxymethylpyridine})_2]_n$

7.2.1. Synthesis

0.29 g $\text{Co}(\text{NO}_3)_2 \cdot 6\text{H}_2\text{O}$ (1 mmol), 0.18 g sodium dicyanamide (2 mmol) and 0.22 g 4-hydroxymethyl-pyridine (2 mmol) were dissolved in 20 mL distilled H_2O . The solution was heated up to 80°C and stirred for 2 hours and 30 minutes. After filtration the pink solution was stirred at the same temperature for 40 minutes and then cooled down to RT. After 24 hours pink plate-like crystals were obtained. Anal. Calculated for $\text{C}_{16}\text{H}_{14}\text{CoN}_8\text{O}_2$ (409.28 g/mol) : 46.96% C; 3.45% H; 27.38% N; Found: 46.76 % C; 3.44% H; 27.37 % N; IR (ATR, cm^{-1}): 3551(w), 3481 (w), 2269 (w), 2245 (m), 2170 (s), 1606 (m), 1564 (w), 1504 (w), 1426 (m), 1293 (s), 1202 (m), 1023 (vs), 799 (m), 607 (w), 533 (s), 493 (m)

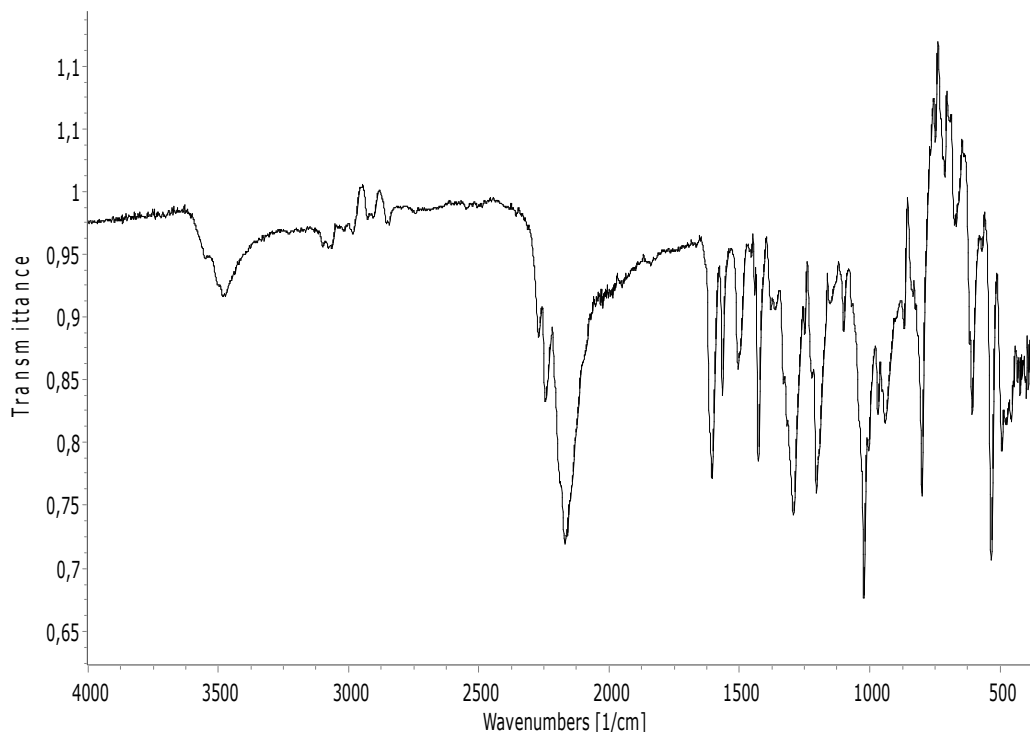


Figure 7.4.: IR spectrum of $[\text{Co}(\text{dca})_2(4\text{-HOMepy})_2]_n$

7. 4-hydroxymethylpyridine complexes

7.2.2. Structural characterization

A packing view of $[\text{Co}(\text{dca})_2(4\text{-HOMepy})_2]_n$ is given in fig. 7.6 and a perspective view of a section of the polymeric chain in fig. 7.5. Selected bond parameters are summarized in table 7.3. The Co(1) center is located on an inversion center. It is coordinated by pyridine N donor atom of two 4-MeOpy molecules in trans configuration and four N atoms of dicyanamide anions (acting in the bis- $\mu(1,5)$ -bridging mode) generating polymeric chains of polyhedra. These are oriented along the c-axis of the monoclinic unit cell. The CoN_6 chromophore has an almost regular octahedron, with Co-N bond distances varying from $2.116(4)$ to $2.126(4)$ Å, and N-Co-N bond angles deviating only by 1.16° from the values of ideal octahedral geometry. The dca bridges possess the following bond parameters: Co-N-C: $163.3(4)$ and $158.5(4)^\circ$; N-C-N: $177.0(5)$ and $176.5(5)^\circ$; C-N-C: $114.7(4)^\circ$; C-N(nitril) $1.146(7)$ and $1.156(7)$ Å; C-N(amide): $1.317(7)$ and $1.326(7)$ Å. The intra-chain $\text{Co} \cdots \text{Co}$ distance of $7.213(3)$ Å is longer than the shortest inter-chain metal \cdots metal separation of $7.076(3)$ Å. Along the a-axis of the unit cell the OH-group of the pyridine derivative ligand forms a hydrogen bond. This bond is of the type O-H \cdots N and is connected to the central N(3) atom of the adjacent dicyanamide anion ($\text{O}(1)\text{-H}(90) \cdots \text{N}(3\#1) = 152(7)^\circ$, $\text{O}(1)\text{ce}^{***}\text{N}(3\#1) = 2.954(7)$ Å; (#1): $1+x, y, z$).

Table 7.3.: Selected bond lengths (Å) and angles (°) for $[\text{Co}(\text{dca})_2(4\text{-HOMepy})_2]_n$. Symmetry codes: (a) $1-x, 1-y, -z$; (b) $1-x, 1-y, 1-z$; (c) $-1+x, y, z$; (d) $x, y, 1+z$; (e) $1-x, 1-y, -1-z$.

Co(1)-N(1a)	$2.126(4)$	Co(1)-N(4a)	$2.124(5)$
Co(1)-N(2a)	$2.116(4)$	N(3)-C(7)	$1.317(7)$
N(2)-C(7)	$1.146(7)$	N(3)-C(8b)	$1.326(7)$
N(4)-C(8)	$1.156(7)$		
N(2)-Co(1)-N(4)	$90.34(17)$	N(2a)-Co(1)-N(1a)	$91.16(17)$
N(4)-Co(1)-N(1a)	$90.47(17)$	N(2)-Co(1)-N(2a)	180.0
Co(1)-N(2)-C(7)	$163.3(4)$	N(2)-C(7)-N(3)	$177.0(5)$
Co(1)-N(4)-C(8)	$158.5(4)$	N(4)-C(8)-N(3b)	$176.5(5)$
C(7)-N(3)-C(8b)	$114.7(4)$		

7. 4-hydroxymethylpyridine complexes

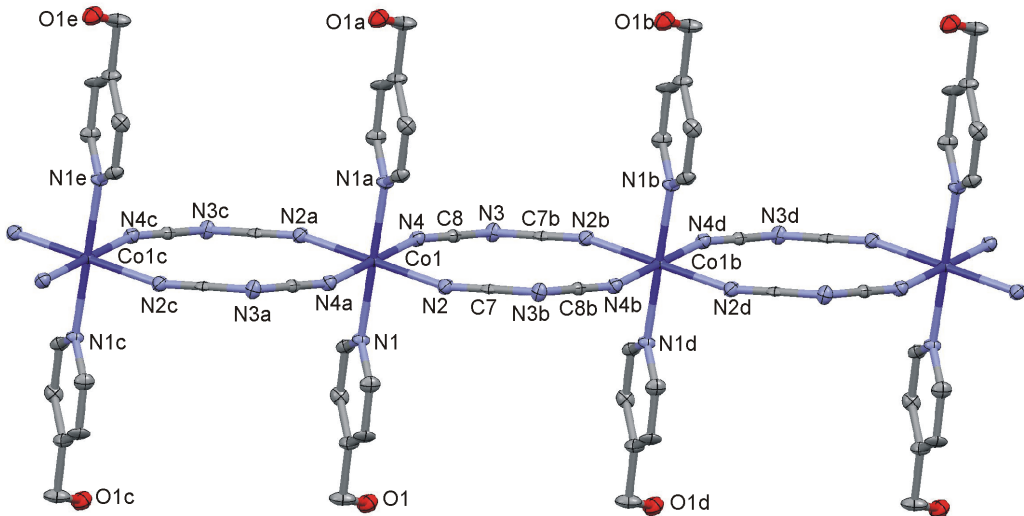


Figure 7.5.: Perspective view of a section of the polymeric chain of $[\text{Co}(\text{dca})_2(4\text{-HOMepy})_2]_n$ together with the atom numbering scheme. Symmetry codes: (a) $1-x, 1-y, -z$; (b) $1-x, 1-y, 1-z$; (c) $-1+x, y, z$; (d) $x, y, 1+z$; (e) $1-x, 1-y, -1-z$.

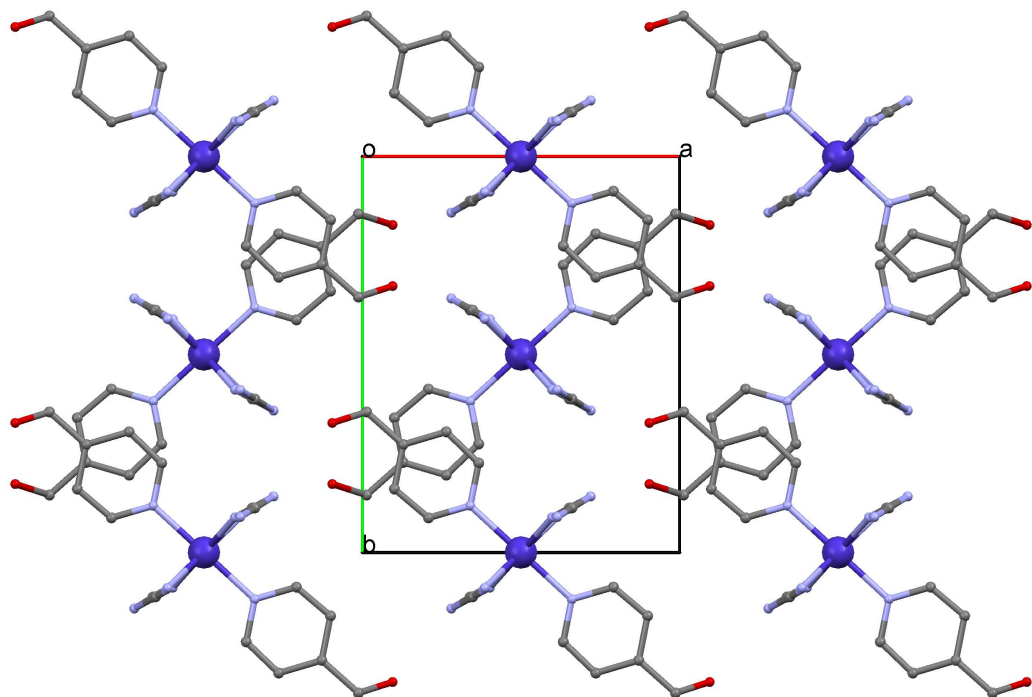


Figure 7.6.: Packing plot of $[\text{Co}(\text{dca})_2(4\text{-HOMepy})_2]_n$.

7. 4-hydroxymethylpyridine complexes

Table 7.4.: Crystallographic data and processing parameter of $[\text{Co}(\text{dca})_2(4\text{-HOMepy})_2]_n$

Empirical formula	$\text{C}_{16}\text{H}_{14}\text{CoN}_8\text{O}_2$
Formula mass	409.28
System	monoclinic
Space group	$\text{P}2_1/\text{c}$
a (Å)	10.347(4)
b (Å)	12.175(5)
c (Å)	7.213(3)
α (°)	90
β (°)	109.435(6)
γ (°)	90
V (Å ³)	856.9(6)
Z	2
T (K)	100(2)
μ (mm ⁻¹)	1.033
D_{calc} (Mg/m ³)	1.586
Crystal size (mm)	0.22 x 0.14 x 0.08
θ max (°)	26.34
Data collected	6380
Unique refl./ R _{int}	1720 / 0.0474
Parameters	127
Goodness-of-Fit on F ²	1.274
R1 / wR2 (all data)	0.0814 / 0.2004
Residual extrema (e/Å ³)	1.66 / -0.86

7. 4-hydroxymethylpyridine complexes

7.3. $[\text{Cu}(\text{dca})_2(4\text{-hydroxymethylpyridine})_2]_n$

7.3.1. Synthesis

40 mL of aqua dest. were used to dissolve 0.48 g $\text{Cu}(\text{NO}_3)_2 \cdot 3 \text{H}_2\text{O}$ (2 mmol), 0.36 g sodium dicyanamide (4 mmol) and 0.44 g 4-hydroxymethylpyridine (4 mmol). A two-hour stirring of the mixture was conducted at 70°C. Before cooling it to room temperature, the blue solution was filtrated and stirred at the same temperature (15 minutes). After 24 hours blue plate-like crystals were obtained. Anal. Calculated for $\text{C}_{16}\text{H}_{14}\text{CuN}_8\text{O}_2$ (413.90 g/mol): 46.43% C; 3.41% H; 27.07% N; Found: 46.31 % C; 3.36% H; 27.30 % N; IR (ATR, cm^{-1}): 3500(w), 2294(m), 2245 (m), 2170 (s), 1605 (s), 1566 (m), 1509 (w), 1426 (m), 1293 (m), 1205 (m), 1023 (s), 800 (m), 607 (w), 533 (m), 493 (w)

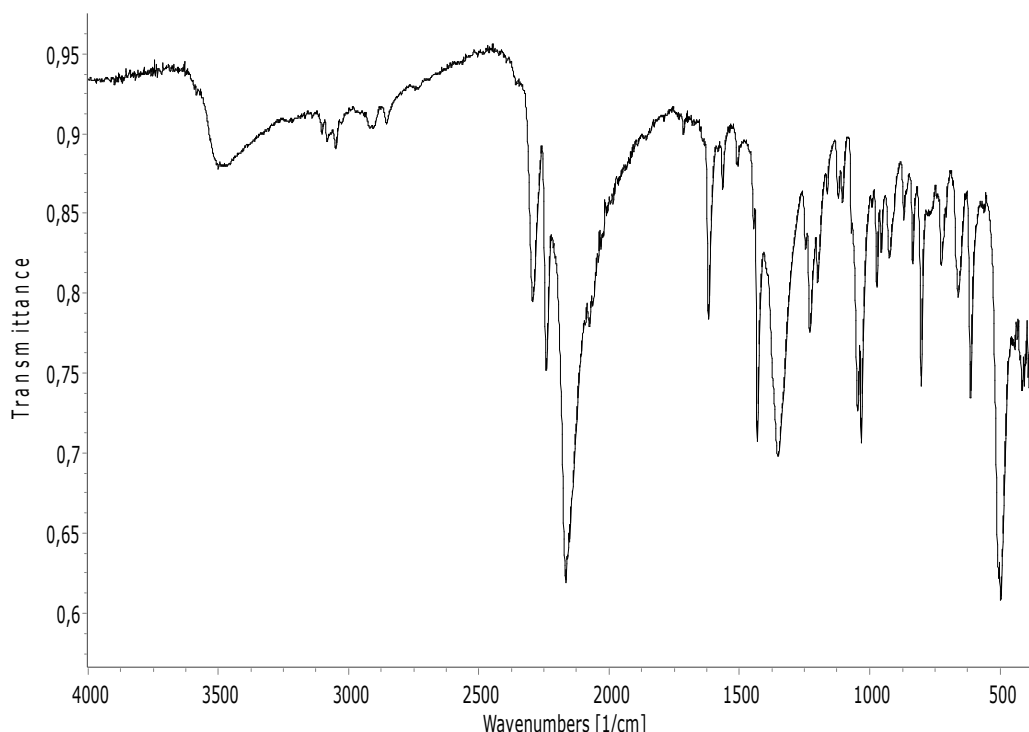


Figure 7.7.: IR spectrum of $[\text{Cu}(\text{dca})_2(4\text{-HOMepy})_2]_n$

7. 4-hydroxymethylpyridine complexes

7.3.2. Structural characterization

Selected bond parameters of $[\text{Cu}(\text{dca})_2(4\text{-HOMepy})_2]_n$ are summarized in tab. 7.5, a perspective view of a section of the polymeric chain is given in fig. 7.8 and a packing view in fig. 7.9. The Cu(1) is located on an inversion center. This metal cation is coordinated by pyridine N donor atom of two 4-methanolpyridine molecules in trans configuration and four N atoms of dicyanamide anions. The latter act in the bis- $\mu(1,5)$ -bridging mode to generate polymeric chains of polyhedra oriented along the c-axis of the monoclinic unit cell. The CuN_6 chromophore possesses an elongated square bipyramidal geometry, with short Cu(1)-N(1) and Cu(1)-N(2) bond distances of 2.014(4) and 1.990(4) Å, respectively. Its semi-coordinative Cu(1)-N(4b,c) bond distances equals 2.488(5) Å. The asymmetric dicyanamide bridges have the following bond parameters: Cu-N-C: 171.1(4) and 134.0(5)°; N-C-N: 174.8(6) and 174.1(7)°; C-N-C: 121.1(5)°; C-N(nitril) 1.148(7) and 1.147(7) Å; C-N(amide): 1.299(7) and 1.302(7) Å. The intra-chain Cu...Cu distance of 7.2754(12) Å is similar to the shortest inter-chain metal..metal separation of 7.2432(12) Å. The hydroxy-group of the pyridine derivative ligand forms hydrogen bond of type O-H · · · N to N(3) and N(4) atom of adjacent dicyanamide anions. This generates a 3D supramolecular network system (O(1)-H(90) · · · N(3#1) = 124(5)°, O(1) · · · N(3#1) = 3.199(8) Å; [O(1)-H(90) · · · N(4#2) = 141(6)°, O(1) · · · N(4#2) = 3.101(7) Å(#1): 1+x,y,z]; (#2): 1+x,1/2-y,-1/2+z).

Table 7.5.: Selected bond lengths (Å) and angles (°) for $[\text{Cu}(\text{dca})_2(4\text{-HOMepy})_2]_n$; Symmetry codes: (a) -x,1-y,-z; (b) -x,1-y,1-z; (c) x,y,-1+z; (d) x,y,1+z; (e) -x,1-y,-1-z.

Cu(1)-N(1a)	2.014(4)	Cu(1)-N(4b)	2.488(5)
Cu(1)-N(2a)	2.1990(4)	N(3)-C(7)	1.299(7)
N(2)-C(7)	1.148(7)	N(3)-C(8)	1.302(7)
N(4)-C(8)	1.147(7)		
N(2)-Cu(1)-N(1)	90.51(17)	N(2a)-Cu(1)-N(1a)	91.16(17)
N(4)-Cu(1)-N(1a)	90.37(17)	N(2)-Cu(1)-N(2a)	180.0
Cu(1)-N(2)-C(7)	171.1(4)	N(2)-C(7)-N(3)	174.8(6)
Cu(1)-N(4)-C(8)	134.0(5)	N(4)-C(8)-N(3)	174.1(7)
C(7)-N(3)-C(8)	121.1(5)		

7. 4-hydroxymethylpyridine complexes

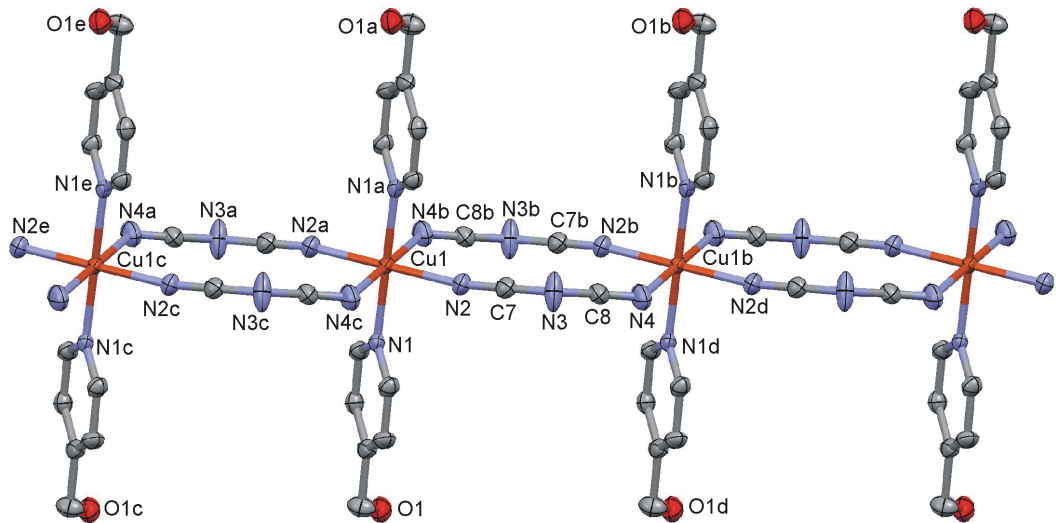


Figure 7.8.: Perspective view of a section of the polymeric chain of $[\text{Cu}(\text{dca})_2(4\text{-HOMepy})_2]_n$ together with the atom numbering scheme. Symmetry codes: (a) $-x, 1-y, -z$; (b) $-x, 1-y, 1-z$; (c) $x, y, -1+z$; (d) $x, y, 1+z$; (e) $-x, 1-y, -1-z$.

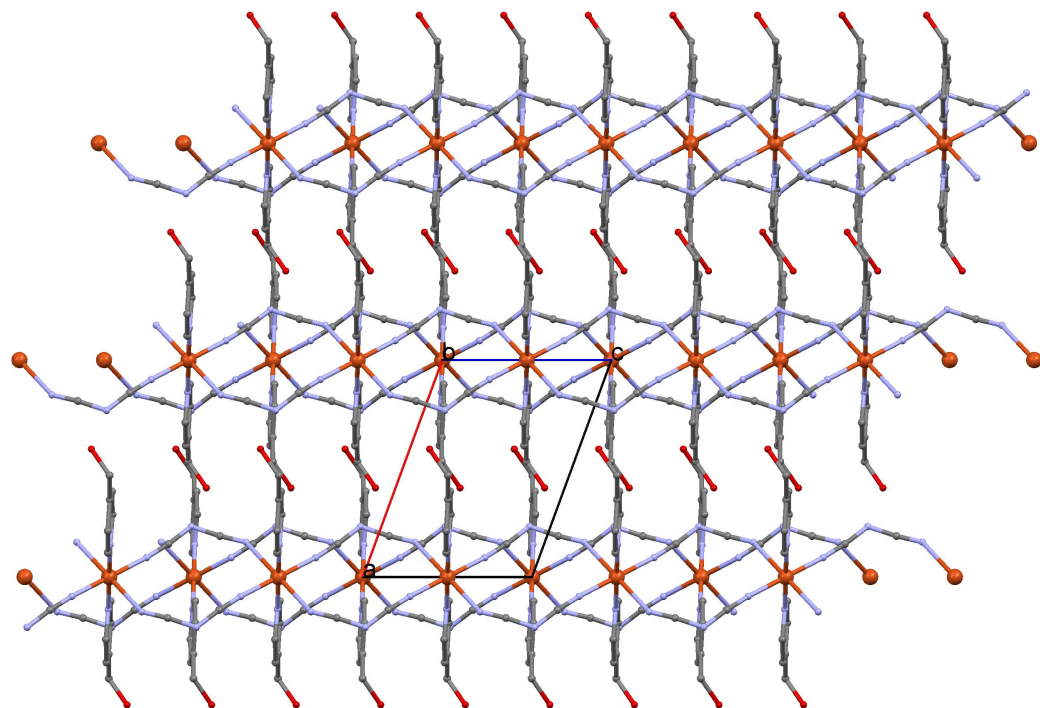


Figure 7.9.: Packing plot of $[\text{Cu}(\text{dca})_2(4\text{-HOMepy})_2]_n$

7. 4-hydroxymethylpyridine complexes

Table 7.6.: Crystallographic data and processing parameter of $[\text{Cu}(\text{dca})_2(4\text{-HOMepy})_2]_n$

Empirical formula	$\text{C}_{16}\text{H}_{14}\text{CuN}_8\text{O}_2$
Formula mass	413.90
System	monoclinic
Space group	$\text{P}2_1/\text{c}$
a (Å)	9.9292(14)
b (Å)	12.527(2)
c (Å)	7.2754(12)
α (°)	90
β (°)	110.109(7)
γ (°)	90
V (Å ³)	849.8(2)
Z	2
T (K)	100(2)
μ (mm ⁻¹)	1.317
D_{calc} (Mg/m ³)	1.618
Crystal size (mm)	0.41 x 0.26 x 0.05
θ max (°)	26.35
Data collected	6328
Unique refl./ R _{int}	1728 / 0.0533
Parameters	127
Goodness-of-Fit on F ²	1.337
R1 / wR2 (all data)	0.0743 / 0.1685
Residual extrema (e/Å ³)	1.26 / -0.95

7. 4-hydroxymethylpyridine complexes

7.4. $[\text{Cu}(\text{SCN})_2(4\text{-hydroxymethylpyridine})_2]_2$

7.4.1. Synthesis

0.48 g $\text{Cu}(\text{NO}_3)_2 \cdot 3\text{H}_2\text{O}$ (2 mmol), 0.39 g KSCN (4 mmol) and 0.44 g 4-hydroxymethyl-pyridine (4 mmol) were dissolved in 35 mL distilled H_2O . The solution was heated up to 70°C and stirred for 2 hours. After filtration the green solution was stirred again for 20 minutes at the same temperature and then cooled down to RT. After a few hours small green crystals were obtained. Anal. Calculated for $\text{C}_{28}\text{H}_{28}\text{Cu}_2\text{N}_8\text{O}_4\text{S}_4$ (795.92 g/mol) : 42.25% C; 3.55% H; 14.08% N; 16.11% S; Found: 42.19 % C; 3.58% H; 14.15 % N; 15.60% S; IR (ATR, cm^{-1}): 3456 (w), 3275 (m), 2093 (s), 1616 (m), 1561 (w), 1504 (w), 1423 (s), 1365 (m), 1195 (w), 1101 (vw), 1050 (m), 1019 (s), 801 (vs), 743 (w), 714 (w), 665 (w), 610 (m), 513 (w), 490 (m), 462 (m)

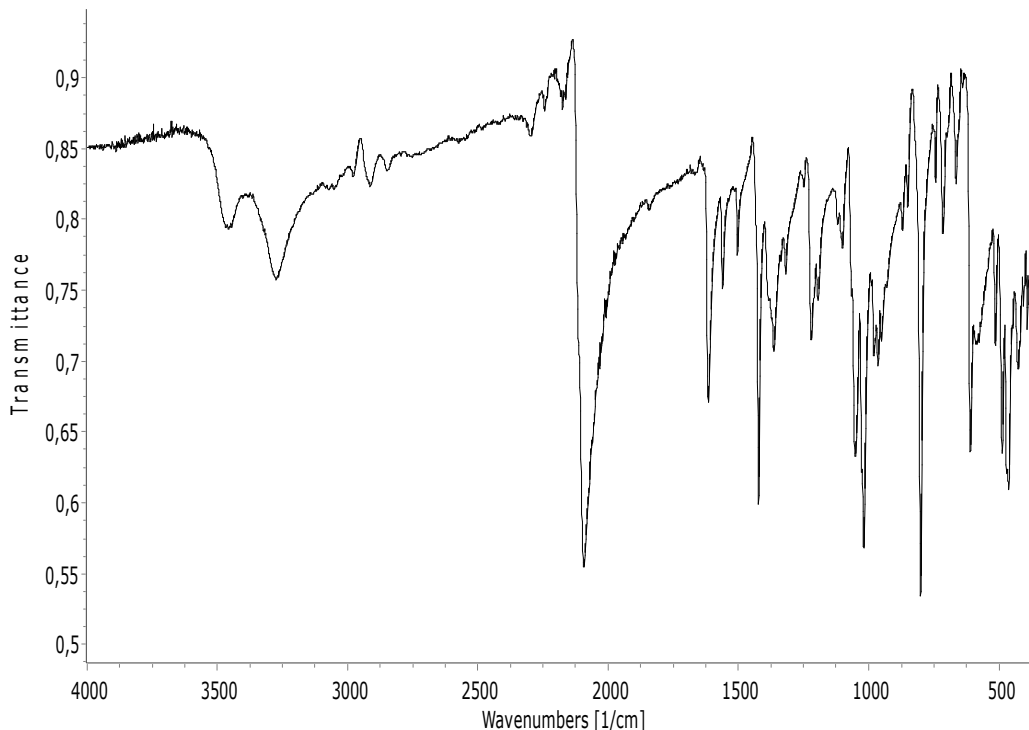


Figure 7.10.: IR spectrum of $[\text{Cu}(\text{SCN})_2(4\text{-HOMepy})_2]_2$

7. 4-hydroxymethylpyridine complexes

7.4.2. Structural characterization

A perspective view of $[\text{Cu}(\text{SCN})_2(4\text{-HOMepy})_2]_2$ is given in fig. 7.11 and a packing view in fig. 7.12. Table 7.7 lists the selected bond parameters. The Cu(1) metal center is penta-coordinated by N(1) and N(2) atoms of two terminal isothiocyanato anions, by N(3) of a terminal 4-hydroxymethylpyridine molecule and further by O(2) and N(4') atoms of two μ (N,O)-bridging 4-hydroxymethylpyridine molecules. The latter connect Cu(1) and Cu(1') polyhedra to form centrosymmetric dinuclear units. The CuN_4O chromophore may be described as slightly distorted square pyramid (SP) with a τ -value of 0.03 (τ -values of 1 and 0 refer to ideal geometries of trigonal bipyramidal (TBP) and square pyramid (SP), respectively) [72]. The apical site is occupied by O(2) [$\text{Cu}(1)\text{-O}(2) = 2.379(4)$ Å]. The basal Cu-N bond distances are in the range of 1.954(4) to 2.041(4) Å. The terminal isothiocyanate anions possess the following bond parameters: N-C: 1.138(6) and 1.156(6) Å, C-S: 1.644(4) and 1.637(4) Å, Cu-N-C: 170.8(4) and 169.0(4)°, N-C-S: 178.0(5) and 178.7(4)°. The $\text{Cu}(1) \cdots \text{Cu}(1')$ distance is 7.9083(14) Å and the shortest inter-dinuclear metal-metal separation is 5.8666(12) Å. Along the c-axis the $\text{Cu}(1) \cdots \text{S}(2c)$ separation is 3.1172(16) Å. Hydrogen bonds of type O-H \cdots S between hydroxy-groups of pyridine derivative ligands and adjacent non-coordinated S atoms of terminal isothiocyanate anions form a supramolecular 2D system oriented along the b- and c-axis of the monoclinic unit cell ($\text{O}(1)\text{-H}(91) \cdots \text{S}(2\#1) = 155(3)$ °, $\text{O}(1) \cdots \text{S}(2\#1) = 3.454(4)$ Å; $\text{O}(2)\text{-H}(92) \cdots \text{S}(1\#2) = 172(3)$ °, $\text{O}(2) \cdots \text{S}(1\#2) = 3.168(3)$ Å; (#1): $x, 1/2 - y, 1/2 + z$; (#2): $x, 1/2 - y, -1/2 + z$). $\text{Cu}(\text{SCN})_2(4\text{-HOMepy})_2$ is isostructural to the corresponding Co(II) complex.

7. 4-hydroxymethylpyridine complexes

Table 7.7.: Selected bond lengths (Å) and angles (°) for $[\text{Cu}(\text{SCN})_2(4\text{-HOMepy})_2]_2$.

$\text{Cu}(1)\text{-N}(1)$	1.973(4)	$\text{Cu}(1)\text{-N}(4')$	2.041(4)
$\text{Cu}(1)\text{-N}(2)$	1.954(4)	$\text{Cu}(1)\text{-O}(2)$	2.379(4)
$\text{Cu}(1)\text{-N}(3)$	2.028(4)	$\text{S}(1)\text{-C}(1)$	1.644(4)
$\text{N}(1)\text{-C}(1)$	1.138(6)	$\text{S}(2)\text{-C}(2)$	1.637(5)
$\text{N}(2)\text{-C}(2)$	1.156(6)		
$\text{N}(2)\text{-Cu}(1)\text{-N}(1)$	177.58(18)	$\text{N}(2)\text{-Cu}(1)\text{-N}(3)$	88.83(16)
$\text{N}(1)\text{-Cu}(1)\text{-N}(3)$	88.87(16)	$\text{N}(2)\text{-Cu}(1)\text{-N}(4')$	91.78(16)
$\text{N}(1)\text{-Cu}(1)\text{-N}(4')$	90.52(16)	$\text{N}(3)\text{-Cu}(1)\text{-N}(4')$	179.39(16)
$\text{N}(2)\text{-Cu}(1)\text{-O}(2)$	93.01(15)	$\text{N}(1)\text{-Cu}(1)\text{-O}(2)$	87.81(15)
$\text{N}(3)\text{-Cu}(1)\text{-O}(2)$	92.30(14)	$\text{N}(4)\text{-Cu}(1)\text{-O}(2')$	87.69(15)
$\text{Cu}(1)\text{-N}(1)\text{-C}(1)$	170.8(4)	$\text{N}(1)\text{-C}(1)\text{-S}(1)$	178.0(5)
$\text{Cu}(1)\text{-N}(2)\text{-C}(2)$	169.0(4)	$\text{N}(2)\text{-C}(2)\text{-S}(2)$	178.7(4)

7. 4-hydroxymethylpyridine complexes

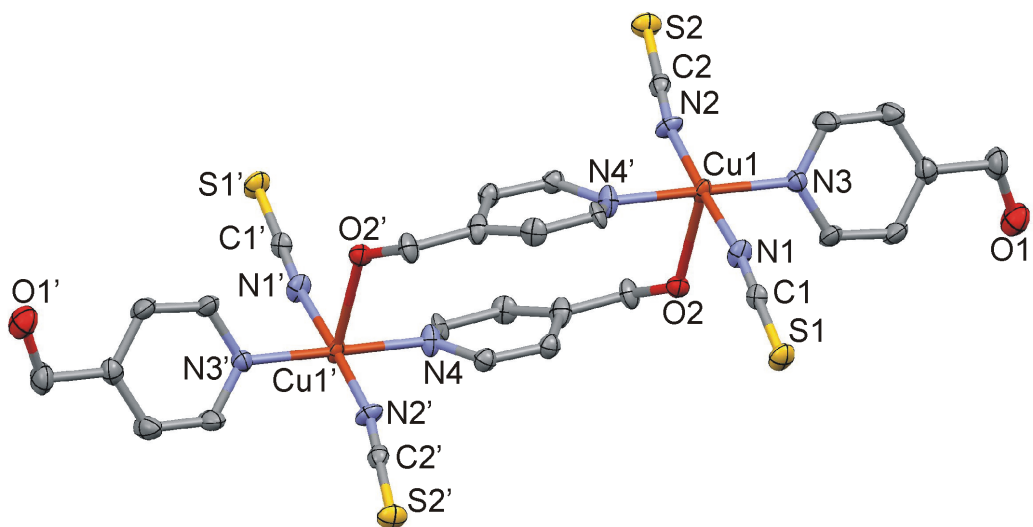


Figure 7.11.: Perspective view of $[\text{Cu}(\text{SCN})_2(4\text{-HOMepy})_2]_2$ with the atom numbering scheme. Symmetry codes: (') $1-x, 1-y, 1-z$.

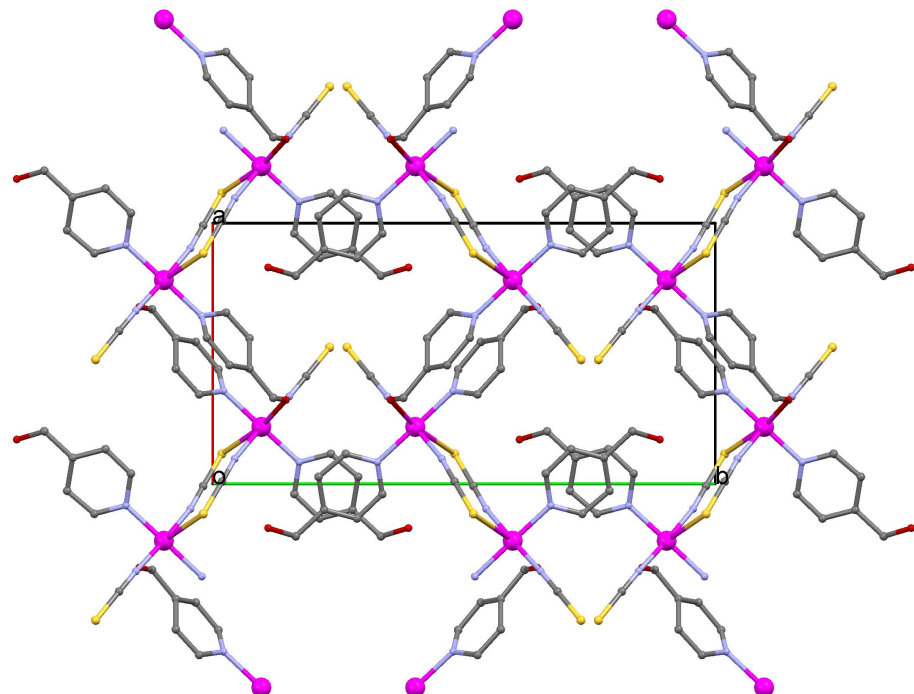


Figure 7.12.: Packing plot of $[\text{Cu}(\text{SCN})_2(4\text{-HOMepy})_2]_2$.

7. 4-hydroxymethylpyridine complexes

Table 7.8.: Crystallographic data and processing parameter of $[\text{Cu}(\text{SCN})_2(4\text{-HOMepy})_2]_2$

Empirical formula	$\text{C}_{28}\text{H}_{28}\text{Cu}_2\text{N}_8\text{O}_4\text{S}_4$
Formula mass	795.92
System	monoclinic
Space group	$\text{P}2_1/c$
a (Å)	10.9582(14)
b (Å)	19.6859(18)
c (Å)	8.0786(12)
α (°)	90
β (°)	111.469(2)
γ (°)	90
V (Å ³)	1621.8(4)
Z	2
T (K)	100(2)
μ (mm ⁻¹)	1.617
D_{calc} (Mg/m ³)	1.630
Crystal size (mm)	0.26 x 0.20 x 0.13
θ max (°)	25.28
Data collected	11792
Unique refl./ R _{int}	2934 / 0.0714
Parameters	250
Goodness-of-Fit on F ²	1.360
R1 / wR2 (all data)	0.0880 / 0.1735
Residual extrema (e/Å ³)	0.99 / -0.73

7. 4-hydroxymethylpyridine complexes

7.5. $[\text{Zn}(\text{SCN})_2(4\text{-hydroxymethylpyridine})_2]$

7.5.1. Synthesis

0.13 g ZnCl_2 (1 mmol), 0.19 g KSCN (2 mmol) and 0.22 g 4-OH-Me-py (2 mmol) were dissolved in 15 mL distilled H_2O . The solution was heated up to 50-60°C and stirred for 1 hour. After filtration the clear solution was stirred again for 1 hour (50°C) and then cooled down to RT. After 24 hours clear white crystals were obtained. Anal. Calculated for $\text{C}_{14}\text{H}_{14}\text{N}_4\text{O}_2\text{S}_2\text{Zn}$ (399.80 g/mol) : 42.06% C; 3.53% H; 14.01% N; 16.04 % S; Found: 41.84 % C; 3.54% H; 14.00 % N; 15.89% S; IR (ATR, cm^{-1}): 3409 (s), 2075 (s), 1621 (s), 1562 (w), 1508 (vw), 1452 (w), 1429 (m), 1340 (w), 1277 (w), 1224 (m), 1105 (w), 1034 (s), 949 (w), 807 (m), 722 (w), 657 (vw), 607 (m), 472 (s)

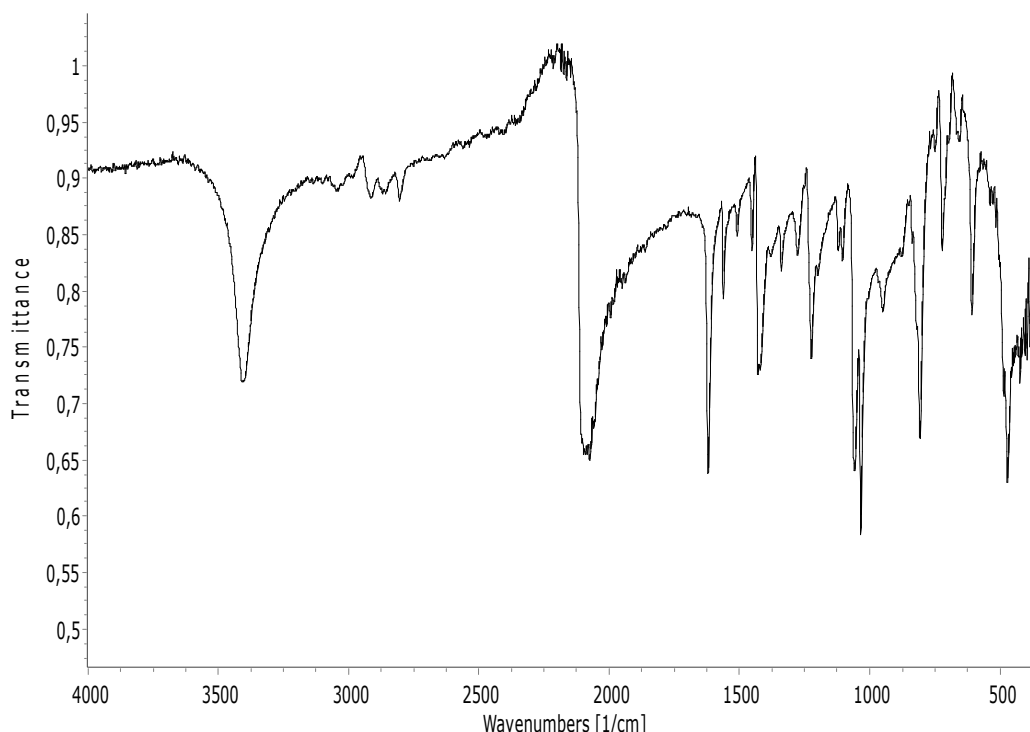


Figure 7.13.: IR spectrum of $[\text{Zn}(\text{SCN})_2(4\text{-HOMepy})_2]$

7. 4-hydroxymethylpyridine complexes

7.5.2. Structural characterization

The crystal structure of $[\text{Zn}(\text{SCN})_2(4\text{-HOMepy})_2]$ consists of two crystallographically independent mononuclear and neutral Zn(II) complexes. A packing view is shown in fig. 7.14, a perspective view in fig. 7.14 and selected bond parameters are listed in table 7.9. Each Zn(1) is tetrahedrally coordinated by N atoms of two terminal isothiocyanato anions, and by N atoms of two neutral 4-hydroxymethylpyridine molecules. The Zn-N bond distances range from 1.939(2) to 2.019(2) Å, and the bond angles within the ZnN_4 tetrahedron vary from 103.81(9) to 124.28(15)°. The bond parameters of terminal N-coordinated NCS- anions are: Zn-N-C = 169.0(2) and 174.3(2)°, N-C-S = 177.8(3) and 177.6(3)°, N-C = 1.159(4) and 1.158(4) Å, C-S = 1.627(3) and 1.627(3) Å. The shortest metal-metal separation is 5.0296(9) Å. Hydrogen bonds of type O-H · · · S form a supramolecular 2D system [O(1)-H(91) · · · S(2#1)(#1: x,2-y,1/2+z) = 165(5)°, O(1) · · · S(2#1) = 3.238(3) Å; O(2)-H(92) · · · S(1#2)(#2: x,-1-y,-1/2+z) = 162(3)°, O(1) · · · S(2#1) = 3.263(3) Å].

Table 7.9.: Selected bond lengths (Å) and angles (°) for $[\text{Zn}(\text{SCN})_2(4\text{-HOMepy})_2]$; Symmetry codes: '): -x,y,-z+1/2; ''): 1-x,y,-z+1/2

Zn(1)-N(1')	1.939(2)	Zn(2)-N(2'')	1.943(2)
Zn(1)-N(3)	2.019(2)	Zn(2)-(N(4))	2.018(2)
N(1)-C(1)	1.159(4)	S(1)-C(1)	1.627(3)
N(2)-C(2)	1.158(4)	S(2)-C(2)	1.627(3)
N(1)-Zn(1)-N(1')	124.28(15)	N(2)-Zn(2)-N(2'')	121.03(15)
N(1')-Zn(1)-N(3)	105.90(10)	N(2'')-Zn(2)-N(4)	103.53(9)
N(1')-Zn(1)-N(3')	105.23(9)	N(2'')-Zn(2)-N(4'')	108.81(9)
Zn(1)-N(11)-N(12)	109.92(13)	N(4)-Zn(2)-N(4'')	111.17(13)
Zn(1)-N(1)-C(1)	169.0(2)	N(1)-C(1)-S(1)	177.8(3)
Zn(2)-N(2)-C(2)	174.3(2)	N(21)-C(2)-S(2)	177.6(3)

7. 4-hydroxymethylpyridine complexes

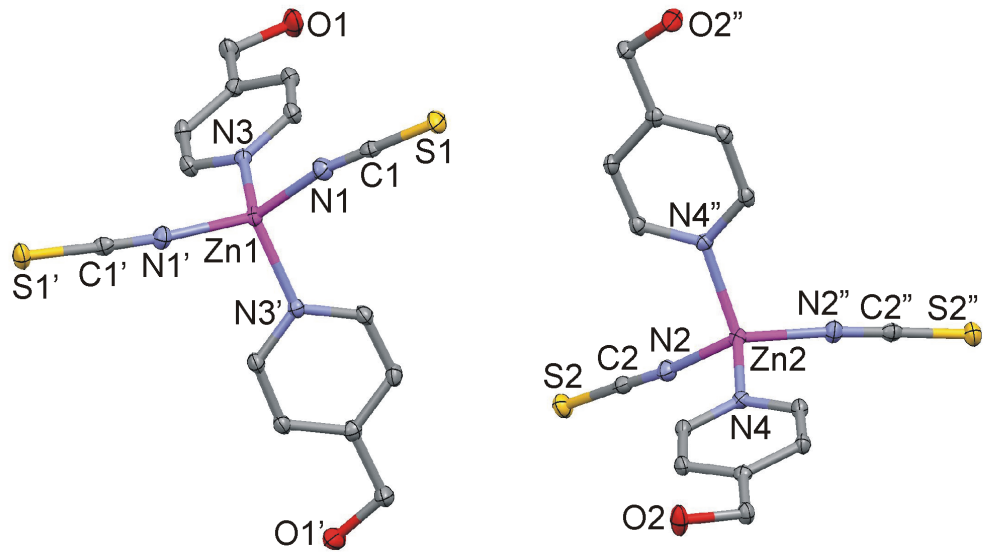


Figure 7.14.: Perspective view of $[\text{Zn}(\text{SCN})_2(4\text{-HOMepy})_2]$ with the atom numbering scheme. Symmetry codes: (''): $-x, y, -z + 1/2$; ('''): $1-x, y, -z + 1/2$.

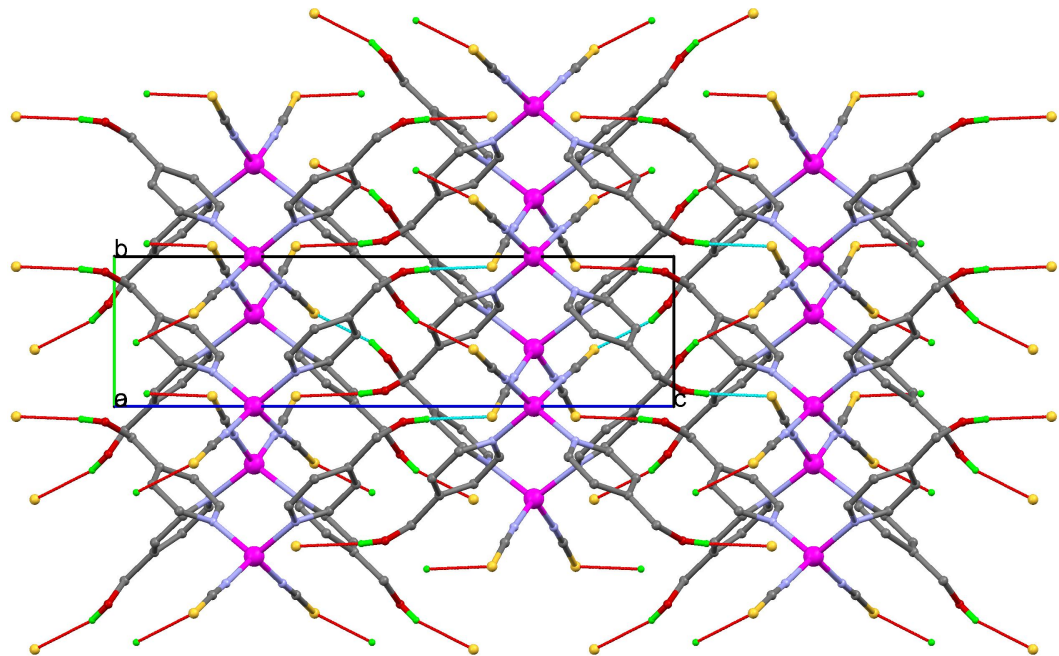


Figure 7.15.: Packing view of $[\text{Zn}(\text{SCN})_2(4\text{-HOMepy})_2]$

7. 4-hydroxymethylpyridine complexes

Table 7.10.: Crystallographic data and processing parameter of $[\text{Zn}(\text{SCN})_2(4\text{-HOMepy})_2]$

Empirical formula	$\text{C}_{14}\text{H}_{14}\text{N}_4\text{O}_2\text{S}_2\text{Zn}$
Formula mass	399.80
System	monoclinic
Space group	P2/c
a (Å)	18.349(2)
b (Å)	5.0296(7)
c (Å)	24.937(3)
α (°)	90
β (°)	161.136(4)
γ (°)	90
V (Å ³)	1733.3(4)
Z	4
T (K)	100(2)
μ (mm ⁻¹)	1.670
D _{calc} (Mg/m ³)	1.532
Crystal size (mm)	0.27 × 0.19 × 0.11
θ max (°)	26.33
Data collected	12908
Unique refl./ R _{int}	3529 / 0.0403
Parameters	215
Goodness-of-Fit on F ²	1.112
R1 / wR2 (all data)	0.0429 / 0.0973
Residual extrema (e/Å ³)	0.84 / -0.44

8. UV-VIS spectra

The synthesized complexes were investigated via UV-VIS-spectroscopy. No absorption bands were observed in the UV-Vis-spectra of the colorless complexes of Zn and Cd. Cobalt and azide-copper complexes showed three and one absorption band, respectively. The spectra are shown in the appendix and the absorption bands of cobalt complexes are found in table 8.1.

Table 8.1.: Absorption bands of cobalt complexes in nm

complex	structure	v ₃	v ₂	v ₁
Co(N ₃) ₂ (4-Me-O-py) ₄	octahedral	337	505	1137
Co(OCN) ₂ (4-Me-O-py) ₄	octahedral	302	484	1063
Co(SCN) ₂ (4-Me-O-py) ₄	octahedral	324	494	1049
Co(dca) ₂ (4-HO-Me-py) ₂	octahedral	314	483	1051

The ligand-field splitting parameter Dq and the Racah-parameter B [73] were calculated for Co complexes (d⁷ with octahedral structure) using eq. 8.1 and 8.2.

$$34Dq^2 + 18(v_2 - 2 * v_1)Dq + v_1^2 - v_1 * v_2 = 0 \quad (8.1)$$

$$B = \frac{v_2 - 2v_1 + 30Dq}{15} \quad (8.2)$$

The calculated Dq and B-values are listed in table 8.2. The allowed transitions are ⁴T_{1g}(F) → ⁴T_{2g}(F), ⁴T_{1g}(F) → ⁴T_{2g}(P) and ⁴T_{1g}(F) → ⁴A_{2g}. The

8. UV-VIS spectra

Co complexes don't possess perfect octahedral structures, therefore the calculated Dq and B-values don't fit in the Tanabe-Sugano-diagramm in figure 8.1

Table 8.2.: Dq and Racah-parameter(B) of the Co complexes in cm^{-1}

complex	Dq	B
$\text{Co}(\text{N}_3)_2(4\text{-Me-O-py})_4$	478	1104
$\text{Co}(\text{OCN})_2(4\text{-Me-O-py})_4$	511	1146
$\text{Co}(\text{SCN})_2(4\text{-Me-O-py})_4$	518	1113
$\text{Co}(\text{dca})_2(4\text{-HO-Me-py})_2$	517	1145

8. UV-VIS spectra

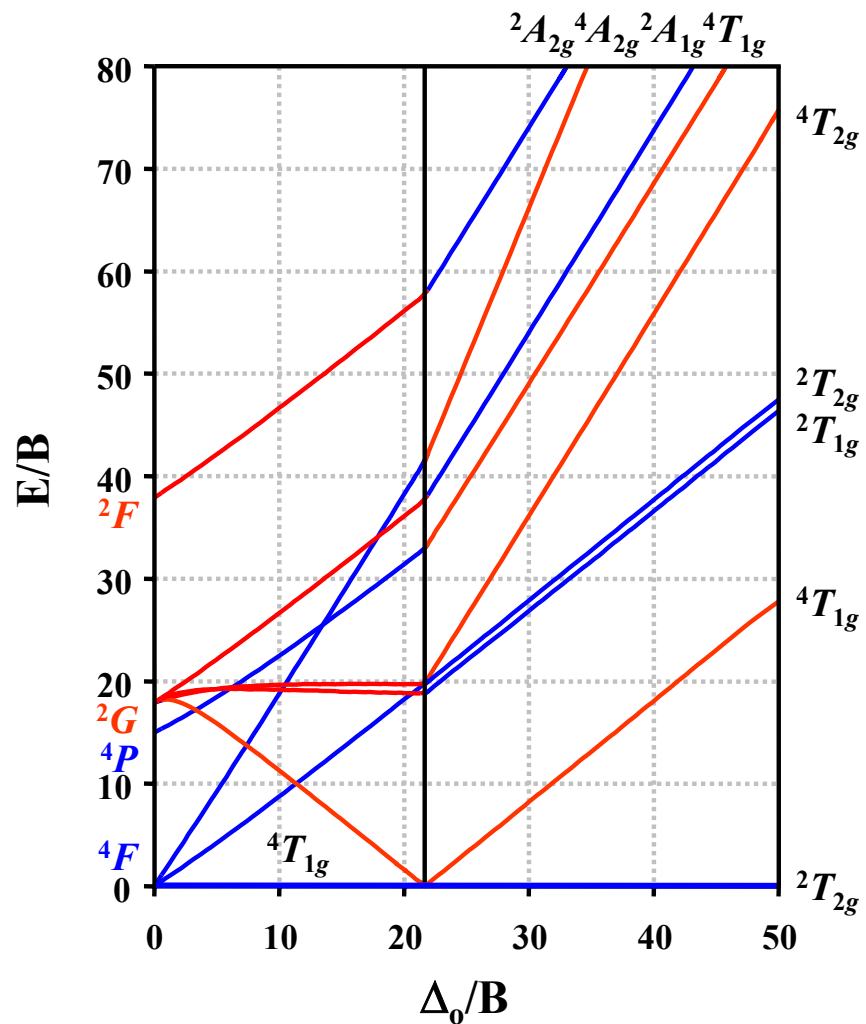


Figure 8.1.: Tanabe-Sugano-Diagramm of the d^7 - configuration of an octahedral structure [74]

9. Discussion

9.1. Dicyanamide complexes

Table 9.2 contains a list of in the CCDC published dicyanamide complexes [1] which possess a similar ligand arrangement as the five newly synthesized dca complexes in table 9.1. The central metal atom is coordinated to the terminal N-atoms of $4\text{N}\equiv\text{C}-\text{N}^--\text{C}\equiv\text{N}$ and to two other ligands in trans-configuration. In the new compounds these ligands are 4-methoxypyridine and 4-hydroxy-methyl-pyridine, whose N-atoms act as electron pair donor. The N-atoms on the ends of the dca are connected to the central metal atoms and make an end-to end-bridge between these. The metal doesn't bind to the middle N-atom of the dca ligand. The atom-atom-distances are ranging from 2.0 to 2.5 Å(M-N) and 1.1 to 1.3 (N-C). The angles are ranging from 174 to 177 ° (N-C-N angle), 134 to 175 ° (M-N-C), 90 to 180 ° (N-M-N) and 114 to 121 (C-N-C).

Table 9.1.: List of newly synthesized dca complexes

Compound name
$[\text{Cd}(\text{dca})_2(4\text{-methoxypyridine})_2]_n$
$[\text{Cu}(\text{dca})_2(4\text{-methoxypyridine})_2]_n$
$[\text{Zn}(\text{dca})_2(4\text{-methoxypyridine})_2]_n$
$[\text{Co}(\text{dca})_2(4\text{-hydroxymethylpyridine})_2]_n$
$[\text{Cu}(\text{dca})_2(4\text{-hydroxymethylpyridine})_2]_n$

9. Discussion

Table 9.2.: List of structures of in the CCDC published dca complexes [1]

Compound name	Identifier
catena-(bis((μ_2 -Cyanocyanamido-N ₁ ,N ₅)-(1H-imidazol-3-yl))-nickel) [75]	BUHZUA
catena-(bis(μ_2 -Dicyanamide)-dipyridyl-manganese(II)) [76]	CERDUY
catena-(bis(μ_2 -Dicyanamido)-bis(imidazole-N ₃)-cadmium) [77]	EMIMUJ
catena-(bis(μ_2 -1,5-Dicyanamido)-bis(methanol)-copper(II)) [78]	HETREE
catena-[tetrakis(μ_2 -Dicyanamido)-bis(m ₂ -4,4'-ditriazolylmethane)-di-manganese(II)] [79]	IPEFAK
catena-(bis(μ_2 -Dicyanamido-N,N'')-bis(2-aminopyrimidine)-copper(II)) [80]	KEQWIM
catena-(bis((μ_2 -Cyanocyanamido-N ₁ ,N ₅)-(1H-imidazol-3-yl))-cobalt) [81]	KUHXIV01
catena-(bis(μ_2 -Dicyanamide)-bis(3-cyanopyridine)-copper(II)) [82]	LAPGAL
catena-[bis(μ_2 -dicyanamido)-bis(quinoxaline)-zinc] [83]	NODJAT

9. Discussion

9.2. 4-MOP and 4-HOMP complexes

This chapter refers to the publications in the CCDC regarding 4-MOP and 4-HOMP complexes shown in table 4.1 (chapter 4.1) and table 4.2 (chapter 4.2). [1] For 4-hydroxy-methyl-pyridine the most common central metal atoms were: copper (9 complexes), Pt (7 complexes), Ni (6 complexes) and Ag (5 complexes). The 4-methoxypyridine complexes offer a wider range in metal atoms like platinum, cobalt, ruthenium or rhenium, to name a few. Other ligands used in these complexes were small ligands like chloride, rhodanide or nitrate and big ligands such as other pyridines. The coordination number ranges from 2 to 6.

Table 9.3 shows the complexes synthesized for this work, of which nine were 4-MOP and five were 4-HOMP complexes. The pseudohalides azide, cyanate, dicyanamide and rhodanide were used as ligands. Some of the ligands like azide, dicyanamide, rhodanide and 4-hydroxymethyl-pyridine acted as bridging ligands connecting metal centers. In the dimeric complex $[\text{Cu}(\text{NCS})_2(4\text{-hydroxymethylpyridine})_2]_2$ the organic ligand act as N,O-bridge, in the other 13 structures of the master thesis the two pyridine derivative ligands function as N-terminal ligands only.

9. Discussion

Table 9.3.: Structures of newly synthesized 4-methoxypyridine and 4-hydroxymethylpyridine complexes

[Co(N ₃) ₂ (4-methoxypyridine) ₄]
[Cu(N ₃) ₂ (4-methoxypyridine) ₂] _n
[Zn(N ₃) ₂ (4-methoxypyridine) ₂]
[Co(OCN) ₂ (4-methoxypyridine) ₄]
[Cd(dca) ₂ (4-methoxypyridine) ₂] _n
[Cu(dca) ₂ (4-methoxypyridine) ₂] _n
[Zn(dca) ₂ (4-methoxypyridine) ₂] _n
[Co(SCN) ₂ (4-methoxypyridine) ₄]
[Cu(SCN) ₂ (4-methoxypyridine) ₂] _n
[Cu(N ₃) ₂ (4-hydroxymethylpyridine)] _n
[Co(dca) ₂ (4-hydroxymethylpyridine) ₂] _n
[Cu(dca) ₂ (4-hydroxymethylpyridine) ₂] _n
[Cu(SCN) ₂ (4-hydroxymethylpyridine) ₂] ₂
[Zn(SCN) ₂ (4-hydroxymethylpyridine) ₂]

10. Summary

14 pseudohalide complexes with 4-methoxypyridine and 4-hydroxy-methylpyridine as coligands were synthesized. This was conducted using the transition metals copper, zinc, cadmium and cobalt as metal center and the pseudohalides azide, rhodanide, dicyanamide and cyanate as ligands. Most complexes possess an octahedral structure, two a tetrahedral and two had the rare coordination number five with a structure between square pyramidal and trigonal bipyramidal.

The crystal structure was solved via single crystal X-ray diffraction; the 4-methoxypyridine complexes are triclinic crystal systems (with the exception of an orthorombic one). One triclinic system aside, the 4-hydroxymethylpyridine complexes are monoclinic.

All 14 complexes were obtained from aqueous solutions, but water molecules were not incorporated in the crystal structures, neither as aqua ligands nor as lattice water molecules. This is due to the two pyridine derivatives which are stronger ligands than water.

The five dicyanamide complexes form a structured series of polymeric chains (1D). In the tetrahedral zinc(II) and octahedral cobalt(II) mononuclear complexes the three-atomic pseudohalide anions N_3^- act as N-terminal ligands only. The copper azide complexes are polyhedral with the azide in bis- μ -1,1-bridging mode in the 4-MOP complex and bis- μ -1,3-bridging mode in the 4-HOMP complex.

Among the four rhodanide complexes one possesses two hydroxymethylpyridines as bridging ligands, resulting in a dimeric structure and one with the

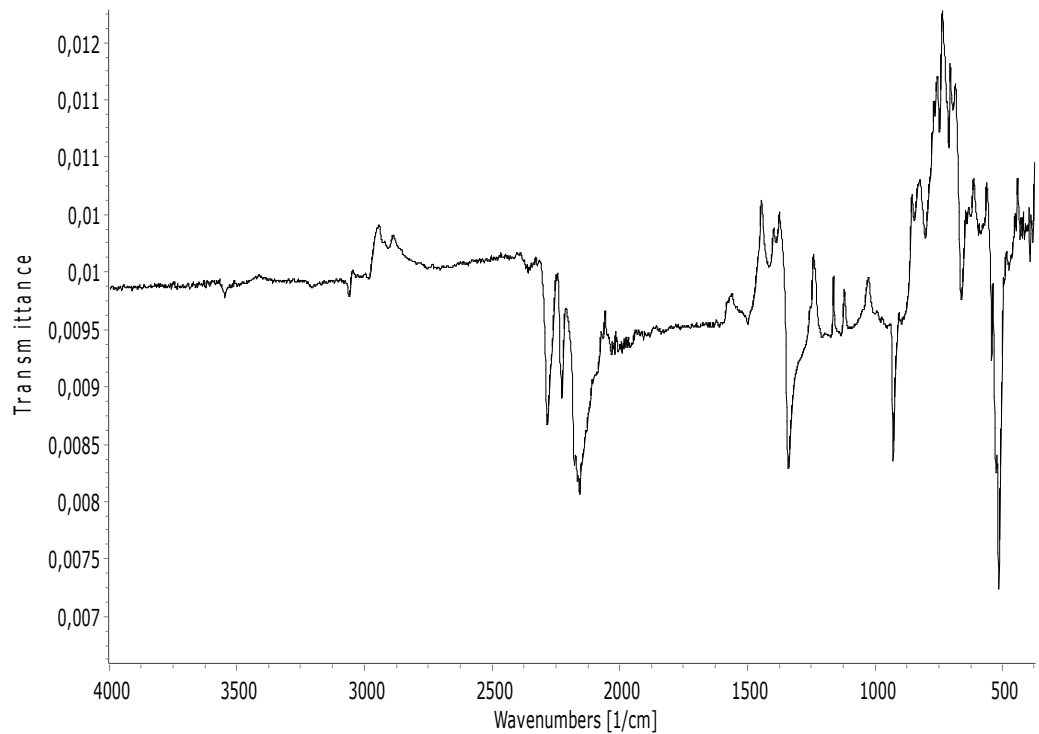
10. Summary

SCN^- ligand in bridging mode creating a 2D-sublattice. The other two are monomeric structures in which SCN^- is a terminal ligand (R-N-C-S). In one complex cyanate act as a pseudohalide ligand in an octahedral monomeric structure.

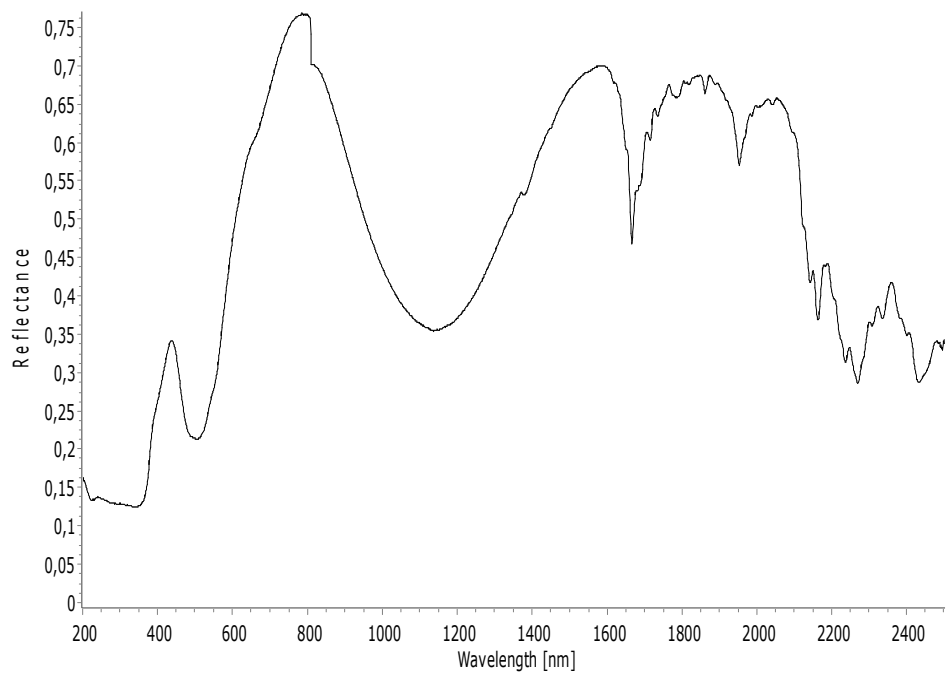
Using UV-Vis spectroscopy, 3 absorption bands are observed for cobalt and one for copper-azide complexes. The colorless zinc and cadmium compounds have no absorption bands in the visible and ultraviolet spectrum.

Appendix

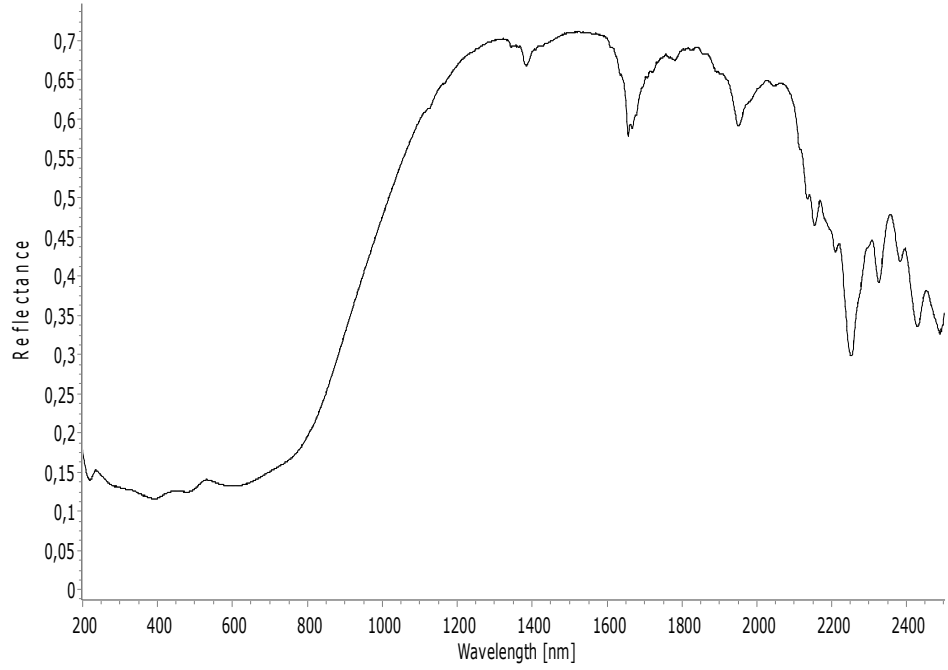
IR (ATR, cm^{-1}): 2284 (m), 2228 (m), 2157(s), 1340(s), 929 (s), 662 (w), 515 (vs)



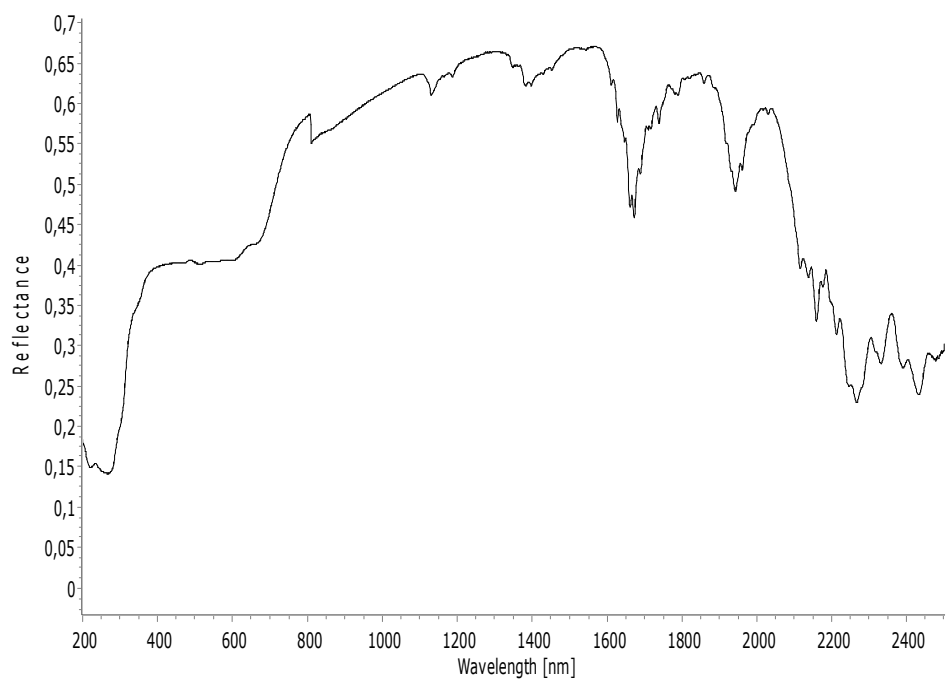
IR spectrum of sodium dicyanamide



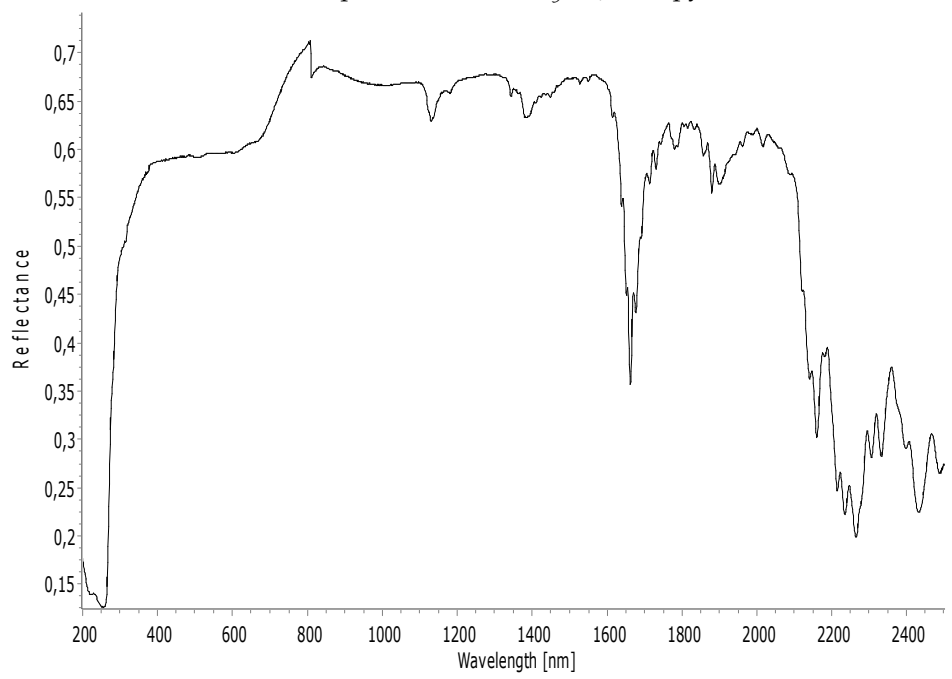
UV-VIS-spectrum of $[\text{Co}(\text{N}_3)_2(4\text{-MeOpy})_4]$



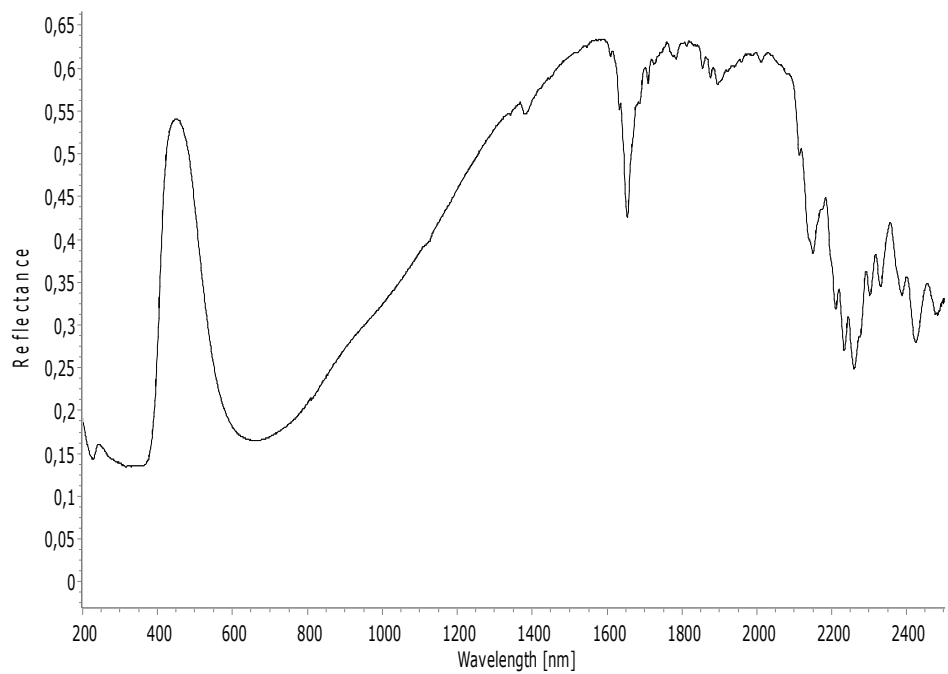
UV-VIS spectrum of $[\text{Cu}(\text{N}_3)_2(4\text{-MeOpy})_2]_n$



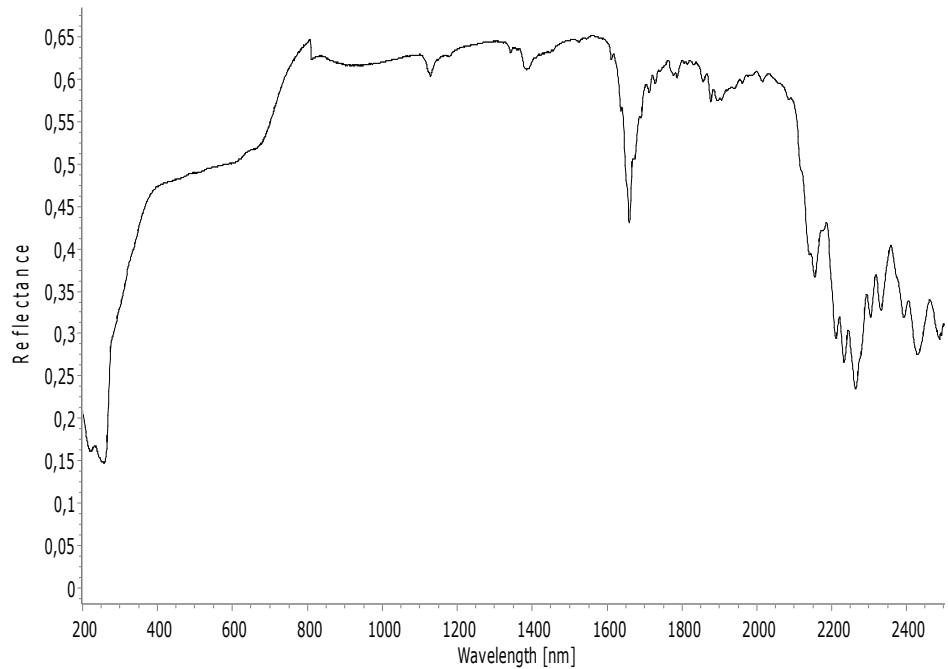
UV-VIS-spectrum of $[\text{Zn}(\text{N}_3)_2(4\text{-MeOpy})_2]$



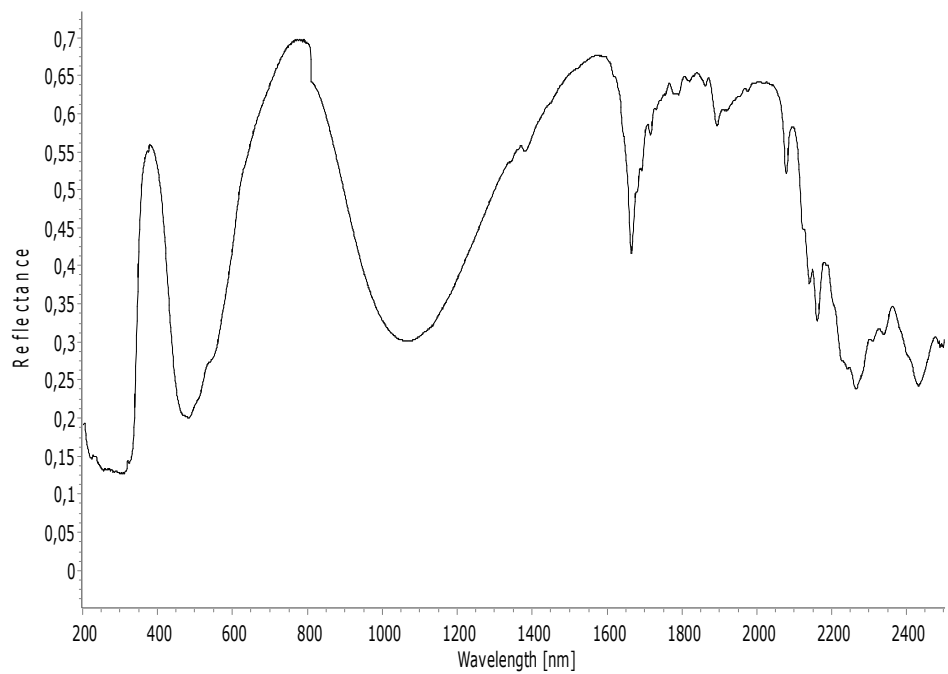
UV-VIS spectrum of $[\text{Cd}(\text{dca})_2(4\text{-MeOpy})_2]_n$



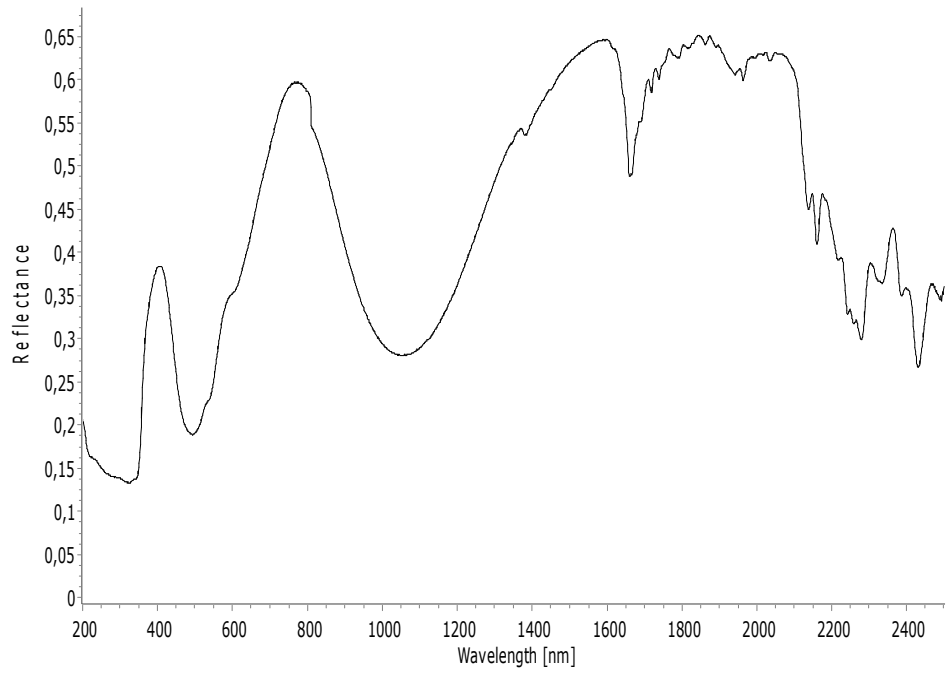
UV-VIS-spectrum of $[\text{Cu}(\text{dca})_2(4\text{-MeOpy})_2]_n$



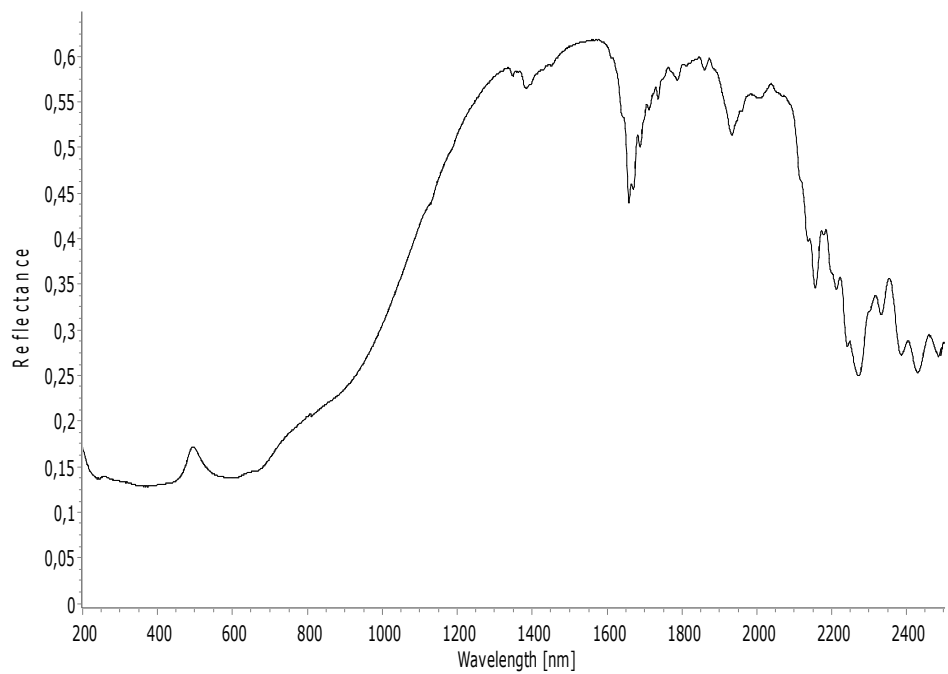
UV-VIS spectrum of $[\text{Zn}(\text{dca})_2(4\text{-MeOpy})_2]_n$



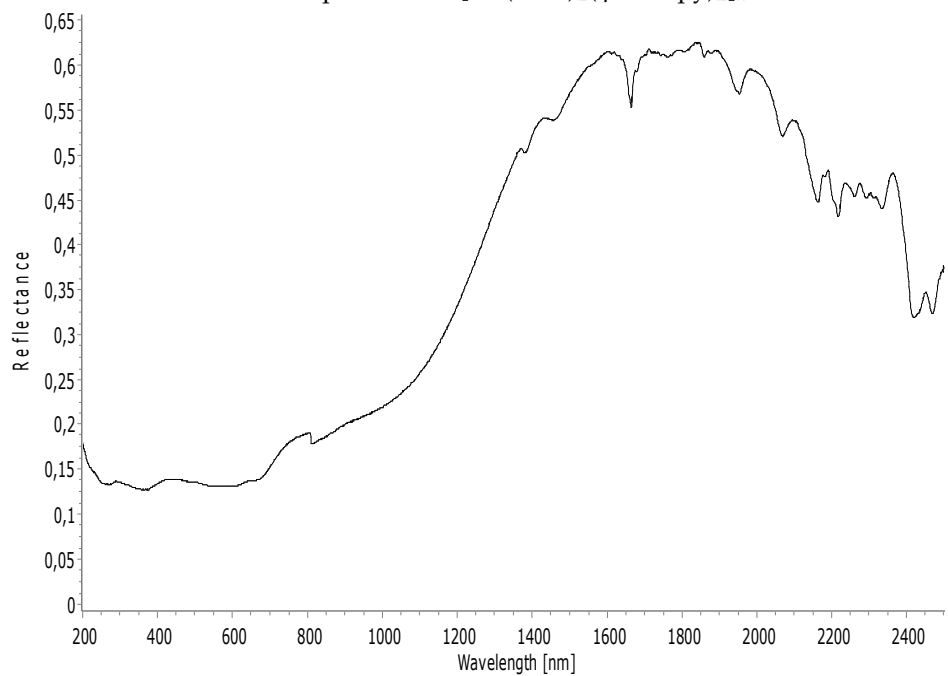
UV-VIS spectrum of $[\text{Co}(\text{OCN})_2(4\text{-MeOpy})_4]$



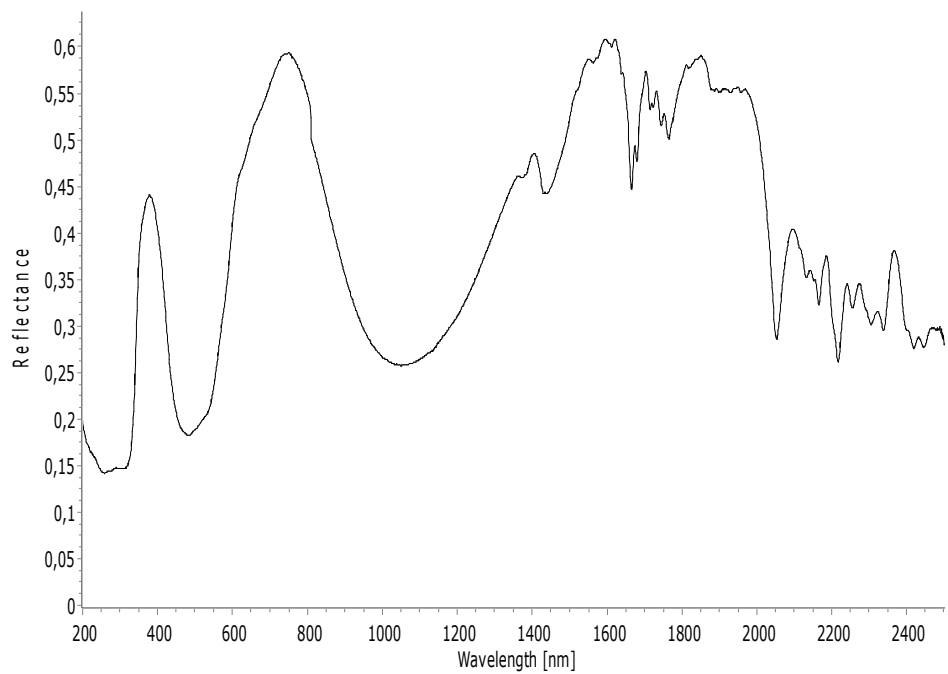
UV-VIS spectrum of $[\text{Co}(\text{SCN})_2(4\text{-MeOpy})_4]$



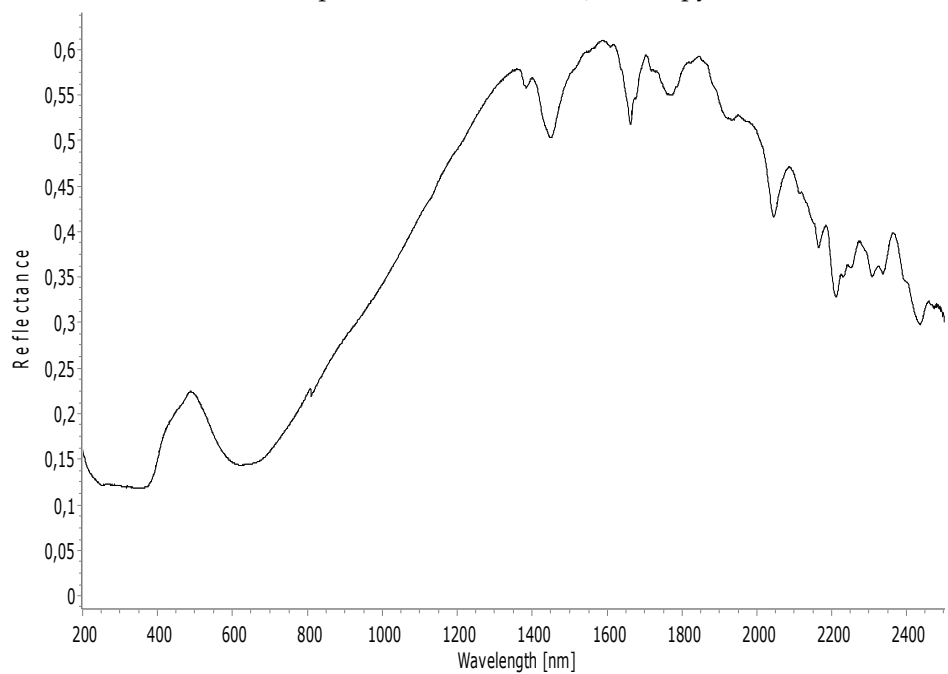
UV-VIS spectrum of $[\text{Cu}(\text{SCN})_2(4\text{-MeOpy})_2]_n$



UV-VIS spectrum of $[\text{Cu}(\text{N}_3)_2(4\text{-HOMepy})]_n$



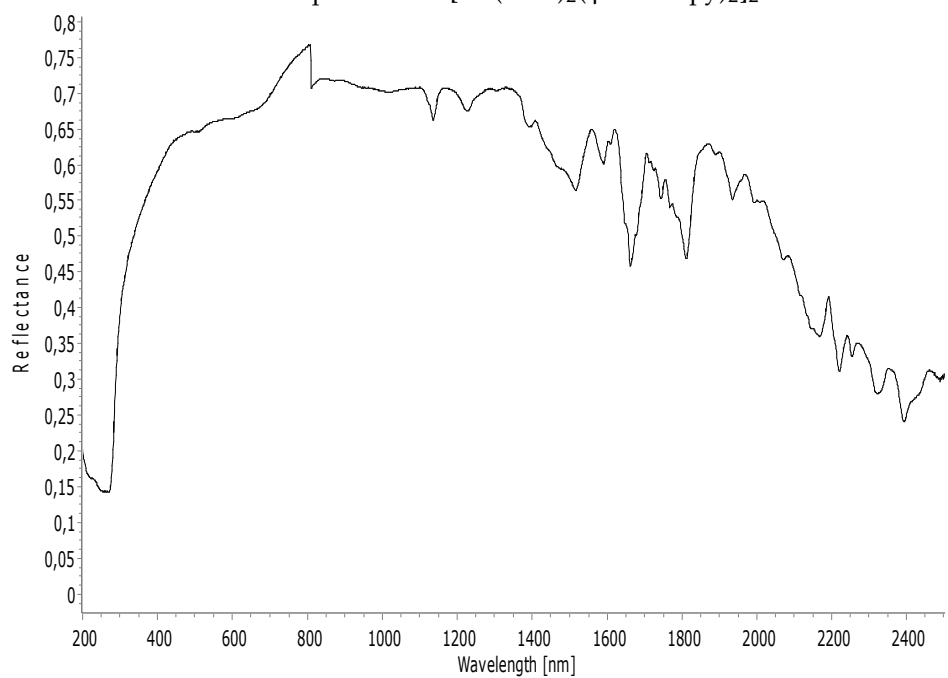
UV-VIS spectrum of $[\text{Co}(\text{dca})_2(4\text{-HOMepy})_2]_n$



UV-VIS spectrum of $[\text{Cu}(\text{dca})_2(4\text{-HOMepy})_2]_n$



UV-VIS spectrum of $[\text{Cu}(\text{SCN})_2(4\text{-HOMepy})_2]_2$



UV-VIS spectrum of $[\text{Zn}(\text{SCN})_2(4\text{-HOMepy})_2]$

Bibliography

- [1] C. R. Groom, I. J. Bruno, M. P. Lightfoot, S. Ward, *Acta Crystallogr.* **2016**, *B72*, 171–179.
- [2] E. Riedel, C. Janiak, *Anorganische Chemie*, 7. Auflage, De Gruyter, **2007**.
- [3] R. S. Berry, *J. Chem. Physics* **1960**, *32*, 933–328.
- [4] W. Massa, *Kristallstrukturbestimmung*, 8th ed., Springer, Wiesbaden, **2015**.
- [5] H. Krischner, *Einführung in die Röntgenfeinstrukturanalyse*, Vol. 2, Vieweg+Teubner Verlag, **1990**, pp. 102–150.
- [6] M. A. Bravais, *J. de l'ecole Polyt.* **1859**, *XIX*, 1.
- [7] W. L. Bragg, *Proc. Cambridge Phil. Soc.* **1913**, *17*, 43.
- [8] P. Debye, *Annalen der Physik* **1913**, 49–92.
- [9] I. Waller, *Zeitschrift für Physik* **1923**, *17*, 398–408.
- [10] N. Walker, D. Stuart, *Acta Crystallogr.* **1983**, *158*.
- [11] D. Harker, J. S. Kasper, *Acta Crystallogr.* **1948**, *70*.
- [12] D. Sayre, *Acta Crystallogr.* **1952**, *60*.
- [13] A. J. C. Wilson, *Acta Crystallogr.* **1949**, *2*, 318.
- [14] A. L. Patterson, *Phys. Rev.* **1934**, *46*, 372.
- [15] A. Holub, H. Köhler, V. Skopenko, *Chemistry of pseudohalides*, Elsevier, **1986**, pp. 15–453.
- [16] U. Müller, *Struct. Bonding* **1973**, *14*, 141.
- [17] S.-D. Han, J.-P. Zhao, S.-J. Liu, X.-H. Bu, *Coordination Chemistry Reviews* **2015**, *289-290*, 32–48.

Bibliography

- [18] R. G. Guy in *Cyanates and Their Thio Derivatives: Volume 2*, John Wiley & Sons Ltd., **1977**, pp. 819–886.
- [19] F. A. Mautner, M. Scherzer, C. Berger, R. C. Fischer, S. S. Massoud, *Polyhedron* **2015**, *85*, 20–26.
- [20] J. Joule, K. Mills, *Heterocyclic Chemistry*, John Wiley & Sons, **2010**, p. 7.
- [21] J. Joule, K. Mills, *Heterocyclic Chemistry*, John Wiley & Sons, **2010**, pp. 125–141.
- [22] F. Ramos-Lima, A. Quiroga, J. M. Perez, C. Navarro-Ranninger, *Polyhedron* **2003**, *22*, 3379–3381.
- [23] T. C. Stamatatos, D. Foguet-Albiol, S. P. Perlepes, C. P. Raptopoulou, A. Terzis, C. S. Patrickios, G. Christou, A. J. Tasiopoulos, *Polyhedron* **2006**, *25*, 1737–1746.
- [24] İ. Uçar, İ. Bulut, A. Bulut, A. Karadağ, *Structural Chemistry* **2009**, *20*, 825–838.
- [25] U. Kalinowska-Lis, A. Felczak, L. Checinska, K. Lisowska, J. Ochocki, *Journal of Organometallic Chemistry* **2014**, *749*, 394–399.
- [26] U. Kalinowska-Lis, J. Ochocki, K. Matlawska-Wasowska, *Coordination Chemistry Reviews* **2008**, *252*, 1328–1345.
- [27] J. Moncol, M. Mudra, P. Lonnecke, M. Koman, M. Melnik, *Journal of Chemical Crystallography* **2004**, *34*, 423–430.
- [28] P. S. Zhao, J. Song, R. C. Shangguan, F. F. Jian, *J. Serb. Chem. Soc.* **2010**, *75*, 1219.
- [29] F.-U. Rahman, I. K. Amjad Ali, R. Guo, L. Chen, H. Wang, Z.-T. Li, Y. Lin, D.-W. Zhang, *Polyhedron* **2015**, *100*, 264.
- [30] J. Maroszova, J. Moncol, Z. Padelkova, T. L. R. Sillanpaa, M. Koman, *Central Eur. J. Chem.* **2011**, *9*, 453.
- [31] R. Murugavel, S. Kuppuswamy, R. Boomishankar, A. Steiner, *Angew. Chem. Int. Ed.* **2006**, *45*, 5536.
- [32] T. C. Stamatatos, D. Foguet-Albiol, S. P. Perlepes, C. P. Raptopoulou, A. Terzis, C. S. Patrickios, G. Christou, A. J. Tasiopoulos, *Polyhedron* **2006**, *25*, 1737.

Bibliography

- [33] Q.-S. Ye, J.-L. Chen, M.-J. Xie, W.-P. Liu, S.-Y. Yang, Z. *Kristallgr.-New Cryst. Struct.* **2011**, *226*, 147.
- [34] E. Escribano, M. Font-Bardia, T. Calvet, J. Lorenzo, P. Gamez, V. Moreno, *Inorg. Chim. Acta* **2013**, *394*, 65.
- [35] M. A. S. Goher, F. A. Mautner, K. Gatterer, M. Abu-Youssef, A. M. A. Badr, B. Sodin, C. Gspan, *J. Mol. Struct.* **2008**, *876*, 199.
- [36] T. R. deBoer, I. Chakraborty, M. M. Olmstead, P. Mascharak, *Cryst. Growth Des.* **2014**, *14*, 4901.
- [37] J. Werner, C. Nather, *Polyhedron* **2015**, *98*, 96.
- [38] J. Moncol, B. Kalinakova, J. Svorec, M. Kleinova, M. Koman, D. Hudecova, M. Melnik, M. Mazur, M. Valko, *Inorg. Chim. Acta* **2004**, *357*, 3211.
- [39] K. K. Klausmeyer, R. A. Adrian, *Acta Crystallogr. Sect. E: Struct. Rep. Online* **2004**, *60*, 1414.
- [40] F. J. Ramos-Lima, O. Vrana, A. G. Quiroga, C. Navarro-Ranninger, A. Halamikova, H. Rybnickova, L. Hejmalova, V. Brabec, *J. Med. Chem.* **2006**, *9*, 2640.
- [41] J. Werner, I. Jess, C. Nather, *Acta Crystallogr. Sect. E: Cryst Commun* **2015**, *73*, 616–619.
- [42] N. N. Hoang, F. Valach, M. Melnik, *Acta Crystallogr. Sect. C: Cryst. Struct. Commun* **1993**, *49*, 467.
- [43] J. Moncol, J. Maroszova, M. Koman, M. Melnik, M. Valko, M. Mazur, T. Lis, *J. Coord. Chem.* **2008**, *61*, 3740.
- [44] D. Chechova, I. Svoboda, K. Jomova, Z. Ruzickova, M. Valko, J. Moncol, *Transition Met. Chem.* **2015**, *40*, 857.
- [45] V. H. L. Wong, A. J. P. White, T. S. A. Hor, K. K. Hi, *Adv. Synth. Catal.* **2015**, *357*, 2485.
- [46] B. N. Gosh, D. Lentz, S. Schlecht, *New J. Chem.* **2015**, *39*, 3536.
- [47] I. Ucar, H. Vural, E. Kucuk, *Spectrochim. Acta Part A* **2015**, *151*, 667.
- [48] A. Canlier, T. Kawasaki, S. Chowdhury, Y. Ikeda, *Inorg. Chim. Acta* **2010**, *363*, 1.

Bibliography

- [49] J. J. Perry, G. J. McManus, M. J. Zaworotko, *J. Chem. Cryst.* **2004**, *34*, 877.
- [50] G. E. Pieslinger, P. Albores, L. D. Step, B. J. Coe, C. J. Timpson, L. M. Baraldo, *Inorg. Chem.* **2013**, *52*, 2906.
- [51] N. Godbert, T. Pugliese, I. Aiello, A. Bellusci, A. Crispini, M. Ghedini, *Eur. J. Inorg. Chem.* **2007**, *32*, 5105.
- [52] P. Saxena, N. Thirupathi, *Polyhedron* **2015**, *98*, 238.
- [53] H. Abourahma, G. J. McManus, B. Moulton, R. D. B. Walsh, M. J. Zaworotko, *Macromol. Symp.* **2003**, *196*, 213.
- [54] T. R. Hayes, P. A. Lyon, C. L. Barnes, S. Trabue, P. D. Benny, *Inorg. Chem.* **2015**, *54*, 1528.
- [55] A. D. Follett., K. A. McNabb, A. A. Peterson, J. D. Scanlon, C. J. Cramer, K. McNeill, *Inorg. Chem.* **2007**, *46*, 1645.
- [56] L. Carlton, L. V. Mokoena, M. A. Fernandes, *Magn. Reson. Chem.* **2013**, *51*, 199.
- [57] M. Dennehy, O. V. Quinzani, A. Granados, R. A. urrow, *Polyhedron* **2010**, *29*, 1344.
- [58] L. Mantilli, D. Gerard, C. Besnard, C. Mazet, *Eur. J. Inorg. Chem.* **2012**, *20*, 3320.
- [59] T. Weilandt, N. L. Low, G. Schnakenburg, J. Daniels, M. Nieger, C. A. Schalley, A. Lutzen, *Chem. Eur. J.* **2012**, *18*, 16665.
- [60] D. W. Wakerley, E. Reisner, *Phys. Chem. Chem. Phys. (PCCP)* **2014**, *16*, 5739.
- [61] Y. Liu, S.-M. Ng, S.-M. Yiu, W.W.W.Y.Lam, X.-G. Wei, K.-C. Lau, T.-C. Lau, *Ang. Chem Int.Ed.* **2014**, *53*, 14468.
- [62] R. D. Schmidt, D. A. Shultz, J. D. Martin, P. D. Boyle, *J. Am. Chem. Soc.* **2010**, *132*, 6261.
- [63] 4-Pyridinemethanol, <http://www.sigmaaldrich.com/catalog/product/aldrich/151629?lang=de®ion=AT>.
- [64] 4-Methoxypyridine, <http://www.sigmaaldrich.com/catalog/product/aldrich/460621?lang=de®ion=AT>.

Bibliography

- [65] K. Nakamoto, *Infrared and Raman spectra of inorganic and coordination compounds*, John Wiley and Sons, Inc, **1986**, pp. 282–291.
- [66] APEX and SAINT, Area Detector Software package and AXS Area Detector integration program, Bruker Analytical X-ray, Madison, WI, **1997**.
- [67] SADABS, AXS Area Detector Absorption program, Bruker Analytical X-ray, Madison, WI, **1997**.
- [68] G. Sheldrick, *Acta Cryst. Sect. A* **2008**, *112*.
- [69] A. L. Spek, PLATON, A Multipurpose Crystallographic tool, Utrecht University, Utrecht, Netherlands, **2005**.
- [70] OPUS-software, Vers. 5, Bruker Optics, Billerica, MA, US.
- [71] UVWin Lab software, Version 5.1; Perkin Elmer LAS, Rodgau - Germany, **2005**.
- [72] A. W. Addison, R. Addison, T. Nageswara, J. Reedijk, J. van Rijn, G. C. Verschoor, *J. Chem. Soc., Dalton Trans.* **1984**, *7*, 1349–1356.
- [73] G. Racah, *Phys. Rev.* **1942**, *62*, 438–462.
- [74] E. Sarina, U. C. Davis, Tanabe-Sugano Diagram, <http://chemistry.bd.psu.edu/jircitano/TSdiagram.pdf>, **2016**.
- [75] R. Sen, A. Bhattacharjee, P. Gutlich, Y. Miyashita, K. Okamoto, S. Koner, *Inorg. Chim. Acta* **2009**, *4663*, 362.
- [76] J. L. Manson, A. M. Arif, C. D. Incarvito, L. M. Liable-Sands, A. L. Rheingold, J. S. Miller, *J. Solid State Chem.* **1999**, *145*, 369.
- [77] K. S. Banu, S. Mondal, A. Guha, S. Das, T. Chattopadhyay, E. Suresh, E. Zangrand, D. Das, *Polyhedron* **2011**, *30*, 163.
- [78] M. Biswas, G. M. Rosair, G. Pilet, S. Mitra, *Inorg. Chim. Acta* **2007**, *360*, 695.
- [79] W. Dong, Q.-L. Wang, Z.-Q. Liu, D.-Z. Liao, Z.-H. Jiang, S.-P. Yan, P. Cheng, *Polyhedron* **2003**, *22*, 3315.
- [80] G. A. van Albada, M. E. Quiroz-Castro, I. Mutikainen, U. Turpeinen, J. Reedijk, *Inorg. Chim. Acta* **2000**, *298*, 221.
- [81] R. Sen, A. Bhattacharjee, P. Gutlich, Y. Miyashita, K. Okamoto, S. Koner, *Inorg. Chim. Acta* **2009**, *362*, 4663.

Bibliography

- [82] M. Du, X.-J. Zhao, S. R. Batten, J. Ribas, *Cryst. Growth Des.* **2005**, *5*, 901.
- [83] P. Chakraborty, S. Mondal, S. Das, A. D. Jana, D. Das, *Polyhedron* **2014**, *70*, 11.